NASA CONTRACTOR REPORT

N73-19269

NASA CR-2191

NASA CR-2191

CASE FILE COPY

WIND TUNNEL INTERFERENCE FACTORS FOR HIGH-LIFT WINGS IN CLOSED WIND TUNNELS

by Robert G. Joppa

Prepared by
UNIVERSITY OF WASHINGTON
Seattle, Wash. 98195
for Langley Research Center

NATIONAL AERONAUTICS AND SPACE ADMINISTRATION • WASHINGTON, D. C. • FEBRUARY 1973

1. Report No. NASA CR-2191	2. Government Accession No.	3. Recipient's Catalog No.
4. Title and Subtitle WIND TUNNEL INTERFERENCE FACTORS FOR HIGH-LIFT WINGS IN CLOSED WIND TUNNELS		5. Report Date February 1973
		6. Performing Organization Code
7. Author(s) Robert G. Joppa		8. Performing Organization Report No.
		10. Work Unit No. 760-61-02-81-23
9. Performing Organization Name and Address University of Washington Seattle, Washington 98195		11. Contract or Grant No. NGL 48-002-010
		13. Type of Report and Period Covered Contractor Report
12. Sponsoring Agency Name and Address National Aeronautics and Space Administration Washington, D.C. 20546		14. Sponsoring Agency Code
15. Supplementary Notes		

16. Abstract

A problem associated with the wind tunnel testing of very slow flying aircraft is the correction of observed pitching moments to free air conditions. The most significant effects of such corrections are to be found at moderate downwash angles typical of the landing approach.

The wind tunnel walls induce interference velocities at the tail different from those induced at the wing, and these induced velocities also alter the trajectory of the trailing vortex system. The relocated vortex system induces different velocities at the tail from those experienced in free air. The effect of the relocated vortex and the walls is to cause important changes in the measured pitching moments in the wind tunnel.

17. Key Words (Suggested by Author(s)) Wind tunnels Wall effects Pitching moments	18. Distribution Statement Unclassified - Unlimited

19. Security Classif. (of this report)	20. Security Classif. (of this page)	21. No. of Pages	22. Price*
Unclassified	Unclassified	125	$ 3.00

*For sale by the National Technical Information Service, Springfield, Virginia 22151

PREFACE

This work was conducted under NASA Grant NGL-48-002-010. Portions of the work presented in Chapter V have previously been published by NASA in CR-845. Portions of the work presented in Chapters IV and VI have been published in the AIAA Journal of Aircraft, May - June 1969, pp. 209-214, are copyrighted by AIAA, and are used here with their permission. This report has been submitted to the Department of Aerospace and Mechanical Sciences, Princeton University, in partial fulfillment of the requirements for the Ph.D. degree.

TABLE OF CONTENTS

Appendices

FIGURE INDEX

WIND TUNNEL INTERFERENCE FACTORS FOR HIGH-LIFT WINGS IN CLOSED WIND TUNNELS

Robert Glenn Joppa

SUMMARY

A problem associated with the wind tunnel testing of very slow flying aircraft is the correction of observed pitching moments to free air conditions. The most significant effects of such corrections are to be found at moderate downwash angles typical of the landing approach.

The wind tunnel walls induce interference velocities at the tail different from those induced at the wing, and these induced velocities also alter the trajectory of the trailing vortex system. The relocated vortex system induces different velocities at the tail from those experienced in free air. The effect of the relocated vortex and the walls is to cause important changes in the measured pitching moments in the wind tunnel.

A method of calculating the interference velocities is presented in which the effects of the altered wake location is included. The flow fields of a lifting system are calculated in free air and in the tunnel, and when compared the differences are charged to tunnel wall interference. Iterative methods are used which require a large computer. The tunnel walls are represented by a vortex lattice and the results compared with classical methods for the undeflected wake case.

Results are presented comparing the tail interference angles, with and without the effect of vortex wake relocation, which show the importance of the wake shift. In some cases the tail angle corrections are reduced to zero and may even change sign. It is concluded that to correctly calculate the interference velocities affecting pitching moments, the effects of vortex wake relocation must be included.

SYMBOLS

$\mathcal{R}$	Aspect ratio
$[A]$	Matrix of coefficients of wall vortex elements
$\{B\}$	Column matrix of coefficients of wing vortex system
b	Wing vortex span
b_g	Wing geometric span
C	Wind tunnel cross-section area
C_L	Wing lift coefficient
e	Distance downstream to wake roll-up
$h_{(\ )}$	Normal distance to a point p from a line containing a vortex segment identified by subscript
$h_{(\ )(\ )}$	Normal distance to a point p from a plane containing vortex segments identified by subscript
H	Height of wind tunnel
$\bar{i},\bar{j},\bar{k}$	Unit vectors in the directions X, Y, Z
L,G	Dimensions of rectangular vortex ring (Fig. 8)
$\bar{n}$	Unit vector normal to vortex ring
p	Point having coordinates X, Y, Z
$R_{(\ )}$	Vector from point (X,Y,Z) to end of a vortex vector $\bar{S}$ indicated by subscript
$R_{(\ )(\ )}$	Magnitude of component of vector $R_{(\ )}$ indicated by second subscript
S_w	Wing area
$\bar{S}$	Vector representing a vortex segment of strength Γ and length S
$S_{(\ )}$	Component of $\bar{S}$ indicated by subscript
$\bar{v}$	Unit vector in the direction of the total velocity vector at a point

$\overline{V}$	Velocity induced at a point
$V_{(\ )}$	Velocity component in direction indicated by subscript
w	Vertical component of wall-induced interference velocity
W	Width of wind tunnel
$\overline{W}$	Vector representing a wing bound vortex of strength Γ_w
X,Y,Z	Cartesian coordinate of a point
β	Angles defining direction to a point from the end of a vortex segment (Fig. 7)
Γ	Circulation strength of a vortex
$\Delta\alpha$	Difference between angle of attack in free air and in wind tunnel
δ	Wind tunnel interference factor
δ_t	δ Evaluated at tail location
δ_w	δ Evaluated at wing location

I. INTRODUCTION

The problem of how to do meaningful testing of high lift systems in wind tunnels has been with us for some time. That wind tunnel testing is necessary for new types of slow flying vehicles is evident because the nature of the problems of stability and control are different than in flight at cruising speeds.

To obtain the necessary lift at low speed requires that incoming air be deflected through a large angle and/or accelerated to a high discharge velocity at a moderate deflection angle. In either case the change in angle or increase of velocity is no longer small, and so linearized assumptions are no longer valid. Pitching moments felt by the airframe due to the large turning angle are generally large and nonlinear, and vary with forward speed as well as with angle of attack.

The gross effects may be estimated by recourse to momentum methods. Unfortunately, the gross effects are modified by real fluid effects that are configuration dependent. Lift is developed by real devices such as rotors, fans, and wings with flaps. These devices are operated at or near their maximum capability, i.e., near the point of flow separation. In many cases, flow separation and re-attachment occur cyclically during normal operations, so that linear relationships such as between forces and angles of attack, do not usually exist.

As a result of all this, classical aerodynamic theory, which is linearized and limited to small angles, is incapable of predicting performance. The only recourse left to the designer, then, is to go to the wind tunnel to determine experimentally the characteristics of a new machine.

Unfortunately, the wind tunnel introduces its own set of problems. While it does indeed permit the solution of the detailed problems of separation and mutual interference by direct analogy, the quality of that solution depends upon the quality of the match of the necessary similarity conditions. These are the exactness of the model and the matching of Reynolds numbers and Mach numbers.

High lift systems usually involve rather intricately detailed parts such as blowing or suction slots, rotors with dampered hinges and important elastic properties, or internal ducting and fans. The accuracy with which these details can be matched imposes some limit on the smallest feasible model size; and, in addition, these elements may be the ones most sensitive to mismatching of Reynolds number and Mach number.

Matching of Reynolds number and Mach number, of course, are mutually exclusive except in the case of a full scale model. Since the flight speeds of concern are usually low, one's first thought is that the test Mach number might be increased in favor of a larger Reynolds number, but this is not usually possible. At high lift coefficients, local flow velocities are often very high and large enough to be affected by the local Mach number. Where rotating parts are in use, the Mach number of an advancing blade is frequently the controlling factor. Thus, the test engineer is forced to do what he has always done; to accept a lower Reynolds number and attempt to extrapolate to full scale results on the basis of previous experience. This experience is not extensive at present and so he does this very reluctantly, insisting on the largest possible model for a given tunnel.

The wind tunnel also introduces another set of problems which are a direct result of the physical presence of the boundaries of the test section. The flow from a high lift system has a large local downwash angle and velocity, and in free air may require several times its own characteristic length to reach final values which may still be very large. The wind tunnel walls force the final value of downwash angle to be zero and alters both the direction and curvature of the flow in the immediate vicinity of the model by an amount which is significant with respect to the camber of the lifting system, especially when the model is long (e.g., a rotor, or a horizontal tail aft of a wing).

That such flow interference exists has of course been recognized from the earliest use of wind tunnels, and classical theory exists for the prediction of the interference effects and for the correction of data. Unfortunately, the classical work depends on the assumption that the downwash velocities are small and that the wake of the lifting system goes straight downstream.

Three methods of coping with this lack of an adequate interference prediction theory are available. One can use a very small model in available tunnels, build bigger wind tunnels, or develop new theory. A criterion for smallness of models was put forth in 1956 (Ref. 1) which suggested that the change in curvature of the flow would be sufficiently small if the interference angle at the lifting system, calculated by linear theory, was never larger than 2°. That this leads to extremely small models is demonstrated by Fig. (1) where it is applied to a helicopter rotor. These small models, of course, aggravate an already serious Reynolds number problem; and so the industry, still having no adequate theory, began in the early 1960's to build larger wind tunnels having test sections of the order of 400 to 1000 square feet. Even this new generation of wind tunnels is inadequate for matching Reynolds number, although the new facilities do permit construction of models large enough that detail can be matched with available fabrication techniques. A considerable amount of effort has been devoted to the wall interference problem but a complete solution is still not available. This paper is devoted to the development of a new method of predicting wind tunnel wall interference for an important class of slow flying vehicles.

II. DEVELOPMENT AND CURRENT STATE OF WALL INTERFERENCE THEORY

In the classical wind tunnel interference problem, it is assumed that the model lifting system can be represented by a lifting line and a pair of vortex filaments which trail downstream in a straight, level line from a point near the wing tips. A cross-section normal to the flow is examined downstream from the plane of the lifting line, and a pattern of other vortex filaments is chosen outside the tunnel walls in such a way that the tunnel walls become streamlines of the flow. The effect at the model of the added vortices then constitutes the interference effect of the walls.

Prandtl presented a solution for the circular wind tunnel (Ref. 2) which required only a single pair of vortices outside the tunnel wall to cancel, at the wall, the effect of the trailing pair inside, but he did not include the effect of the lifting line itself. Consequently, his solution is valid only at the plane of the lifting line and cannot give the longitudinal variation of the interference angles.

Glauert followed (Ref. 3) with a solution for a rectangular tunnel. Since the walls were planes, it was required only that each wall become a plane of symmetry of the vortex lines inside the tunnel and those outside it, thus leading to a doubly infinite set of vortex lines. In the rectangular tunnel there is no problem of how to handle the bound vortex, for its external image clearly joins the images of each trailing pair. His solution then is valid for points fore and aft of the lifting line, and it was possible to show that the effect of the tunnel walls was different at the tail than at the wing.

Other authors have developed solutions for other tunnel shapes, but no proper image system has been presented for any other shape than the rectangular tunnel. Lotz (Ref. 4) was successful in developing solutions for circular and elliptical cross section tunnels which accounted for the effect of the bound vortex. She added to the image system of Prandtl, a potential function expressed in infinite series form, which was required to cancel at the wall the normal velocities at the wall caused by the bound vortex and also expressed in infinite series form. The accuracy of the results depends on the evaluation of the truncated series, and no indication is given in the original report of the probable error.

Clearly the basic assumption of the straight downstream wake trajectory had to be modified for the consideration of the high downwash systems of interest here. The most successful change to date was made by Heyson (Ref. 5) who let the wake be straight, but at an angle downward until it struck the tunnel floor. The zero size lifting system was represented by a point doublet and the wake by a string of such doublets. When extending to a finite span wing, a series of such point systems are placed side by side; and, since internal singularities cancel each other, the result is equivalent to a lifting line and a single trailing pair of vortex filaments. The angle of descent of the trailing system was taken originally as 1/2 the final downwash angle calculated by momentum theory for the span-circle mass of air required to produce the lift of the system. In a later publication (Ref. 6), he modified this to 1/4 of the final downwash angle, agreeing with a calculation by the author that vortex filaments of a wake move downward at approximately 1/5 the final momentum downwash value. Thus, the angle of descent used in later work is representative of the final wake trajectory, in free air, of the trailing vortex system. Image systems are then constructed outside the tunnel (rectangular cross-section). At the point where the trailing wake strikes the floor, it is met by the first image wake, and they are assumed to change direction and move aft together in the plane of the floor.

With the image system constructed as described, it was possible to sum the interference velocities at the model due to the external vortex system. It should be noted that the doublets, normal to the plane of the downward trailing pair, have fore and aft components as well as vertical components; and, consequently, longitudinal as well as vertical interference velocities exist. At the floor intersection, only the vertical components are canceled; the longitudinal components add and are retained.

Some controversy exists about the degree to which these interference calculations are applicable. Evidence has been presented (Ref. 6,7,8) to show that good results are achieved when calculating interference velocities at the model and using them to correct lift and drag. The method has not been uniformly successful in correcting pitching moments, however. As an indication of the controversy, it may be said that another laboratory has offered evidence that wind tunnel and flight stability data may agree more closely when no corrections whatever are applied (Ref. 9).

The solutions of Heyson, and others who have tried to do something similar, are deficient in at least two respects. The first and most obvious is that the assumed wake position is not correct. Others have attempted to improve on the wake trajectory by using other assumptions or by modeling experimentally measured wakes, and then using Heyson's computations to calculate the interference velocities due to images of these more correct wakes. Results are reported to be little changed at the model location, but they are still inadequate for pitching moments.

The second deficiency is the one which is the more important and which no one has yet attempted to account for. This is the direct effect on the model of the fact that the wake trails along a different trajectory in the tunnel than in free air. The effect arises this way. The presence of the boundaries (as made evident by the image system) causes upwash velocities which are felt everywhere in the tunnel; by the model tail and also by the vortex wake itself. The result of these upwash velocities is to cause the vortex wake to be higher in the tunnel than in free air. This new higher position is different with respect to the tail. For example, if the tail is above the wake in free air, the wake will now be raised closer to the tail and will induce on the tail a stronger downwash than in free air. This effect may equal or exceed the wall or image induced upwash, and thereby dominate the pitching moment interference.

III. A NEW APPROACH TO INTERFERENCE CALCULATIONS

A new approach to the problem is offered in this paper which attempts to remove the two deficiencies of former methods. The interference must be computed for the correct wake shape, and the direct effects of the relocated wake must be included. In order to do this, the flow field of the lifting system must be predicted both in the free air case and in the wind tunnel, and the differences in flow velocities be charged to wall interference. In order to develop the method, certain restrictions to the problem were defined for practical reasons.

The principal effect which it is desired to show is that the relocation of the wake by the interference of the walls contributes a major influence on pitching moment interference, which may be added to or subtracted from the usual interference calculations. It is not difficult to show that the effect of a shift in the wake position will have a maximum effect when the wake is only moderately deflected with respect to the tail or the plane of a rotor. Figure (2) shows a section taken (Trefftz plane) at a location representative of a tail with a pair of trailing vortices at a distance h below the tail. The downwash is given by the Biot-Savart equation, and is

$$w = \frac{\Gamma}{\pi \frac{b}{2} \left[1 + \left(\frac{h}{b/2}\right)^2\right]}$$

The ratio of the downwash velocity to that experienced when the wake is at the same height as the tail, $(h = 0)$, is given by

$$\frac{w}{w_{(h=0)}} = \frac{1}{1 + \left(\frac{h}{b/2}\right)^2}$$

The maximum rate of change of downwash with height occurs when $\frac{h}{b/2} = \sqrt{\frac{1}{3}} = 0.577$.

If the length of the model is of the same order as the span, and the model is in a level attitude, then this corresponds roughly to a downwash angle of the vortex wake of about 16°. Helmbold (Ref. 10), has shown that the maximum lift possible due to circulation alone will produce a wake trajectory angle of just over 20°. Therefore, the attainable values of circulation lift place the wake in the region where changes in its location will produce the maximum effect on the downwash at the tail.

Greater wake trajectory angles are of course produced by highly powered lifting systems where the power is used to increase the mass rate of flow through the system. Analysis of highly powered systems is not included here for two principal reasons. First, the larger downwash angles remove the wake vorticity further from the tail plane, and so the effects of wake relocation become less important. If the downwash angles are large enough, the tail is almost unaffected by changes in wake location, and in this case the methods of Heyson become appropriate, and indeed have given good results.

A more practical reason for avoiding larger downwash angles is that at some point interaction with the tunnel walls produces an impossible situation. In the limiting case of hovering inside a test section, the forces measured are clearly different from those in free air because of recirculation of the air. For a range of forward speeds above hovering, recirculation still exists in the tunnel where it will not in free flight, even near the ground. At speeds just above recirculation, experiments by Rae (Ref. 11) indicate that forces measured are so far from what is expected that test results are highly doubtful and may be useless. Apparently the rotor wash is interacting with the entire tunnel flow and producing a large circulation very close downstream in a way which has yet to be satisfactorily explained. His test results show that a fairly definite point can be determined at which this effect (which he calls flow breakdown) disappears and one expects credible results. This limit probably determines the lower speed bound (maximum downwash angle) for corrections of any type. Consequently, this region will not be examined here, and the problem will be confined to lifting systems which can be said to produce only circulation lift.

This type of system is simply represented as a lifting vortex line with a single trailing pair of vortices. Such a mathematical model could represent a simple wing with some sort of boundary layer control so that the large values of circulation can be developed. It may also represent a helicopter rotor operating in the translational lift region. Since we are primarily concerned with the flow field at a distance from the model (at the tunnel walls), details near the model are of lesser interest and a relatively simple model representation can be used.

It is assumed that the trailing sheet of vorticity rolls up immediately into a cylindrical core of vorticity which can be represented by a single filament located at the center of gravity of the original vortex sheet. Actually, this assumption is not really necessary. It only need be shown that the effect of the singular representation of one half of the trailing sheet on the center of gravity of the other half is not significantly different from the effect of the real sheet. It is demonstrated in Appendix A that the effect of the undeflected sheet trailing from one half of an elliptically loaded wing is only 2½% larger than the corresponding effect of a singularity at the center of gravity. After roll-up, the vortex sheet becomes axially symmetrical and it is easily shown that the effect at any external point of a uniform cylindrical vortex sheet is identical to that of a filament at its center having the same total strength.

Evidence that the wake does roll up quickly is given by Sprieter and Sacks (Ref. 12) who report the roll-up distance as a fraction of the geometric wing span to be

$$\frac{e}{b_g} = 0.28\left(\frac{A\!\!\!R}{C_L}\right)$$

In the high-lift case of interest here, $A\!\!\!R/C_L$ is about 1.0, so the roll-up distance would be of the order of a chord length downstream.

That a helicopter rotor can be represented by the lifting line and trailing pair is graphically shown by data taken by Heyson, (Ref. 13). Figure (3), taken from NACA TR 1319, shows that for a rotor having a momentum downwash angle of 15°, two clearly defined vortex cores are already well developed at a plane only just downstream of the rotor trailing edge. It also shows that the cores are deflected less than one half as much as the air mass, calculated by momentum theory.

In summary, the problem that will be presented is the calculation of the interference due to the walls of a closed test section wind tunnel, on a high-lift wing having a moderately large downwash angle, taking account of the direct effect of the relocation of the vortex wake on the longitudinal distribution of downwash. The problem is approached by first calculating the trajectory of the wake of a simple lifting system and its flow field in free air. The lifting system is then placed in a wind tunnel and its new trajectory and flow field are compared at the same values of remote wind speed and model circulation strength; differences are interpreted in terms of tunnel wall interference. In order to determine the flow field in the wind tunnel, a new method of representing the wind tunnel walls was developed and is also presented.

IV. THE FREE AIR TRAJECTORY

Figure (4) shows a sketch of the vortex wake representing a plane elliptical wing and indicates the induced velocity due to an element of the vortex acting at an arbitrary point. The element of induced velocity is evaluated by the Biot-Savart law, and when integrated over the entire wake, the direction of the flow at a point can be determined. The flow direction is first determined along an initially assumed wake trajectory and the wake is then deflected to assume the calculated direction. With the wake now deflected, a new calculation of flow direction is made and the solution converges after several iterations.

To facilitate the solution, the vortex system is broken into a series of short straight line segments. The bound vortex lies on the quarter chord line and has a span of $\pi/4$ times the geometric span, which is appropriate for representing an elliptical wing. The first trailing segments lie in the plane of the wing, extending from the bound vortex tips to the trailing edge. The downstream vortices are assumed to spring from the trailing edge at that point and are divided into segments whose length is approximately 1/10 of the vortex span. The angle of the first segment, being in the plane of the wing, is determined by adding the induced angle of attack and the effective angle of attack at the plane of symmetry. The induced angle of attack of the wing is computed at the lifting line by summing the induced velocities of all the trailing segments and adding them vectorially to the remote velocity. The effective angle of attack is determined by assuming two dimensional flow at the plane of symmetry and setting the normal component of the local velocity vector equal and opposite to the velocity induced by the bound vortex at the three-quarter chord point. See Figure (5).

The direction of each downstream element, in turn, is calculated by summing the individual velocities due to all other elements at its own upstream end. This direction is used to determine the coordinates of the downstream end of the segment; the entire string of segments downstream from that point is translated so that it stays attached, and the next segment direction is determined. Thus, the wake is moved into place by sweeping along its length from the wing aft in several iterations.

When a vortex line lies in a plane and follows a path of varying curvature, it induces on itself velocities normal to the original plane which vary with the curvature. The filament, which leaves the wing at a fixed location, curves upward from its angle of departure, and so each downstream section experiences an inward deflection from its own upstream elements. This vanishes as the trajectory straightens out, but it must leave the final straight wake at a smaller vortex span than it had on leaving the wing. The iteration process must then allow for this lateral freedom, as well as for the vertical motion of the wake.

When the above described process was first attempted, simultaneously calculating both downward and inward deflections, the computation became unstable after only a few iterations. This instability was avoided by a double iteration process. First, one pass is made calculating only downward deflections, and then a second is made allowing only horizontal or inward deflections. By this stepwise process, a trajectory can be found which converges after only three or four such double passes, and which converges before instability develops.

It should be noted that the vortex line is physically unstable in that curvature of the line causes more self-induced curvature. A pair of vortex lines, if disturbed, will break up into segments and eventually produce vortex rings. An example may be observed in the contrails of jet aircraft, where the engine exhaust is drawn into and makes visible the cores of the trailing vortex pair. This instability could be accentuated by round-off errors in the computing machine and places a limit on the number of times an iteration can be carried out.

A computer program with instructions and card listing for the solution for the vortex trajectory from a lifting wing is given in Appendix B.

V. REPRESENTATION OF THE WIND TUNNEL WALLS

While the image systems described earlier are correct, and could be used with proper modification for finding the interference velocities due to the tunnel walls, they still leave something to be desired. Since the vortex wake of the lifting system in the tunnel will be curved, the external images would also have to be curved; and furthermore, since the final solution will have to be iterative, the geometry of the image system will have to change also for each iteration. These problems can be handled by a computer, but the method has some more basic restrictions. Proper images are available only for rectangular tunnels and the concept of an image implies that the tunnel is of infinite length. Tunnels in use for high lift testing are not all rectangular and, more important, many of the special tunnels being built today have such short test sections that some doubt exists about their adequacy. Therefore, in an effort to satisfy these objections a new approach was developed.

In this method the image concept was abandoned and the tunnel walls are represented by a vortex lattice. The strength of each element of the lattice is found by simultaneously requiring that the normal component of velocity vanish at a control point in the center of each lattice element. This method has the computational advantage that the geometry of this system is unchanged during each iteration, and that the large matrix of coefficients need be inverted only once for a series of computations.

Further, it is applicable to any tunnel cross section to the extent that it can be approximated by a polygon of equal length elements, and the effects of finite length can be explored. In order to prove the method, it was first applied to the classical problem of the undeflected wake. The development follows.

Problem Statement

The problem is to find that distribution of vorticity lying in the tunnel walls which will prevent any flow through the wall due to the action of a lifting system in the wind tunnel. The lifting surface is assumed to be uniformly loaded and is represented by a simple horseshoe vortex with the trailing pair undeflected. In principle, any desired distribution of lift could be built up of several such simple elements.

The walls are represented by a tubular vortex sheet of finite length composed of a network of circumferential and longitudinal vortices having equal spacing. Helmholtz' theorem that a vortex filament can neither end nor begin in the flow is satisfied most readily by constructing the network of square vortex rings lying wholly within the plane of the walls. Each square has a vortex strength Γ_i , and each side is coincident with the side of the neighboring square. Thus, the strength of any segment is the difference between the strengths of the two adjoining squares. The boundary condition that the wall must be impervious to flow is satisfied at a control point in the center of each square. This results in a set of simultaneous equations, one written for each control point, in which the unknowns are the Γ_i .

A large number of equations results if the tube is very long, thus some judgment is required in choosing the geometric arrangement. The use of square vortex rings requires a tunnel of constant cross-section. One notes that for a wing mounted in the center of the tunnel, lateral symmetry always exists; and, if the wake is undeflected, vertical symmetry also exists, thus reducing the number of unknowns. The trailing edge of a finite length tube which represents the long tunnel requires a slightly different treatment. At a far downstream section, only longitudinal vorticity should exist. This is represented by elongating the last ring of squares by a large amount, while keeping the control point at the same location with respect to the last circumferential station. Figure (6) shows the arrangement for a rectangular tunnel with filleted corners.

Equation Setup and Solution

A right-hand axis system is established with the X-axis on the longitudinal centerline of the tunnel, positive downstream. The Y-axis is taken positive upward and the Z-axis positive to the right side of the tube facing downstream.

Since the surface of the tunnel is to be made of square elements, its cross-section is a polygon of equal segments arranged to approximate the desired cross-section shape. In this development, the cross-section will be assumed to be symmetrical about the X , Y plane.

In general, the velocity induced at any point p (Fig. 7) due to a vortex segment may be written:

$$\overline{V} = \frac{\Gamma}{4\pi h} (\cos \beta_1 + \cos \beta_2) \overline{v} \qquad (1)$$

where $\bar{v}$ is a unit vector to establish direction. The terms required are written as follows:

$$\cos \beta_1 + \cos \beta_2 = \frac{R_1+R_2}{2R_1R_2S}\left[S^2 - (R_1-R_2)^2\right]$$

$$\bar{v} = \frac{\bar{R}_1 \times \bar{S}}{|\bar{R}_1 \times \bar{S}|} = \frac{\begin{vmatrix} \bar{i} & \bar{j} & \bar{k} \\ R_{1_x} & R_{1_y} & R_{1_z} \\ S_x & S_y & S_z \end{vmatrix}}{R_1 S \sin \beta_1}$$

Noting that $\sin \beta_1 = \dfrac{h}{R_1}$,

$$\bar{v} = \frac{\left(R_{1_y}S_z - R_{1_z}S_y\right)\bar{i}}{Sh} - \frac{\left(R_{1_x}S_z - R_{1_z}S_x\right)\bar{j}}{Sh} + \frac{\left(R_{1_x}S_y - R_{1_y}S_x\right)\bar{k}}{Sh}$$

Finally, the velocity induced at a point due to a vortex segment is:

$$\frac{\bar{V}}{\Gamma/4\pi h} = \frac{R_1+R_2}{2R_1R_2S^2h}\left[S^2-(R_1-R_2)^2\right]\left[\left(R_{1_y}S_z-R_{1_z}S_y\right)\bar{i}\right.$$

$$\left. +\left(R_{1_z}S_x-R_{1_x}S_z\right)\bar{j} + \left(R_{1_x}S_y-R_{1_y}S_x\right)\bar{k}\right] \quad (2)$$

One could then add the contributions of all four sides of a vortex square, but it is more convenient to take advantage of the lateral symmetry and sum the effects due to a pair of symmetrically located vortex squares of the same strength. The arrangement is shown in Fig. (8) and the following equation results:

$$
\begin{aligned}
\frac{\bar{V}}{\Gamma/8\pi L} = {} & h_{AB}\left\{\frac{R_{NA}+R_{NB}}{h_{N_1}^2 R_{NA}R_{NB}}\left[L^2-(R_{NA}-R_{NB})^2\right]-\frac{R_{MA}+R_{MB}}{h_{M_1}^2 R_{MA}R_{MB}}\left[L^2-(R_{MA}-R_{MB})^2\right]\right\}\bar{i}\\
& + h_{DC}\left\{\frac{R_{ND}+R_{NC}}{h_{N_2}^2 R_{ND}R_{NC}}\left[L^2-(R_{ND}-R_{NC})^2\right]-\frac{R_{MD}+R_{MC}}{h_{M_2}^2 R_{MD}R_{MC}}\left[L^2-(R_{MD}-R_{MC})^2\right]\right\}\bar{i}\\
& + \cos\phi_B\left\{\frac{R_{NA}+R_{NB}}{h_{N_1}^2 R_{NA}R_{NB}}\left[L^2-(R_{NA}-R_{NB})^2\right]+\frac{R_{ND}+R_{NC}}{h_{N_2}^2 R_{ND}R_{NC}}\left[L^2-(R_{ND}-R_{NC})^2\right]\right\}(X-X_N)\ \bar{j}\\
& + \cos\phi_B\left\{\frac{R_{MA}+R_{MB}}{h_{M_1}^2 R_{MA}R_{MB}}\left[L^2-(R_{MA}-R_{MB})^2\right]+\frac{R_{MD}+R_{MC}}{h_{M_2}^2 R_{MD}R_{MC}}\left[L^2-(R_{MC}-R_{MD})^2\right]\right\}(X_M-X)\ \bar{j}\\
& + \left\{\frac{R_{MA}+R_{NA}}{h_A^2 R_{MA}R_{NA}}\left[L^2-(R_{MA}-R_{NA})^2\right](Z-Z_A)+\frac{R_{NB}+R_{MB}}{h_B^2 R_{NB}R_{MB}}\left[L^2-(R_{MB}-R_{NB})^2\right](Z_B-Z)\right\}\bar{j}\\
& + \left\{\frac{R_{NC}+R_{MC}}{h_C^2 R_{NC}R_{MC}}\left[L^2-(R_{NC}-R_{MC})^2\right](Z_C-Z)+\frac{R_{ND}+R_{MD}}{h_D^2 R_{ND}R_{MD}}\left[L^2-(R_{ND}-R_{MD})^2\right](Z-Z_D)\right\}\bar{j}\\
& + \sin\phi_B\left\{\frac{R_{NA}+R_{NB}}{h_{N_1}^2 R_{NA}R_{NB}}\left[L^2-(R_{NA}-R_{NB})^2\right]-\frac{R_{NC}+R_{ND}}{h_{N_2}^2 R_{NC}R_{ND}}\left[L^2-(R_{NC}-R_{ND})^2\right]\right\}(X_N-X)\ \bar{k}\\
& + \sin\phi_B\left\{\frac{R_{MC}+R_{MD}}{h_{M_2}^2 R_{MC}R_{MD}}\left[L^2-(R_{MC}-R_{MD})^2\right]-\frac{R_{MA}+R_{MB}}{h_{M_1}^2 R_{MA}R_{MB}}\left[L^2-(R_{MA}-R_{MB})^2\right]\right\}(X_M-X)\ \bar{k}\\
& + \left\{\frac{R_{NA}+R_{MA}}{h_A^2 R_{NA}R_{MA}}\left[L^2-(R_{NA}-R_{MA})^2\right]-\frac{R_{NC}+R_{MC}}{h_C^2 R_{NC}R_{MC}}\left[L^2-(R_{NC}-R_{MC})^2\right]\right\}(Y_A-Y)\ \bar{k}\\
& + \left\{\frac{R_{ND}+R_{MD}}{h_D^2 R_{ND}R_{MD}}\left[L^2-(R_{ND}-R_{MD})^2\right]-\frac{R_{NB}+R_{MB}}{h_B^2 R_{NB}R_{MB}}\left[L^2-(R_{NB}-R_{MB})^2\right]\right\}(Y_B-Y)\ \bar{k}
\end{aligned}
\tag{3}
$$

Similarly, the velocity induced at point p by a simple horseshoe vortex located in the center of the tunnel is derived from Fig. (9) using Eq. (1). Summing the contributions from the three segments yields:

$$\frac{\bar{V}}{\Gamma_w/8\pi b} = \frac{R_{W1}+R_{W2}}{h_b^2\, R_{W1}R_{W2}} \left[b^2 - (R_{W1}-R_{W2})^2 \right] R_{W1_y} \quad \bar{i}$$

$$+ \left\{ \frac{2\,b}{h_2^2} \left(1 + \frac{X-X_w}{R_{W2}} \right) R_{W2_z} - \frac{2\,b}{h_1^2} \left(1 + \frac{X-X_w}{R_{W1}} \right) R_{W1_z} \right. \tag{4}$$

$$\left. - \frac{R_{W1}+R_{W2}}{h_b^2\, R_{W1}R_{W2}} \left[b^2 - (R_{W1}-R_{W2})^2 \right] R_{W1_x} \right\} \bar{j}$$

$$+ \left\{ \frac{2\,b}{h_1^2} \left(1 + \frac{X-X_w}{R_{W1}} \right) R_{W1_y} - \frac{2\,b}{h_2^2} \left(1 + \frac{X-X_w}{R_{W2}} \right) R_{W2_y} \right\} \bar{k}$$

The normal velocity at a point on the wall is constructed by taking the dot product of the induced velocity vector with the unit outer normal at that point. $V_n = \bar{V} \cdot \bar{n}$. The normal is constructed using the cross product of a unit vector in the downstream direction and a vortex ring vector lying in the Y - Z plane

$$\bar{n} = \frac{\bar{i} \times (\bar{R}_1 - \bar{R}_2)}{|i \times (\bar{R}_1 - \bar{R}_2)|}$$

The boundary condition is expressed at each control point by summing all the normal velocities due to the wall vortex rings and setting it equal and opposite to the normal velocity induced at the same point by the wing vortex. The result is expressed in a matrix equation

$$[A] \left\{ \Gamma \right\} = \Gamma_w \left\{ B \right\}$$

in which the $\{\Gamma\}$ are the unknown strengths of the wall vortex elements, and the matrix $[A]$ is fixed by the dimensions and shape of the tunnel and the locations of the vortex rings and control points. The column $\{B\}$ describes the influence of the lifting wing at the tunnel walls, and is developed from the dot product of Eq. (4) with the unit outer normal at each control point.

Because of the lateral symmetry assumed in writing Eq. (3), it is necessary only to take control points on one side of the tunnel. If the wing is also placed on the vertical ℄ and the tunnel is vertically symmetrical, then the Γ_i will also be symmetrical but of opposite sign. It is then necessary only to take control points in one quarter of the tunnel. The matrix $[A]$ is inverted, since it is fixed for a given tunnel shape, and the values of Γ_i may then be found for a variety of wing spans by changing only the column matrix $\{B\}$.

Once the Γ_i are known, the induced velocity due to the walls can be calculated at any point in the tunnel by the use of Eq. (3) summed over all the vortex rings in the tunnel walls. The interference is expressed as an angle whose tangent is the vertical component of interference velocity, w , divided by the tunnel wind speed, V . In the linear, undeflected wake case, the tangent is approximately equal to the angle. Results are expressed in terms of the classical interference factor δ , defined by the equation:

$$\Delta\alpha = \delta \frac{S_w}{C} C_L$$

The factor is computed in terms of wing circulation and vortex span

$$\delta = \frac{w \quad C}{2b \; \Gamma_w}$$

Results are presented graphically to show the longitudinal variation of the factor δ for different wing spans in a variety of tunnels. A computer program with instructions and card listing for the solution of the interference factor δ is given in Appendix C.

Results and Comparison with Classical Results

In order to test the validity of the method, it was compared with classical solutions where those were available. Results of calculations made for three representative tunnel shapes are presented in the form of graphs of the wall interference factor δ. Values of δ were calculated at points along the tunnel centerline from the wing location downstream for several values of wing vortex span. These are presented for a circular, a square, and a 3:5 rectangular tunnel in Figs. (10), (11), and (12). The average value of this interference factor over the vortex span of the uniformly loaded wing was also calculated and is shown as a function of vortex span for each of these tunnels along with the centerline values in Fig. (13).

Square tunnel.--Glauert's concept of an infinite array of images of the wing located outside the tunnel is applicable only to rectangular (including square) tunnels and has been applied by Silverstein and White in Ref. (14). Results are presented there for square and 2:1 rectangular tunnels; only the square tunnel results are used here for comparison, since 2:1 tunnels are not common.

The number of line segments, each corresponding to the side of a vortex square, to be used to adequately represent the square tunnel cross-section was determined by making a series of calculations with increasing numbers of segments. Fig. (14) shows the results of using 12, 16, and 20 segments to make up the periphery of the square cross-section. The results for 16 and 20 segments differ only slightly and correspond very closely to the data taken from Ref. (14). The excellent agreement shown indicates that 16 segments are enough to represent satisfactorily the square cross-section tunnel.

Circular tunnel.--In the case of the circular tunnel, no exact solution is available for the downstream interference factors, so two approximate results are compared with the new calculations in Fig. (15). The results presented by Lotz (Ref. 4) depend on the value of a truncated infinite series, and the reference gives no indication of the accuracy expected in its evaluation. The result taken from Silverstein and White (Ref. 14) was arrived at by following their suggestion that the downstream interference factors for the circular tunnel be taken as the same as for the square tunnel of the same area.

Four different approximations to the circular tunnel were used for this calculation. Two regular polygons having 12 or

16 sides were used for the cross-section shape; each was rotated so that either points or flats of the polygon were at the top and side centerline. All four calculations yielded the same curve, with values within one-tenth of one percent. Thus, it is concluded that a twelve-sided polygon is adequate to represent the circular tunnel.

Length effect. -- The effect of length of the tunnel to be used in calculations was explored for the circular tunnel. A twelve-sided polygon was used in the calculation, with the model vortex span equal to 0.4 of the tunnel diameter. It is evident from Fig. (16) that a length-to-diameter ratio of 3 or 4 is ample for convergence. The reason for this may be seen in an examination of the distribution of the wall vorticity. The bound vortex of the wing requires some circumferential vorticity in the walls, but only in the region quite near to the wing. Longitudinal vorticity is not required far upstream, and far downstream only longitudinal filaments exist to control the trailing pair from the wing. By using the artifice of a very long last ring, the proper conditions are met far downstream, and the vortex lattice need only be long enough to provide the circumferential vorticity needed in the immediate vicinity of the wing. In fact, all the vorticity in the circumferential rings is quickly transferred to the longitudinal filaments.

Figure (17) shows the wall vortex strengths taken from calculations made for circular tunnels of various lengths. The circumferential vorticity strengths were taken at the floor near the center of the tunnel where they are the strongest; the longitudinal vortex filament strength is that along the side wall at model height. It is evident that the details of the distribution are not strongly affected by the presence or absence of tunnel walls more than about one diameter up or downstream from the wing.

Conclusion

The excellent agreement shown by the examples presented verifies the hypothesis that the walls of the tunnel may be adequately represented by a rather coarse network of vortex rings. The advantage of this method is that any tunnel cross-section can be represented by using an equivalent polygon of 16 or more equal length sides arranged to approximate the actual geometry.

VI. THE FINAL SOLUTION

The solution for the wake trajectory in the wind tunnel is an iterative combination of the free air trajectory solution and the wind tunnel wall vortex lattice solution. The lifting system, represented by a horseshoe vortex, is placed inside a vortex lattice tube representing the tunnel, and is given an initial value of circulation strength and an undeflected wake. A solution is found for the wall vorticity exactly as described in the earlier section. The wake location is then found exactly as in the free air solution, with the exception that the velocities induced by the wall vorticity found for the undeflected wake are added to those induced by the wing on itself. After an equilibrium trajectory is found, a second solution for the wall vorticity is made with the wake in its deflected position, followed by a second iteration of the wake location. In general, the two systems do not interact strongly for the short span to tunnel size ratios one expects to use in testing of high lift systems; and so only two or three such cycles are usually necessary for convergence.

Determination of the Interference Factors

In order to find the total interference effect, one should compare the flow patterns of the system, operating at the same conditions, in and out of the tunnel. The same conditions, as used here, mean at the same circulation and remote velocity. When the solutions are complete, they yield the complete velocity field both in free air and in the tunnel, as well as the separate contributions to that field by the wall vortex lattice and the lifting system.

The interference velocities are then defined by stating that the difference between the velocity at a point in the tunnel and the velocity at the same point in free air is the total interference velocity. Both the horizontal and vertical components of the interference velocity should properly be considered, but because the moderate wake deflections of the examples considered here cause only very small longitudinal interference (3% in the extreme cases), only the effects of the vertical component are presented. The vertical component of the interference is felt as a change in the angle of attack so it is convenient to present the interference in those terms. Thus

$$\Delta\alpha = \alpha_{\text{tunnel}} - \alpha_{\text{free air}}$$

These angles are not small enough to allow the use of the small angle approximation so they are defined by their tangents.

$$\Delta\alpha = \tan^{-1}\left(\frac{V_y}{V_x}\right)_T - \tan^{-1}\left(\frac{V_y}{V_x}\right)_{F.A.}$$

This data is usually presented in terms of a value of δ defined by the equation

$$\Delta\alpha = \delta \frac{S_w}{C} C_L$$

but since we are comparing at equal values of Γ instead of C_L, we use the relation

$$C_L = \frac{2L}{\rho V^2 S_w} = \frac{2\rho\Gamma V b}{\rho V^2 S_w} = \frac{2\Gamma b}{V S_w}$$

Thus

$$\Delta\alpha = \delta \frac{2\Gamma b}{CV}$$

so that

$$\delta = \left[\frac{CV}{2\Gamma b}\right]\left[\tan^{-1}\left(\frac{V_y}{V_x}\right)_T - \tan^{-1}\left(\frac{V_y}{V_x}\right)_{F.A.}\right]$$

A computer program listing is given in Appendix D for the combined solution for the interference factor δ for a lifting wing with deflected wake in a closed tunnel.

Results

Calculations are presented for a plane wing, at lift coefficients approaching the maximum theoretically possible for an unpowered system. In order to achieve the highest wake deflection angles, the aspect ratio of sample calculations was taken at 3.0 so that high C_L/AR values could be attained.

The wing vortex span was taken as one half the tunnel width, and the tunnel had a rectangular test section of height to width ratio 1:1.5 .

Figure (18) shows the trajectory of the wake in free air and in the wind tunnel for the sample wing. The difference in location of the wake in the tunnel is evident. In Fig. (19) the value of the interference factor δ is shown as a function of $C_L/Æ$ at the location of the wing and for three tail locations assumed to be on the tunnel centerline.

The tail interference angle is taken as the difference between the interference angles at the wing and at the tail, and presented as the difference between the values of δ at these two points. Figure (19) also shows the tail interference factor $(\delta_t - \delta_w)$. This curve shows that, for the geometry chosen, the pitching moment corrections may become small or even negative at the higher lift coefficients.

In order to demonstrate the effect of the wake shift, Fig. (20) was prepared for comparison with Fig. (19). The same factors were calculated, but the contribution of the deflected wake was left out. The interference angle was calculated using only the velocities induced by the wall vortex lattice. The wake location as computed in the tunnel was used, so these results accurately represent interference velocities based upon only the wall induced effects. Figure (20) also shows the tail interference factors calculated using only the wall induced velocities. The importance of including the direct effects of the wake relocation is shown when Fig. (20) is compared with Fig. (19).

Tail location is an important parameter, for if the tail is initially below the vortex wake in free air, then the wake shift upward in the tunnel will accentuate the wall induced upwash. Figures (21) and (22) show this effect for tail heights of 0.2 and 0.4 times the vortex span below the wing, as well as the reversal which takes place when the wake moves past the tail location.

In the preceding examples the interference angle factors were calculated at fixed locations in the tunnel, and do not necessarily represent a physically realizable vehicle. The results can be interpreted to represent a tilt-wing type vehicle in which the body is constrained to a constant angle of attack.

For the case where body attitude changes, it is necessary to calculate and compare flow angles at the tail in free air with those in the tunnel at angles of attack appropriate for the same wing circulation. An example is presented in Fig. (23) for a case where wing and tail are fixed to a body and rotate as a unit. The tail is located above the plane of the wing (0.2 of the vortex span) and three tail lengths are shown. The interference factor shows a minimum where the tail passes through the height of the vortex wake. The large variations of the factor indicate the importance of accounting for the wake shift and for actual tail position.

VII. DISCUSSION OF RESULTS

In this section the results and their implications will be discussed in some detail. Some examples will be worked out showing how corrections would be made using these interference calculations, some of the difficulties encountered in making corrections, and how these difficulties may be resolved by modifying the test program. Additional discussion considers the adequacy of the mathematical model, computational problems, and suggestions for possible future modification or growth of this method.

Examples of Corrections of Test Data

The results presented in the previous section are in the form of the factors δ_w used to calculate the correction to the angle of attack at the wing, and $(\delta_t - \delta_w)$ used to calculate the difference in angle of attack at the tail from that at the wing. These values will be used here to compute examples of actual corrections that should be applied and show their effects on final data.

The factor δ_w is used to calculate the interference angle at the wing in the following formula

$$\Delta\alpha = \delta_w \frac{S}{C} C_L$$

where $\Delta\alpha$ is the increase in angle of attack at the wing caused by the restriction of downwash by the tunnel boundaries. For the examples presented earlier, the following values result. The wing has $AR = 3$ and its vortex span is one-half of the tunnel span. The wing area to tunnel cross section area ratio is then $2/\pi^2$, assuming a vortex span ratio of $\pi/4$. From Fig. (19), the value of δ_w is almost constant at the wing up to $C_L/AR = 0.5$ and is only changed by 10% out to C_L/AR approaching 1.0. The table shows values of the angle of attack interference at selected lift coefficients.

$C_L/\mathcal{R}$	C_L	δ	deflected wake		straight wake	
			$\Delta\alpha$ deg	ΔC_{D_t}	$\Delta\alpha$ deg	ΔC_{D_t}
0.0	0.0	0.111	0.0	0.0	0.0	0.0
0.5	1.5	0.115	2.01	0.0525	1.94	0.0507
0.7	2.1	0.120	2.93	0.1076	2.72	0.0995
0.9	2.7	0.130	4.08	0.1925	3.48	0.1642

The $\Delta\alpha$ shown is a correction to be added to the angle of attack measured in the tunnel. In free air the wing would have to be at the higher angle in order to produce the same lift as in the tunnel.

When the angle of attack is corrected the lift vector is rotated by the same amount. The effect of the rotation of the lift vector then causes a component of the lift to appear as an additional drag, the magnitude being equal to the lift coefficient multiplied by the interference angle in radians. This result is also shown in the table above.

If the wake was not deflected, the value of δ_w would be constant at all lift coefficients, and the corrections would have been smaller. The corresponding values of $\Delta\alpha$ and ΔC_{D_t} for the undeflected wake are also shown in the table. Comparison of the corrections shows that only small changes, of the order of 15% of the drag correction, are due to wake shift. Since the total drag correction is of the order of 25% of the induced drag at the highest lift coefficient, this change is less than 4% of the measured dra .

Calculating the difference in interference at the tail shows a more dramatic effect. In the normal case (undeflected wake and low $C_L/\mathcal{R}$) where δ_t and δ_w are constant over the range of C_L of interest, one calculates the difference in angle of attack at the tail and the wing caused by the interference and uses this angle to calculate a correction to the pitching moment. Since the tail experiences a greater interference angle than the wing, the moments measured in the tunnel are more negative for positive lift coefficients. Because the interference angles are proportional to C_L , the effect is to measure a larger negative value of the slope $d\,C_M/d\,C_L$ in the tunnel, making the model appear more stable than it would be in free air.

Because of the wake deflection, the tail angle correction will be different from what it would be without wake deflection. The curves of Fig. (19), (21), and (23) show this for three different examples.

To calculate the change in pitching moment requires knowledge of the characteristics of the horizontal tail. For an example calculation let us assume that the tail length is equal to the vortex span, the tail volume coefficient $\overline{V}_h = 1.0$, the tail aspect ratio is about the same as the wing, and has a lift curve slope of π/radian. Then the correction to the pitching moment would be

$$\Delta C_M = \frac{dC_M}{d\alpha_t} (\Delta\alpha_t - \Delta\alpha_w)$$

where

$$\frac{dC_M}{d\alpha_t} = \left(\frac{dC_{L_t}}{d\alpha_t}\right) \overline{V}_h \; \eta_t$$

$$(\Delta\alpha_t - \Delta\alpha_w) = (\delta_t - \delta_w) \frac{S}{C} C_L$$

and

$$\eta_t = q_t/q$$

Then, using the assumed values,

$$\Delta C_M = \pi\left(\frac{2}{\pi^2}\right) (\delta_t - \delta_w)\, C_L$$

The following table compares the corrections for the several cases with those expected when the wake goes straight back and the tail is at wing height. In the tilt wing case, the tail remains fixed at wing height while the wing rotates to increase lift. The column headed low tail is also a tilt wing, but the tail is fixed in the tunnel at 0.2b below the wing height. In the moving tail case, the tail is assumed attached to the wing at 0.2b above the plane of the wing, and moves as the wing rotates in the tunnel.

C_L	straight wake ΔC_M	tilt wing ΔC_M	low tail ΔC_M	moving tail ΔC_M
0.0	0.0	0.0	0.0	0.0
0.9	0.0636	0.0522	0.805	0.062
1.5	0.105	0.0679	0.1482	0.134
2.1	0.147	0.0535	0.209	0.268
2.7	0.189	0.0	0.2325	

The tabulated values are plotted in Fig. (24) to show the correction to the pitching moment coefficient for the several cases. If the wake is not deflected, the interference would be proportional to C_L as shown, and the apparent interference is just a change in the stability derivative, dC_M/dC_L, of the aircraft. For the case shown this amounts to a change in that derivative of $\Delta \frac{dC_M}{dC_L} = 0.07$ and is interpreted as a change in the location of the center of gravity for neutral stability of 7% of the wing mean aerodynamic chord.

The other cases are not as simple. The effect of the wake shift changes the correction very much and how it does so is a function of the exact location of the tail with respect to the wing. For the case where the wing tilts and the tail stays fixed in the tunnel at the height of the wing, the total interference may be seen to be the same as for the undeflected wake at low C_L, but reach a maximum and decline to zero at high C_L. If the tail is lower than the wing, the wake shift effect causes the interference to be larger than in the undeflected case because the wake moves closer to the tail. In the case where the entire aircraft rotates so that the tail starts above the wake and moves past it, the curve shows a reversal of initial trend and finally deviates very markedly from the no-deflection case.

The tilt-wing case is perhaps the most interesting of the three cases. At low C_L values, the corrections are identical to those for the undeflected wake, and the stability level in the tunnel is apparently too high by $\Delta \frac{dC_M}{dC_L} = -0.07$. At about $C_L = 1.5$, the interference effect is now constant, so the apparent stability is the correct value. However, a constant ΔC_M is introduced which corresponds to a change in stabilizer angle of about 1.24°. At $C_L = 2.7$ no correction in stabilizer angle will be required, but the apparent stability is now less than the correct value by $\Delta \frac{dC_M}{dC_L} = 0.13$. The effect of this change in pitching moments is to move the location of the neutral point a distance of 20% of the wing chord over the range of available lift coefficients. This is about the same as the usual allowable movement of the center of gravity of a normal aircraft.

These three cases taken together show that the fact that the wake does move with respect to the tail causes the pitching moment interference to vary widely; in the examples, from zero to nearly twice the values calculated in the usual way assuming no wake deflection and tail fixed on tunnel centerline. Because of this wide variation it is not possible to generalize on the results beyond saying that the interference is dependent on the configuration of the aircraft and the wind tunnel, and must be calculated for each case. Because the variations of interference are of the same order as the linear interference and may be of either sign, they are certainly too large to be ignored.

Difficulties in Application

Actual application of these interference calculations is not as easy as presented above, particularly with respect to the computation of the pitching moment correction. As this correction was presented earlier, it was presumed that the tail effectiveness was represented by the derivative $d C_M/d\alpha_t$ and that this value was a constant. In the normal airplane this is often so, but in the case of the STOL aircraft one cannot make that assumption. The specific difficulties are that the local flow angles may be so large that the lift curve slope $dC_L/d\alpha_t$ is in a nonlinear range, and that the dynamic pressure at the tail may not be anywhere near the free stream value due either to being immersed in low energy wakes from wing flaps or high energy wakes from propulsion devices. Consequently, it is usually advisable to measure separately the tail effectiveness by making several runs at different stabilizer angle settings and computing directly from this data the values of $dC_M/d\alpha_t$ over the range of lift coefficients of interst. This much is often done in ordinary wind tunnel work and is even more important in the testing of STOL aircraft.

An additional consequence of the wake shift is now apparent. The energy wakes are shifted in position and so are likely to change the dynamic pressure at the tail. While the process described above of measuring the tail effectiveness derivative will allow correction under the conditions of test in the wind tunnel, these are different from free air conditions. What is desired is that the tail in the wind tunnel be placed in the same air conditions that it would experience in free flight. Since the wake in the tunnel is in a different place than in free air, the tail should be moved to occupy the same position with respect to the wake.

The present method allows one to calculate in advance of the test program what the wake shift will be for each value of the wing circulation. A model could be constructed so that the tail height would be adjustable. Stability testing would then be done at several positions of the tail to produce a family of curves of pitching moment, each one of which will be valid for a given lift coefficient, and final data will be a composite curve taking data from the several curves at the appropriate points. If the wake shifting of the air impinging on the tail is the same as that of the vortex cores, and the tail is moved that amount, then the wake shift effect on the tail moment correction is reduced to zero and only the wall-induced effects would be necessary. Variations of induced velocity across the span of a model are not large (of the order of 10% or less) for models less than two-thirds of the tunnel width, and so this method appears to have promise.

Another uncertainty in the application of these interference results stems from the estimate of the vortex span and the resulting value of the circulation strength which is calculated using the Kutta-Joukowski law. It is apparent that this value should be estimated rather carefully before applying interference corrections to the data. It may be desirable to make some attempt to measure it directly by locating the vortex trajectory in the tunnel. It should be mentioned in passing that this is not a new problem and it has always been necessary in applying classical corrections to make this estimate: because the corrections are larger at higher lift coefficients, the estimate is more important.

Discussion of Accuracy and Computation Method

It will have become apparent in the above discussion that the quality of the interference calculation depends on the representation of the lifting system and the resulting accuracy of the free air flow fields. It is recognized that, if one could actually predict the real flow fields with a high degree of accuracy, the wind tunnel would no longer be necessary; and that, if the accuracy is poor, the interference calculation will have little value. This statement is not as contradictory as it may seem, because there is a difference between the detailed effects felt in the near field and the gross effects in the far field. Regardless of how it may be produced, lift is a result of the generation of circulation about some location fixed in the flow field. Consequently, if lift is measured and the vortex span carefully estimated or measured, the induced effects at points as far away as the tunnel walls are very well predicted by the Biot-Savart law.

A wind tunnel program is designed to measure more detailed effects, particularly those due to local flow separation and those due to mutual interference of the components of the aircraft on each other. No one at this time realistically expects to be able to predict these complex events and so replace the wind tunnel with a computer. Since the interference calculations presented here depend only on the gross induced effects, the accuracy should be adequate for the purose. The representation of the model may be improved as much as desired by superposition of additional vortex systems, and should be modified for other configurations, but the effects at the tunnel wall, and therefore the wall vorticity and the resulting induced velocities, will not be changed very much. What such improvement and modification will do is account more accurately for the direct effect on pitching moments due to wake shift. Certainly such work should be done, but the wide variety of arrangements possible preclude any generalization in advance and so it will be done on an <u>ad hoc</u> basis.

Some remarks are in order on the convergence of the numerical solution, and the instabilities expected in it. Any difficulties to be found would be expected in situations where the wake was forced to curve most sharply, and this would be when the wing is inside a tunnel and operating at the highest lift coefficients. A detailed study was made of such a trajectory over seven iterations for the aspect ratio 3 wing at C_L/AR about 1 . Two regions of the wake were selected which exhibited the two areas of concern -- instability and convergence.

It was expected that in regions of sharp curvature the self-induced effects of adjacent segments of the vortex, made somewhat unreal by being broken up into short straight sections and aggravated by round-off errors, would initiate local curvature anomolies and cause the solution to degenerate.

This effect did indeed appear as a wavy motion of the segments alternating around a mean line. Two or three such zig-zags appeared in the second and third iterations and about twelve segments were involved in the seventh. The amplitude of these motions grew slowly and did not reach 20% of the length of the segments until the seventh iteration. This corresponded to a deviation of the segment direction of 13° or less from a mean line drawn through them. These waves disappeared, in the seventh iteration, at about one wingspan downstream from the wing where the slope of the trajectory had become nearly constant. The effects of these small changes of direction were judged to be negligible and so no smoothing sub-routines were used.

Convergence was examined at a point one vortex span downstream from the wing where the trajectory of the vortex line was straight over a length of about one span. The locus of points of intersection of the vortex line and the tunnel cross section was found to be a spiral over the seven iterations. Convergence was approximately logarithmic with each motion from one iteration to the next being one-half to one-third of the previous one. Thus, the convergence is so rapid that the fifth iteration moves the wake less than 1% of the wingspan.

One concludes from the above that the solution is quite well behaved and no conflict exists between convergence and stability. Acceptable convergence is had at the fourth iteration, and the growing instability is still acceptable at the seventh, leaving a wide region of choice for the user.

Future work could well be done on approximate methods of predicting wake deflection; for example by choosing a general form for the trajectory curve, and finding its amplitude at only a few points. Certainly other approximations will suggest themselves.

The results presented here, and the method of approach, appear to provide as near to an exact solution as is likely to be found, and may be used as a standard to which approximate and more convenient methods may be compared.

VIII. CONCLUSIONS

The problem of determining the wind tunnel wall interferences for high lift wings or lifting systems for slow flight has been examined, and a new method of calculating the interference effects has been developed. It has been shown that the most significant interference is on the measured pitching moments and the apparent longitudinal stability of an aircraft having a tail, or at least having a longitudinal characteristic dimension of the order of its spanwise dimension. The interference is a maximum when the system is operating at moderate downwash angles which are attainable with lifting systems using only small amounts of power and which can be represented by passive systems in potential flow.

The solution developed is based on the use of a vortex lattice to represent the tunnel boundaries, and takes into account the direct effect of the interference-caused relocation of the vortex wake on the flow direction in the region of the tail. A method of testing is proposed which can minimize this effect.

The following conclusions may be stated.

1. Representation of the wind tunnel boundaries by a vortex lattice system may be used to calculate interference velocities for a tunnel of arbitrary cross-section.

2. Simplified representations of lifting systems may be used. The vortex span and point of origin of the trailing system are the most important choices.

3. Wall induced velocities cause the vortex wake and high or low energy wakes to be deflected less in the wind tunnel than in free air.

4. The relocated vortex and energy wakes cause different flow angles and velocities to be felt at the region of a tail and these effects are properly charged to tunnel boundary interference along with the wall-induced velocities.

5. The direct effect of the vortex wake shift on a tail may be of the same order as the usual wall-induced velocities and may be of either sign.

6. The amount and direction of wake shift effects depends strongly on the tail location and so

effects must be calculated for each configuration of interest.

7. Wake shift effects may be reduced or avoided by testing with models whose tail heights can be adjusted to match the energy and vortex wake locations for particular regions of interest.

8. The numerical calculation presented converges rapidly (in about three to four iterations), but may develop instabilities if carried beyond seven or eight such iterations.

9. The quality of the solution presented is as near an exact solution as practical representation of a lifting system will permit, and should serve to guide the formation of approximations and as a standard to evaluate them.

REFERENCES

1. Anscombe, A. and Williams, J., "Some Comments on High-Lift Testing with Particular Reference to Jet Blowing Models," Agard Report 63, August 1956.

2. Prandtl, L., Tragflugeltheorie, Vol. II, C, Gottingen Nachrichten, 1919.

3. Glauert, H., "The Interference of Wind Channel Walls on the Aerodynamic Characteristics of an Aerofoil," R. & M. No. 867, British A.R.C., 1923.

4. Lotz, Irmgard, "Correction of Downwash in Wind Tunnels of Circular and Elliptic Section," T.M. No. 801, NACA, 1936.

5. Heyson, Harry H., "Linearized Theory of Wind Tunnel Jet Boundary Corrections and Ground Effect for VTOL/STOL Models," NASA TR R-124, 1962.

6. Heyson, Harry H. and Grunwald, Kalman J., "Wind Tunnel Boundary Interference for V/STOL Testing," Conference on V/STOL and STOL Aircraft, NASA SP-116, 1966, pp. 409-434.

7. Grunwald, Kalman J., "Experimental Study of Wall Effects and Wall Corrections for a General-Research V/STOL Tilt-Wing Model with Flap," NASA TN D-2887, 1965.

8. Staff of Powered-Lift Aerodynamics Section, NASA Langley Research Center, "Wall Effects and Scale Effects in V/STOL Model Testing," AIAA Aerodynamic Testing Conference, March 1964, pp. 8-16.

9. Hickey, D. H. and Cook, W. L., "Correlation of Wind-Tunnel and Flight-Test Aerodynamic Data for Five V/STOL Aircraft," Agard Report 520, October 1965.

10. Helmbold, H. B., "Limitations of Circulation Lift," Reader's Forum, Journal of the Aeronautical Sciences, Vol. 24, No. 5, March 1957, pp. 237-238.

11. Rae, William H., Jr., "Limits on Minimum-Speed V/STOL Wind-Tunnel Tests," Journal of Aircraft, Vol. 4, No. 3., May-June 1967.

12. Spreiter, John R. and Sacks, Alvin H., "The Rolling Up of the Trailing Vortex Sheet and Its Effect on the Downwash Behind Wings," Journal of the Aeronautical Sciences, Vol. 18, No. 1, January 1951.

13. Heyson, Harry H. and Katzoff, S., "Induced Velocities Near a Lifting Rotor with Non-Uniform Disk Loading," NASA Report 1319, 1957.

14. Silverstein, A. and White, J. A., "Wind-Tunnel Interference with Particular Reference to Off-Center Positions of the Wing and to the Downwash at the Tail," T.R. No. 547, NACA, 1935.

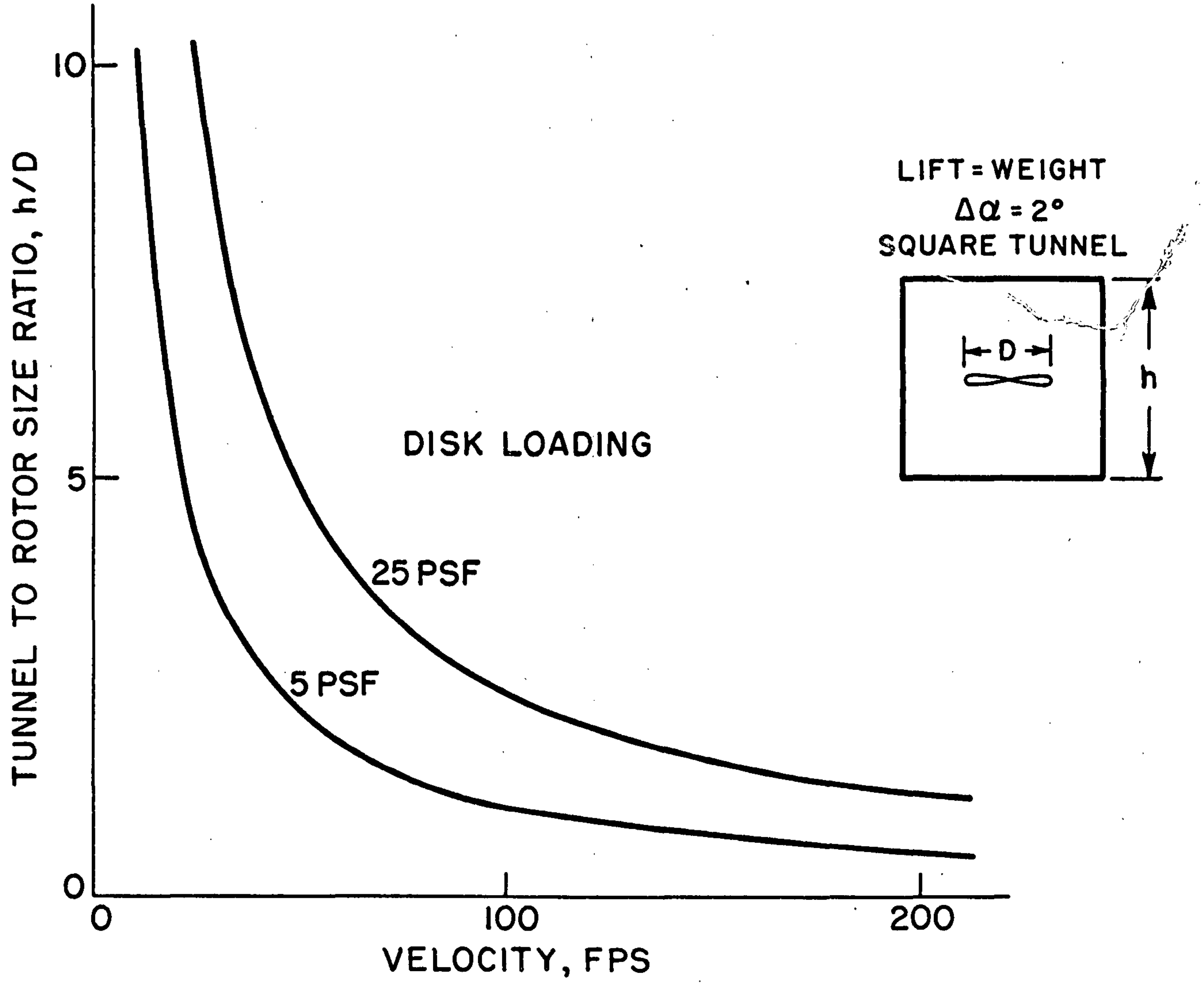

Fig. 1 Tunnel size required to limit wall interference to 2°.

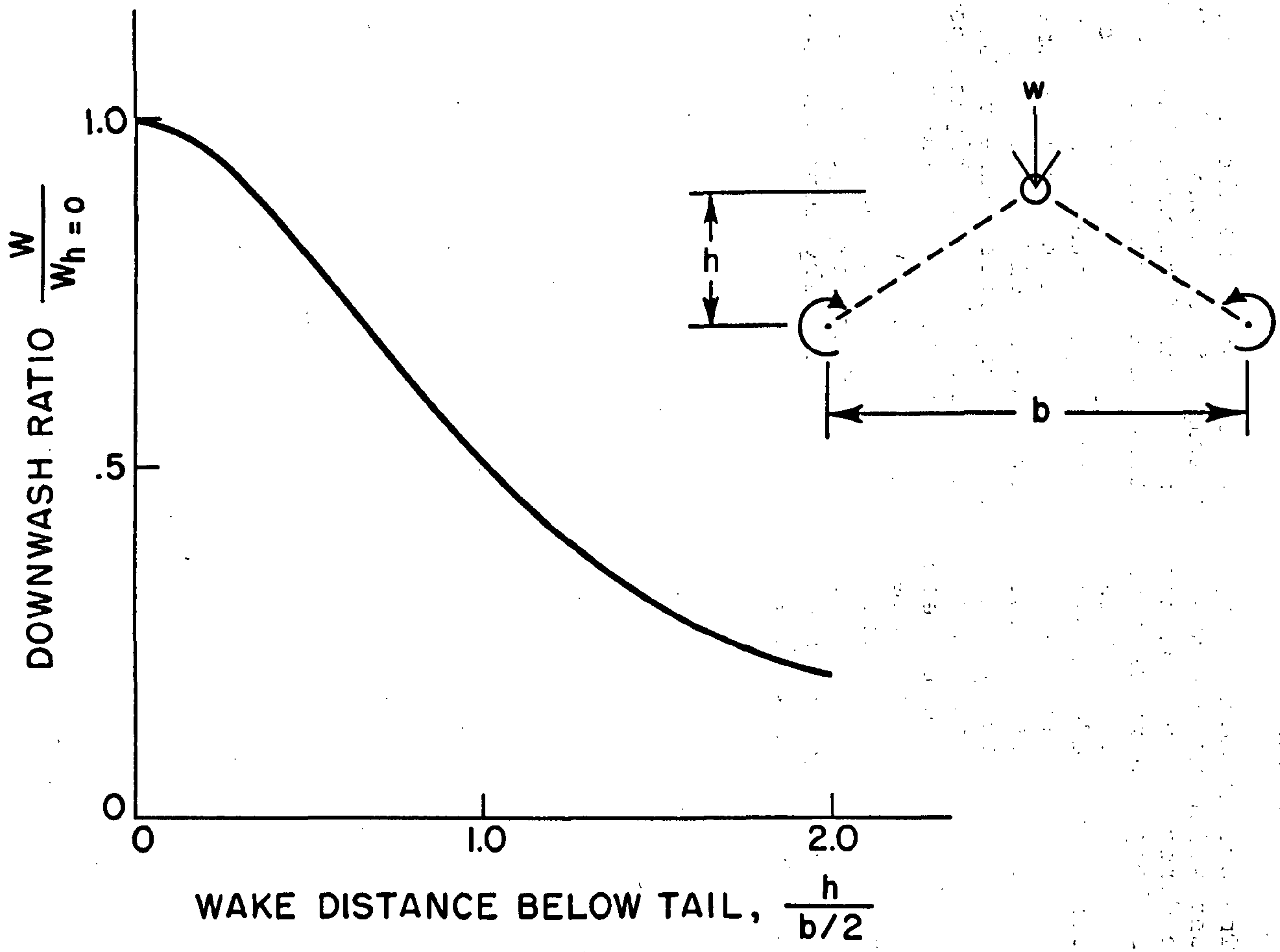

Fig. 2 Downwash at a tail location due to a displaced wake.

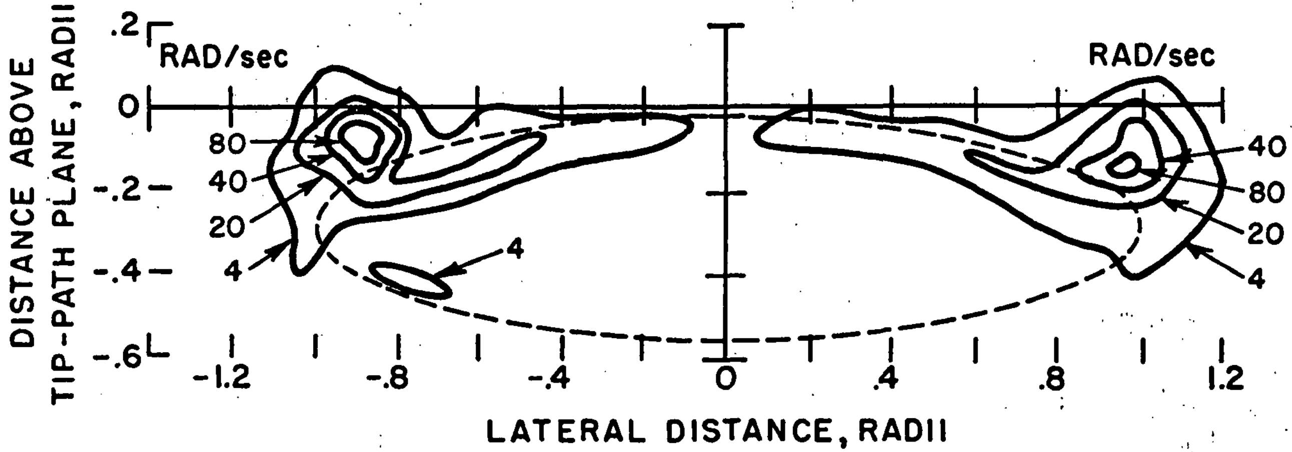

Fig. 3 Vorticity distribution at 7% of radius behind a rotor. Momentum angle is 15°.

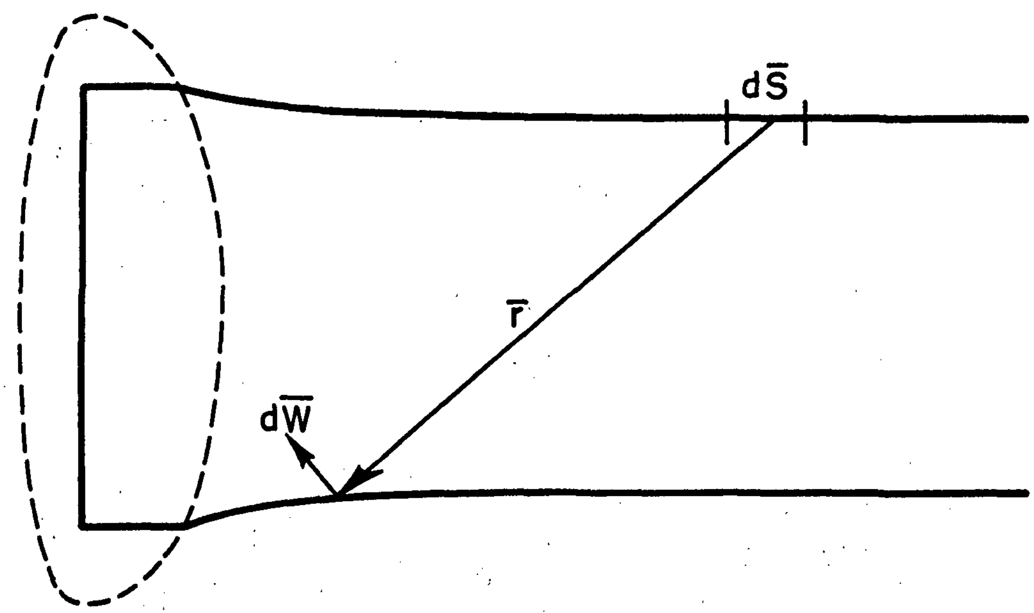

$$d\bar{W} = \frac{\Gamma}{4\pi} \frac{d\bar{S} \times \bar{r}}{|\bar{r}|^3}$$

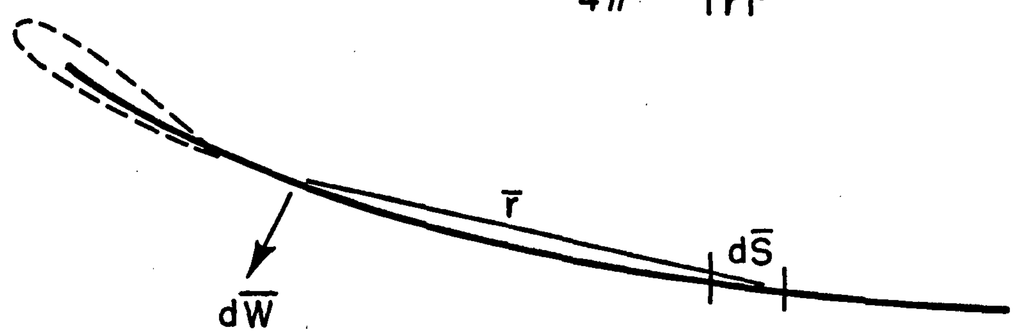

Fig. 4 Velocity induced at a point by a vorticity element.

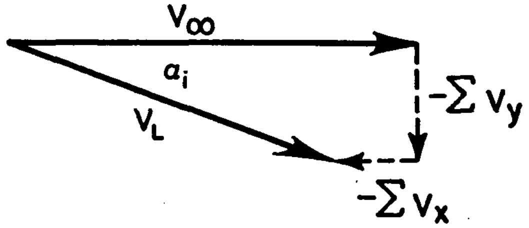

$$\text{Tan } \alpha_i = \frac{\Sigma V_y}{V_\infty + \Sigma V_x}$$

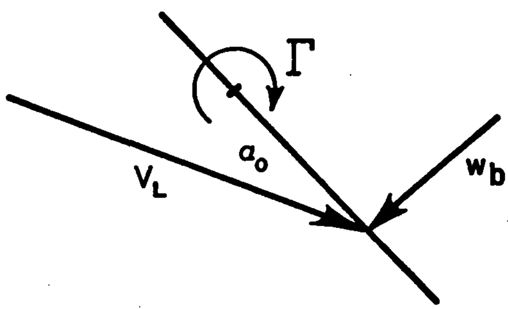

$$\text{Sin } \alpha_o = \frac{w_b}{V_L}$$

Fig. 5 Flow geometry at the wing.

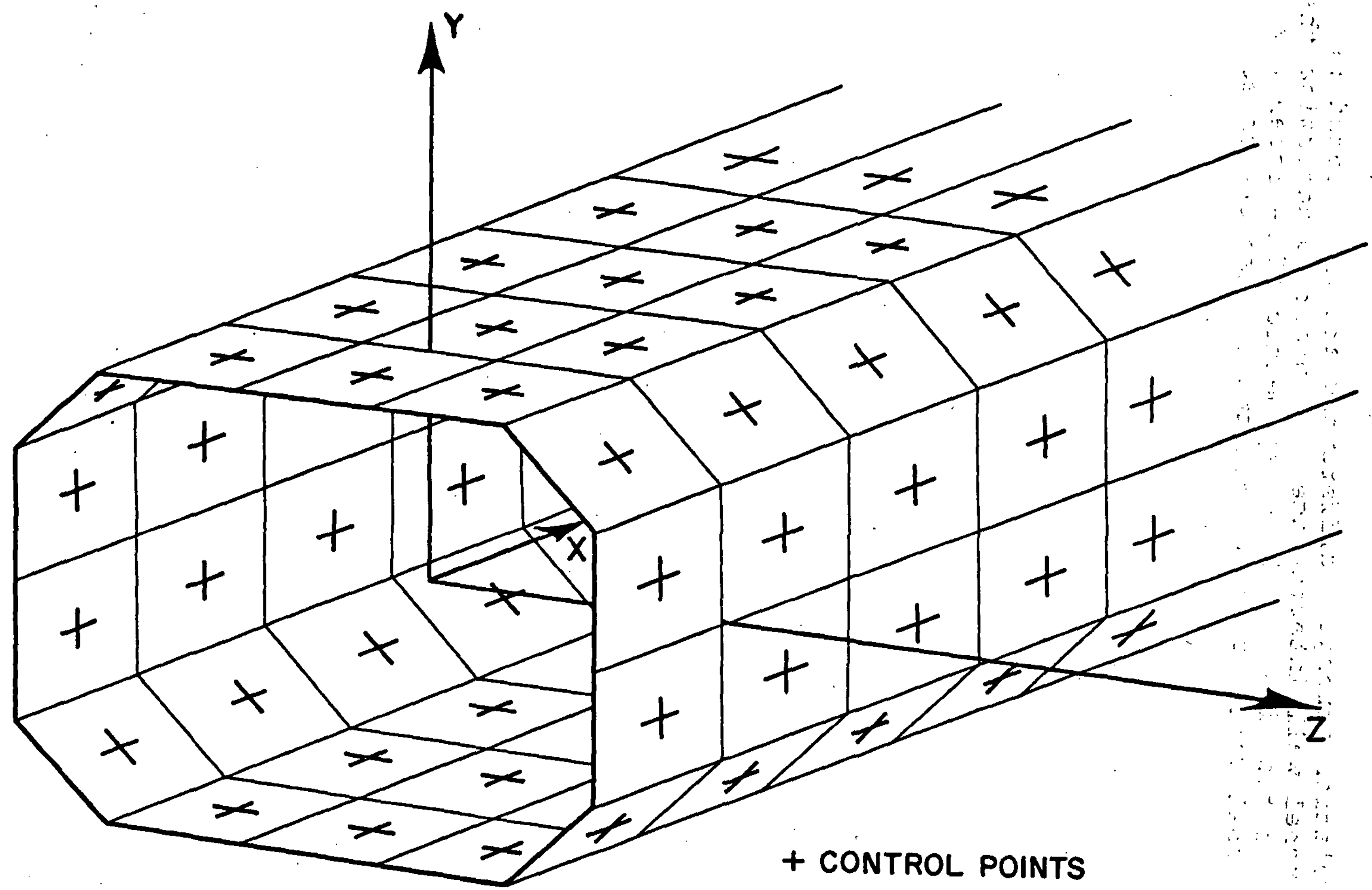

Fig. 6 Representation of a rectangular tunnel with corner fillets by a vortex lattice of square vortex rings lying in the tunnel walls.

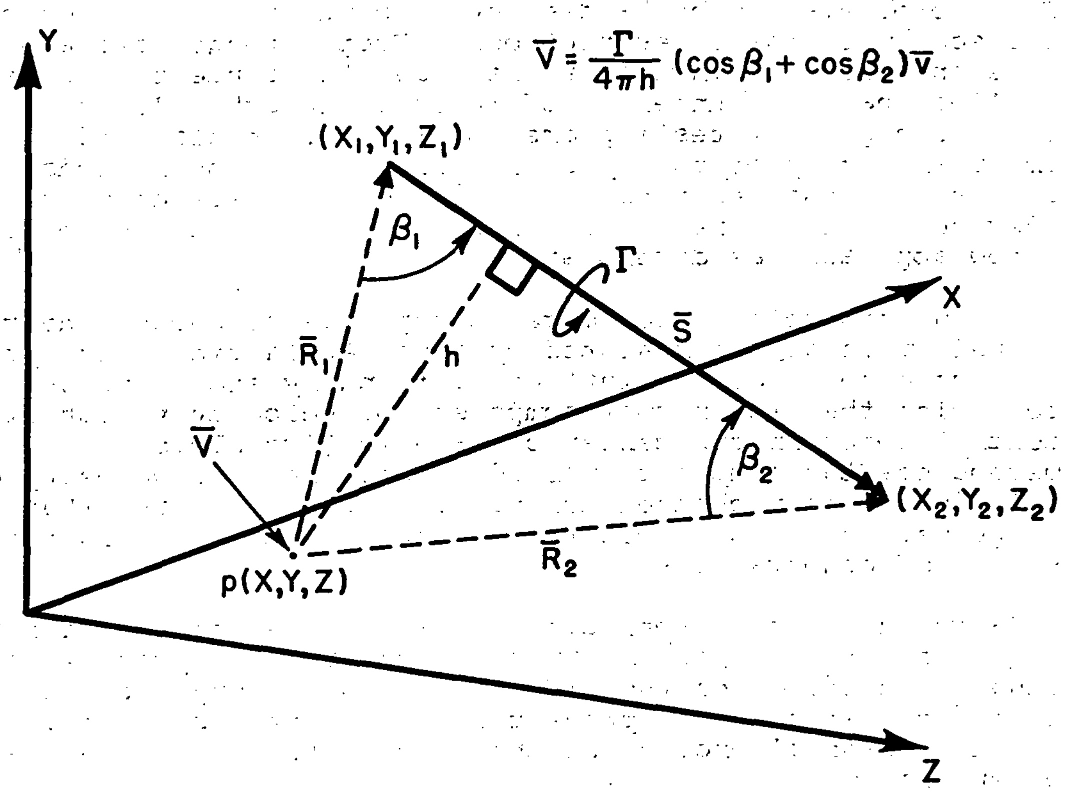

Fig. 7 Velocity induced at a point by an arbitrarily oriented vortex segment.

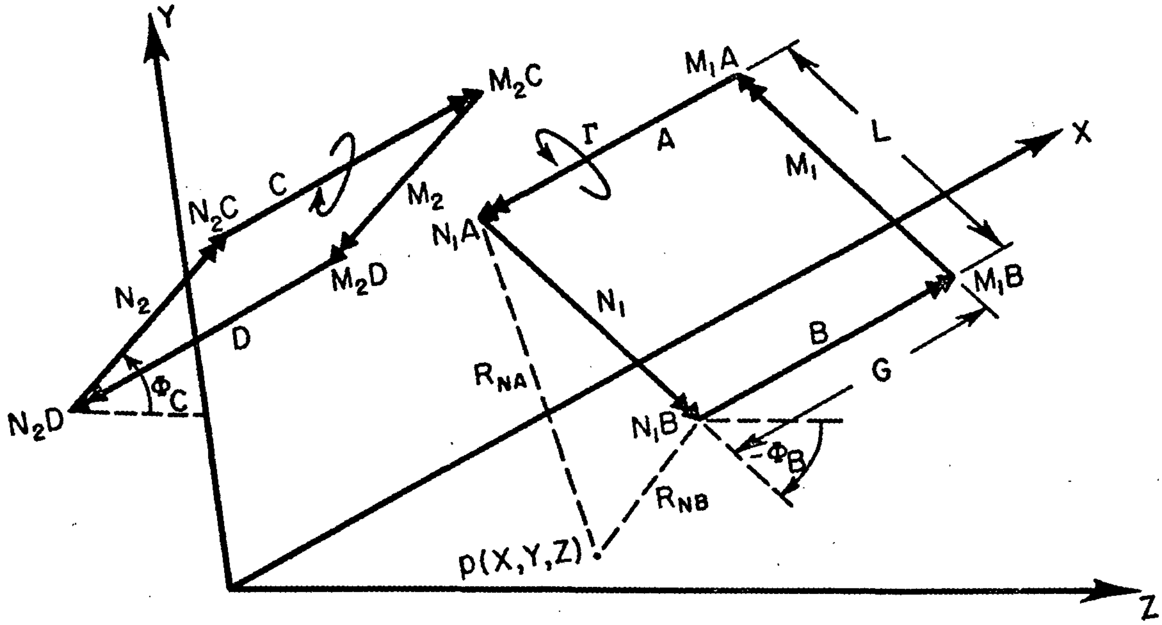

Fig. 8 Definition of angles and distances for a pair of vortex squares oriented symmetrically about the X,Y plane.(Elements A,B,C,and D are parallel to the X-axis)

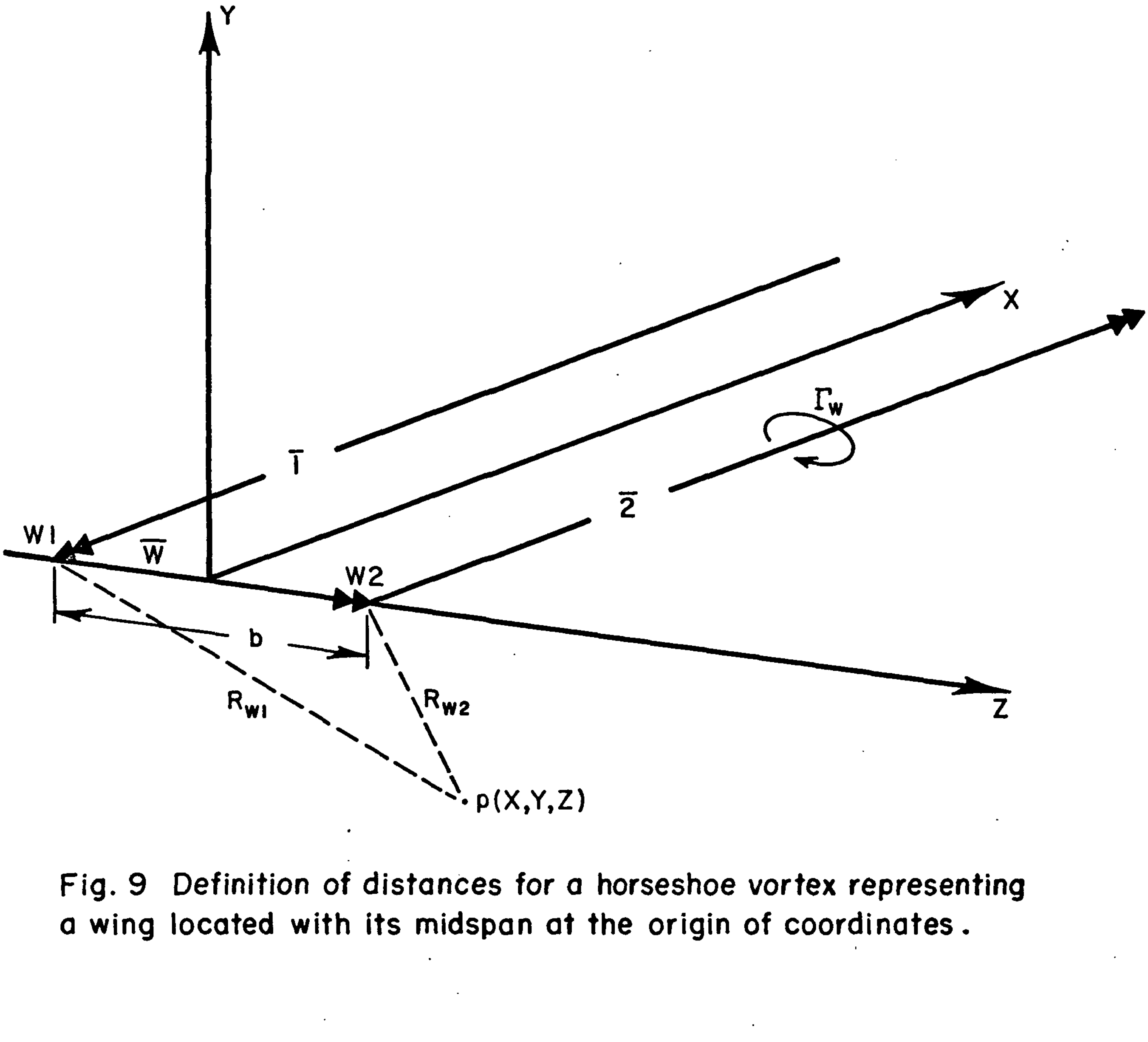

Fig. 9 Definition of distances for a horseshoe vortex representing a wing located with its midspan at the origin of coordinates.

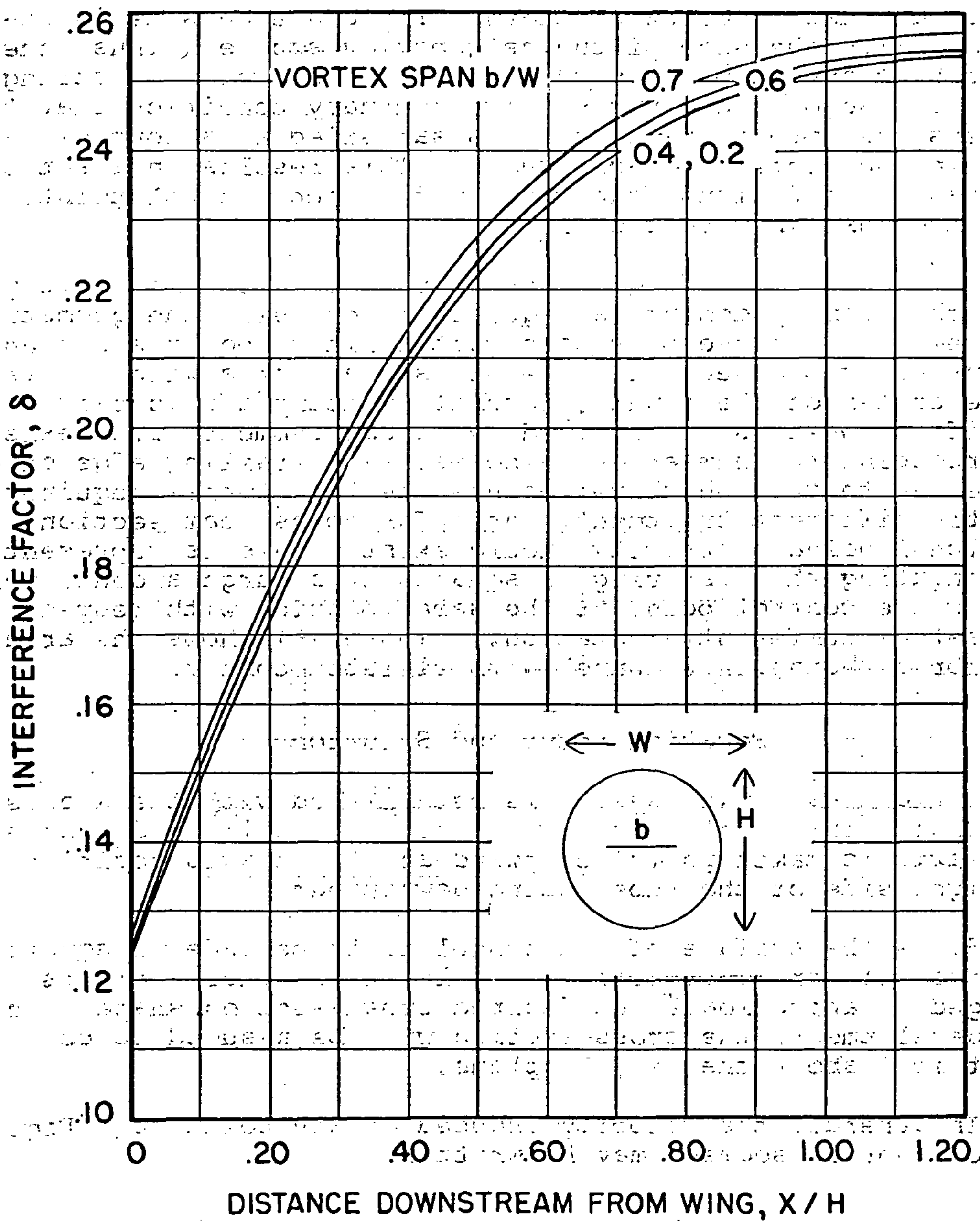

Fig. 10 Wall interference factors for a circular wind tunnel.

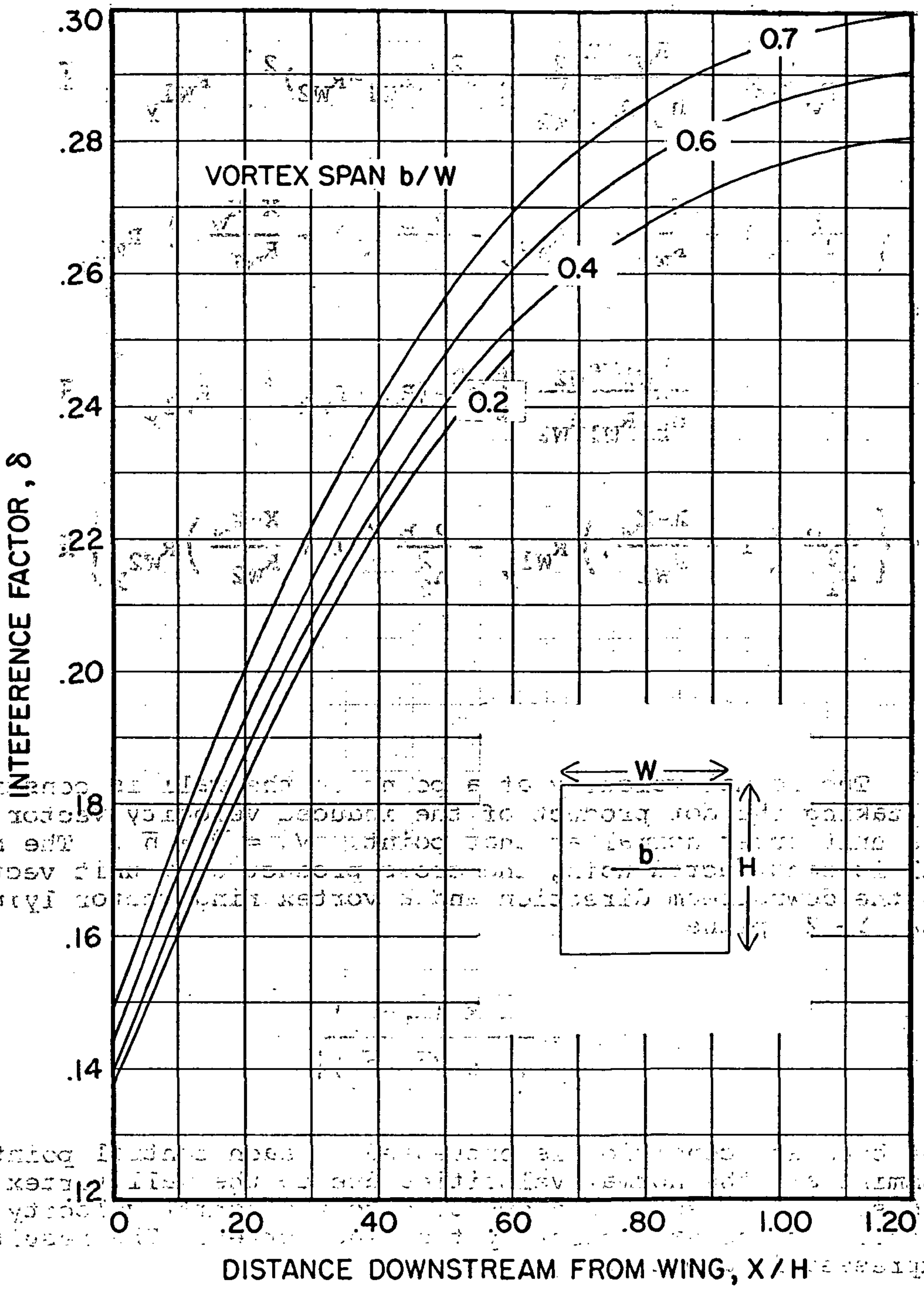

Fig. 11 Wall interference factors for a square wind tunnel.

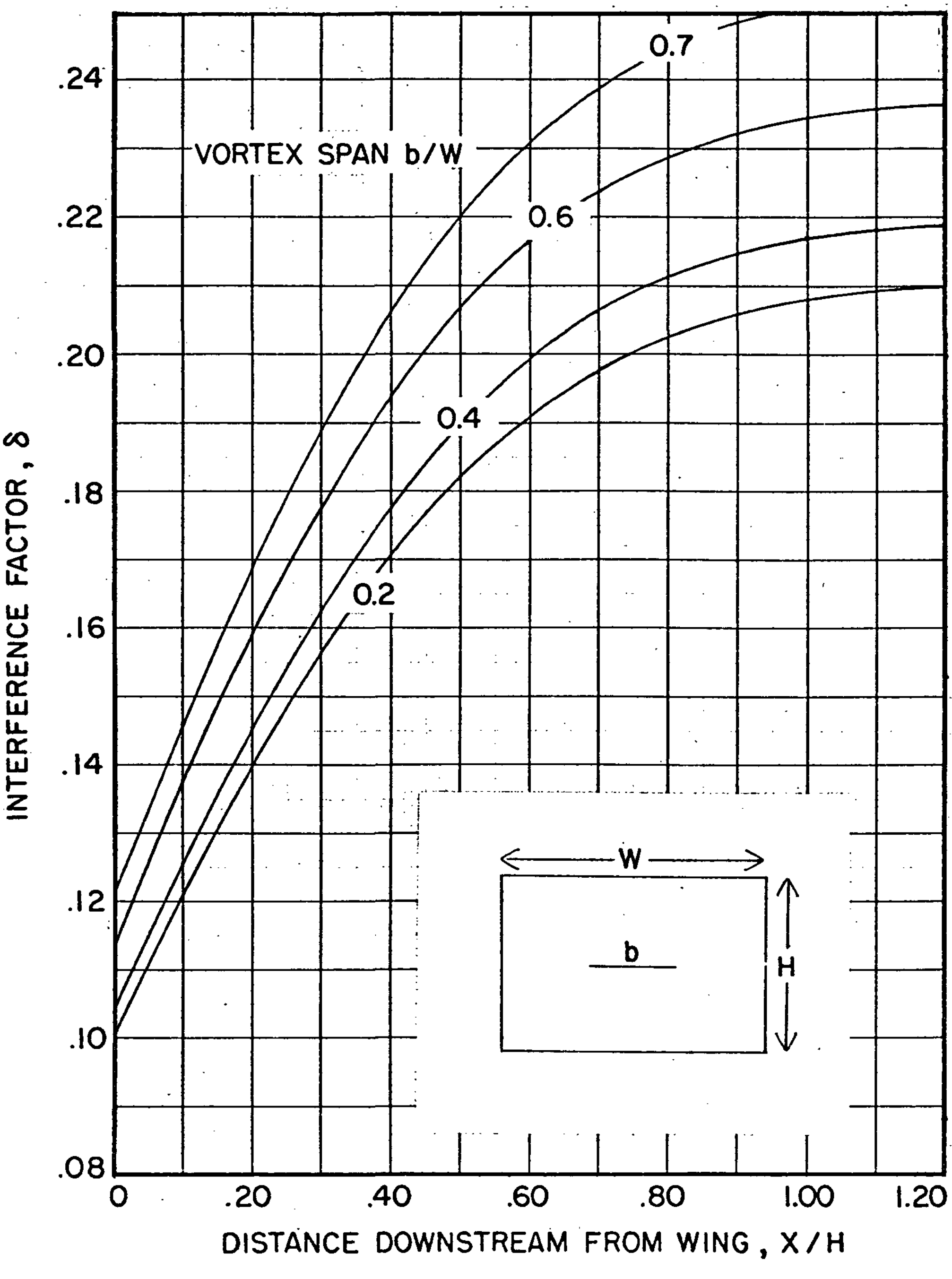

Fig. 12 Wall interference factors for a 3:5 rectangular wind tunnel.

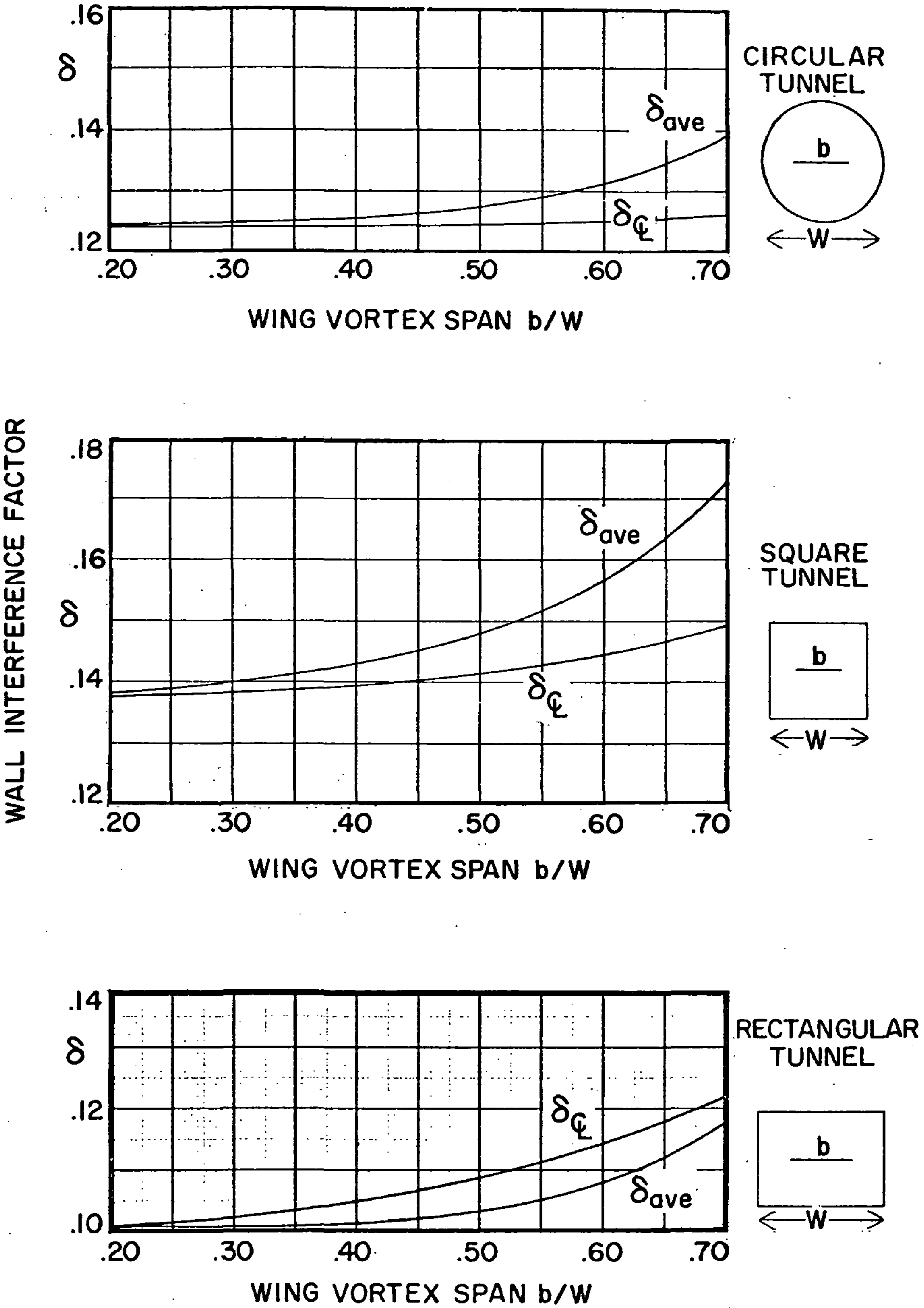

Fig. 13 Effect of wing span on average interference factor and the centerline interference factor at the wing.

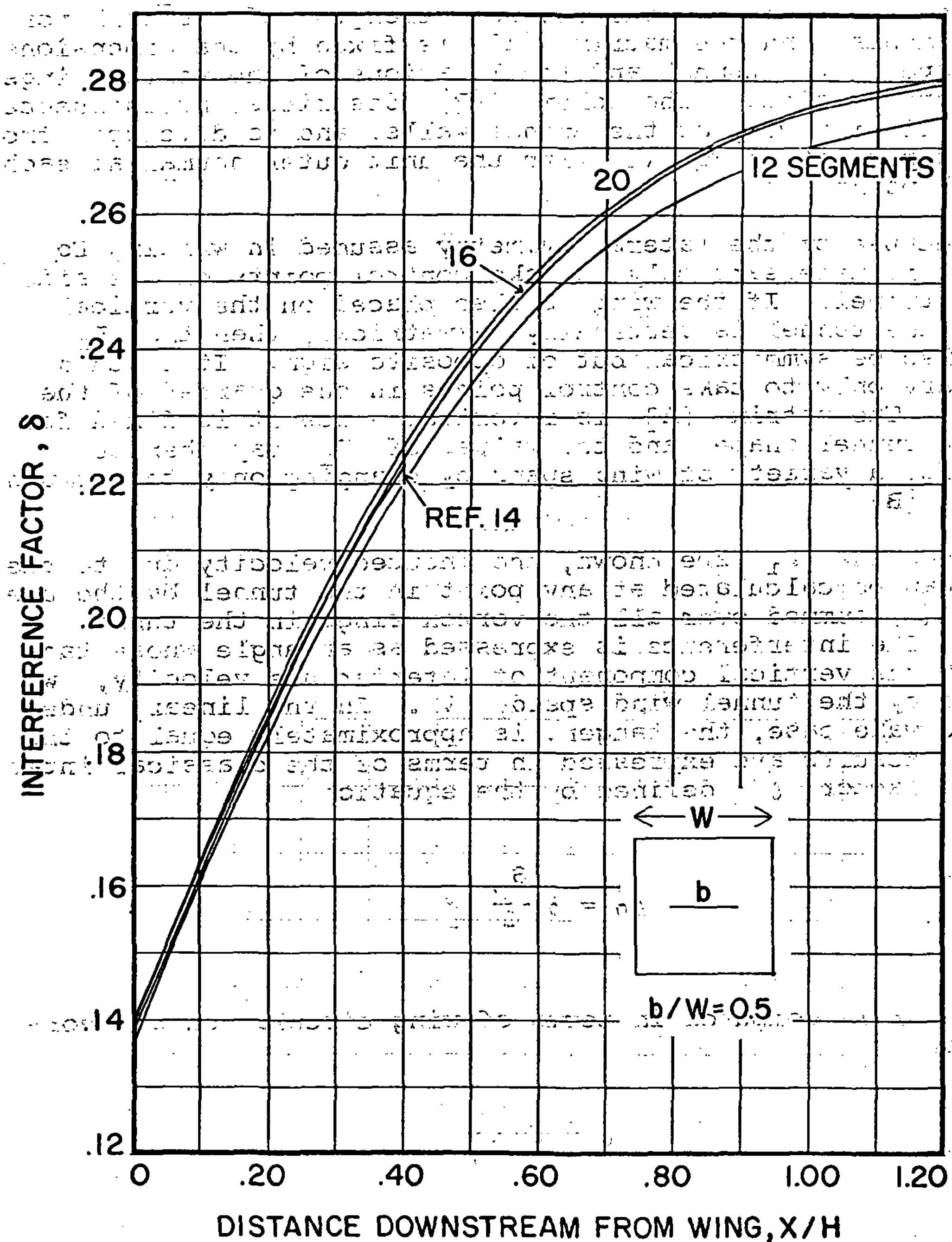

Fig. 14 Comparison of interference factors with classical values for a square tunnel.

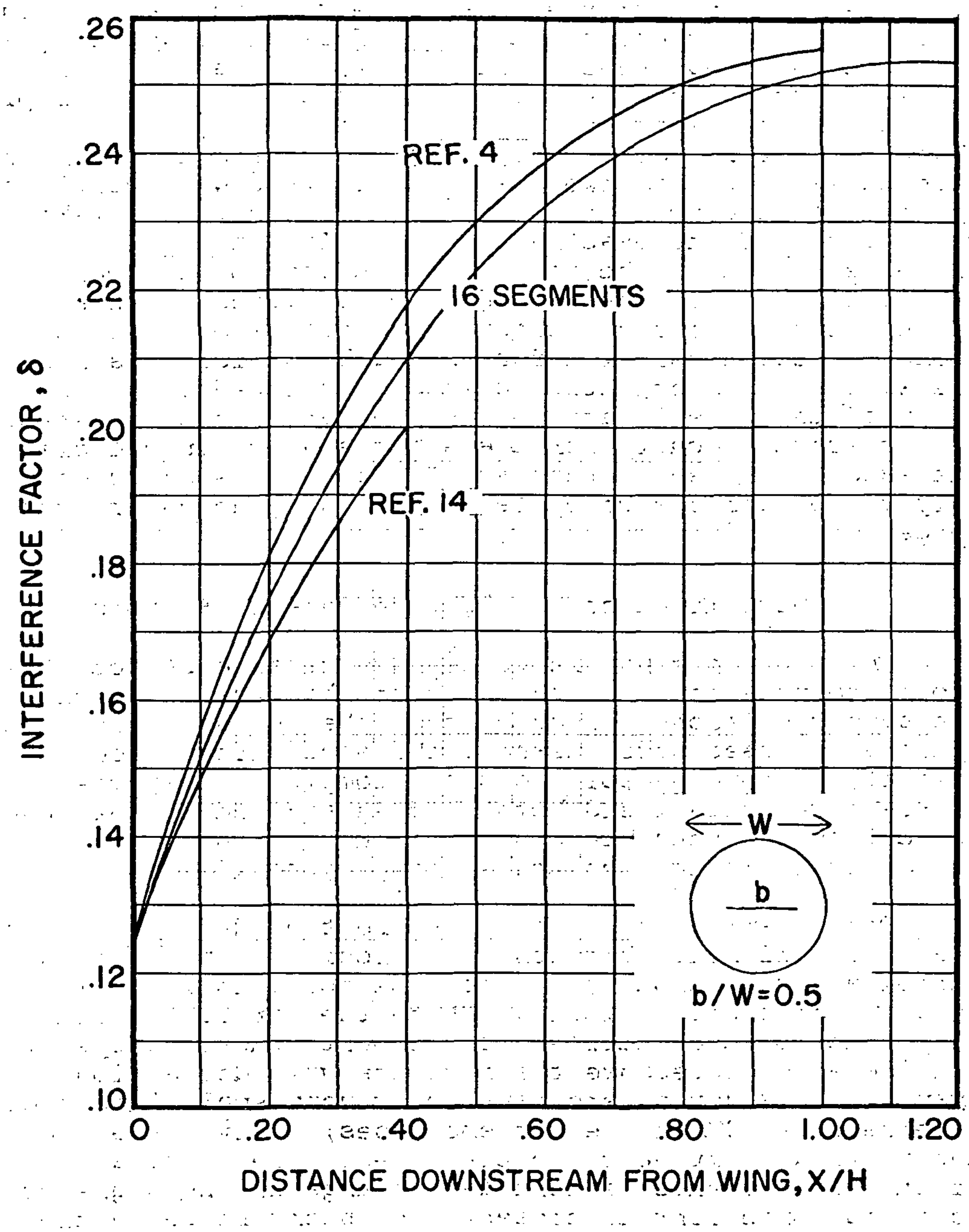

Fig. 15 Comparison of interference factors with classical values for a circular tunnel.

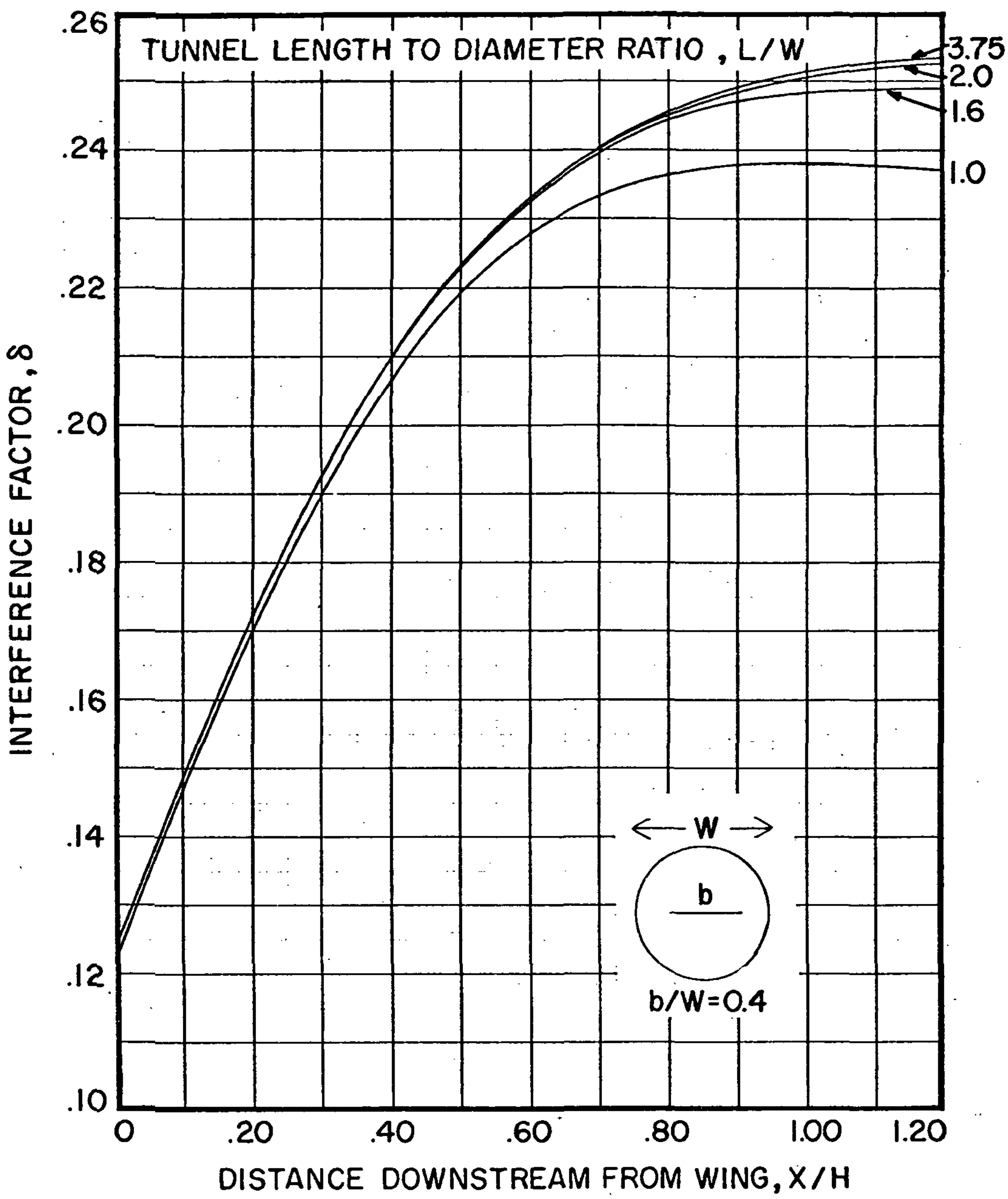

Fig. 16 Effect of tunnel length on interference factors for a circular tunnel.

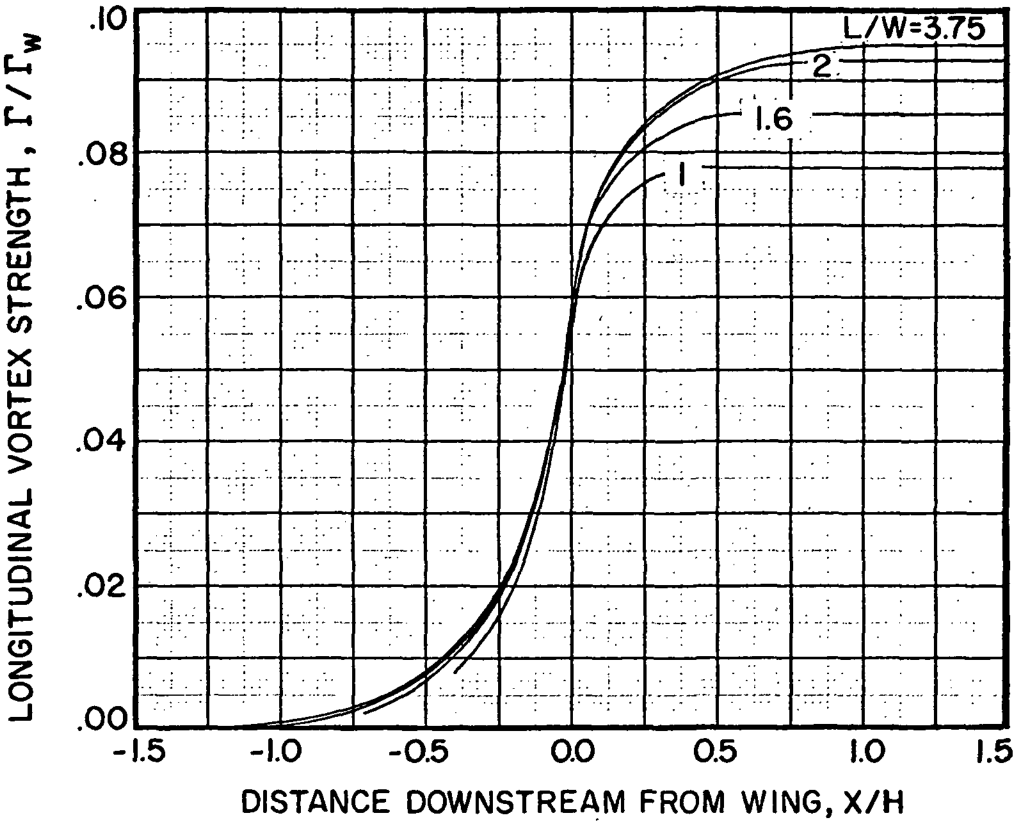

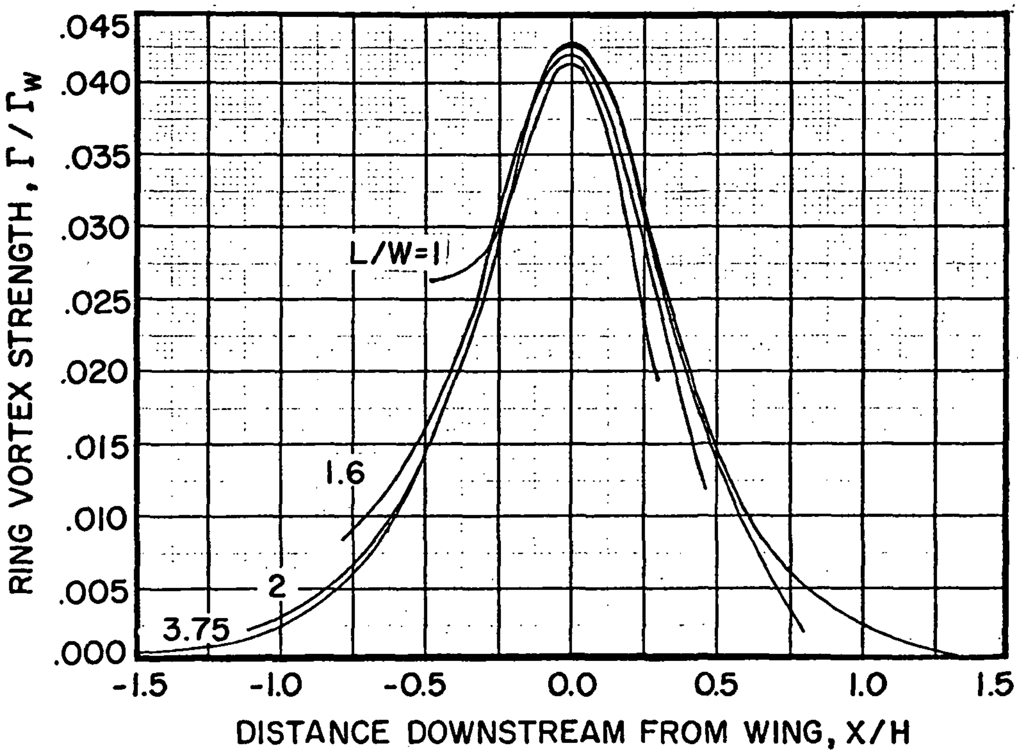

Fig. 17 Effect of tunnel length on wall vorticity distribution for a circular tunnel.

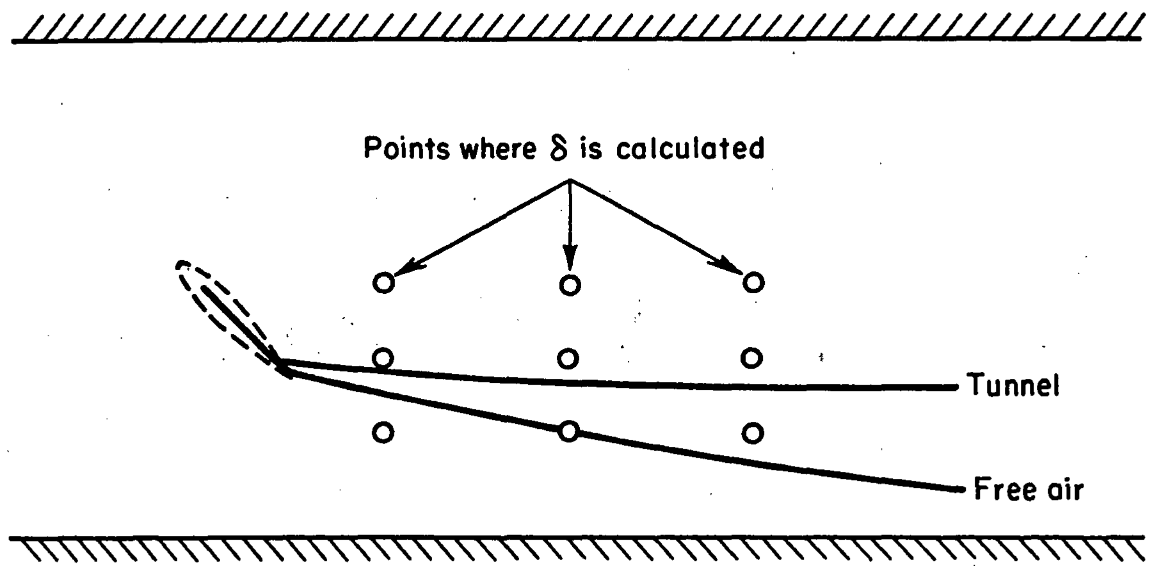

Fig. 18 Effect of tunnel walls on vortex wake trajectory in a 1:1.5 closed tunnel. Vortex span = .5 tunnel width $C_L/AR = .9$.

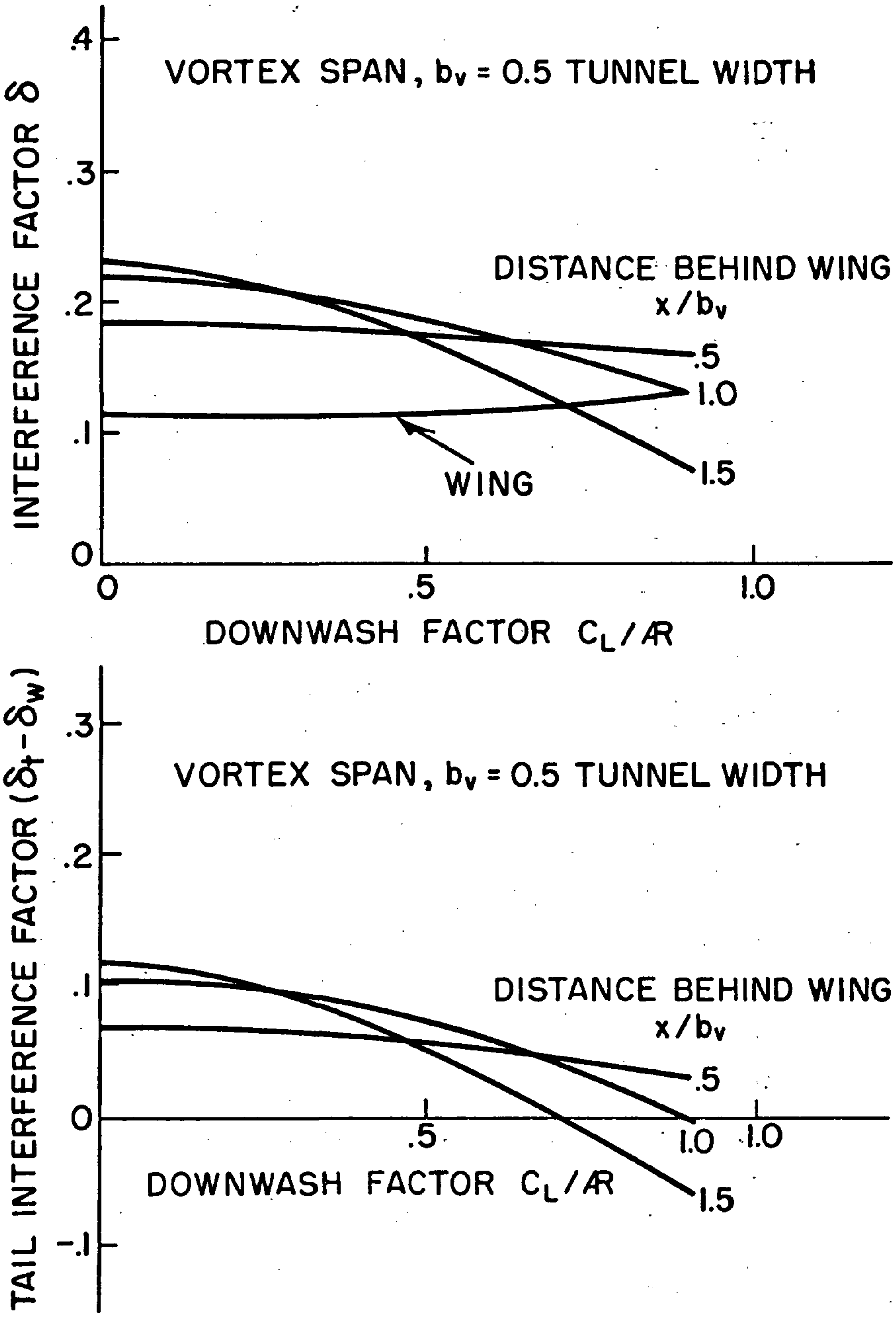

Fig. 19 Interference factors at wing and tail including wake relocation effects. Tail on tunnel centerline.

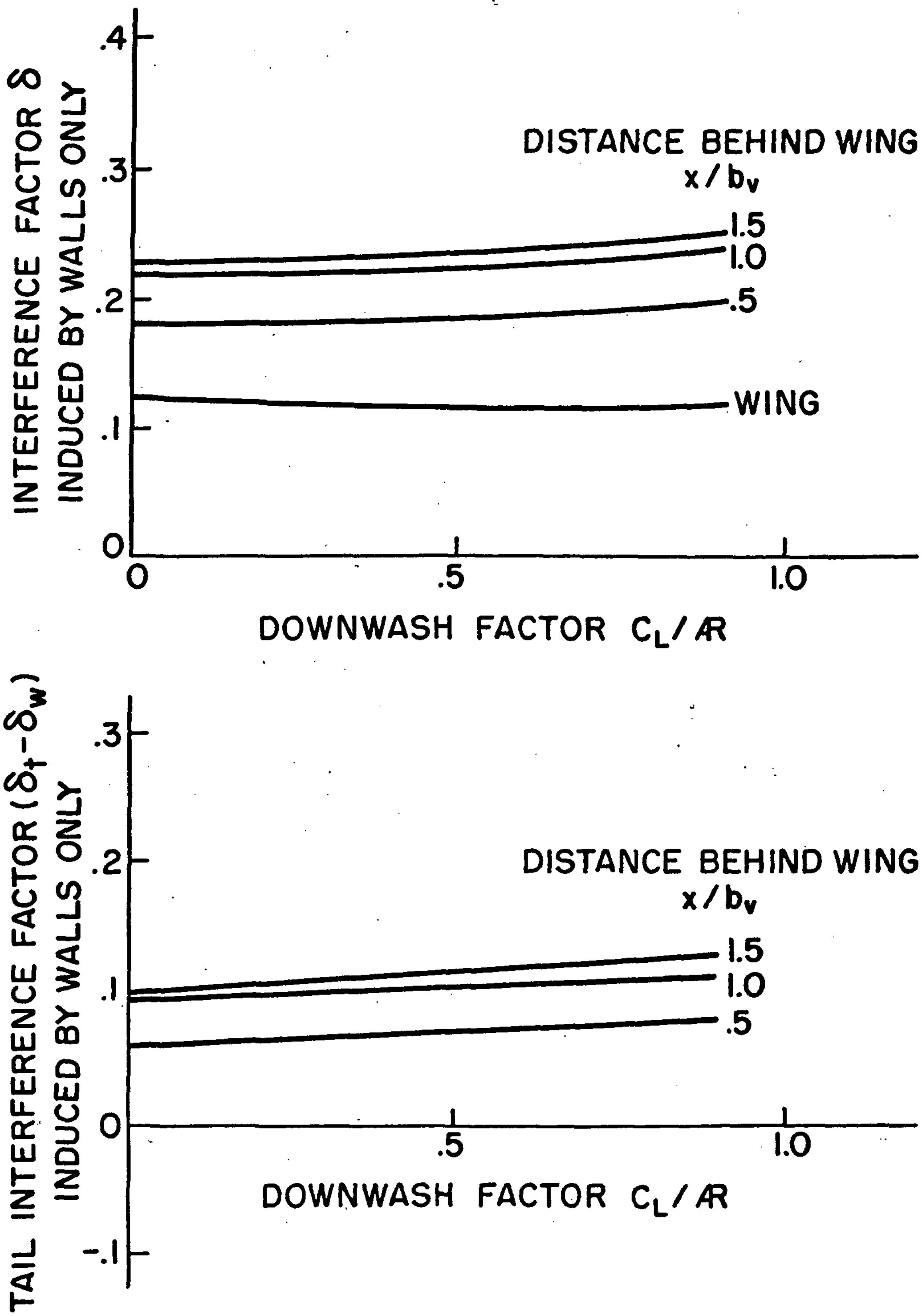

Fig. 20 Interference factors at wing and tail using only wall-induced effects. Tail on tunnel centerline.

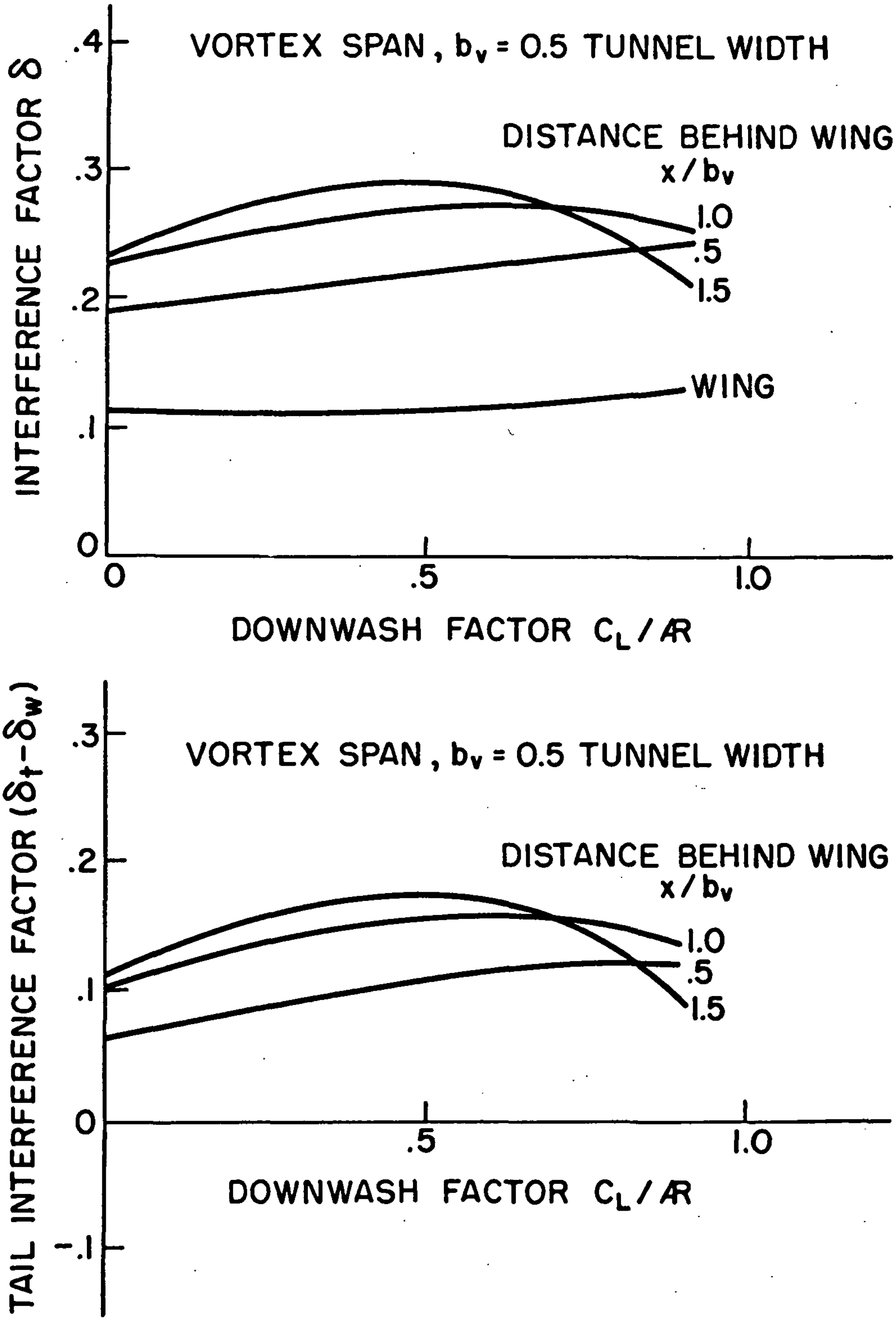

Fig. 21 Interference factors at wing and tail at .2 b_v below tunnel centerline.

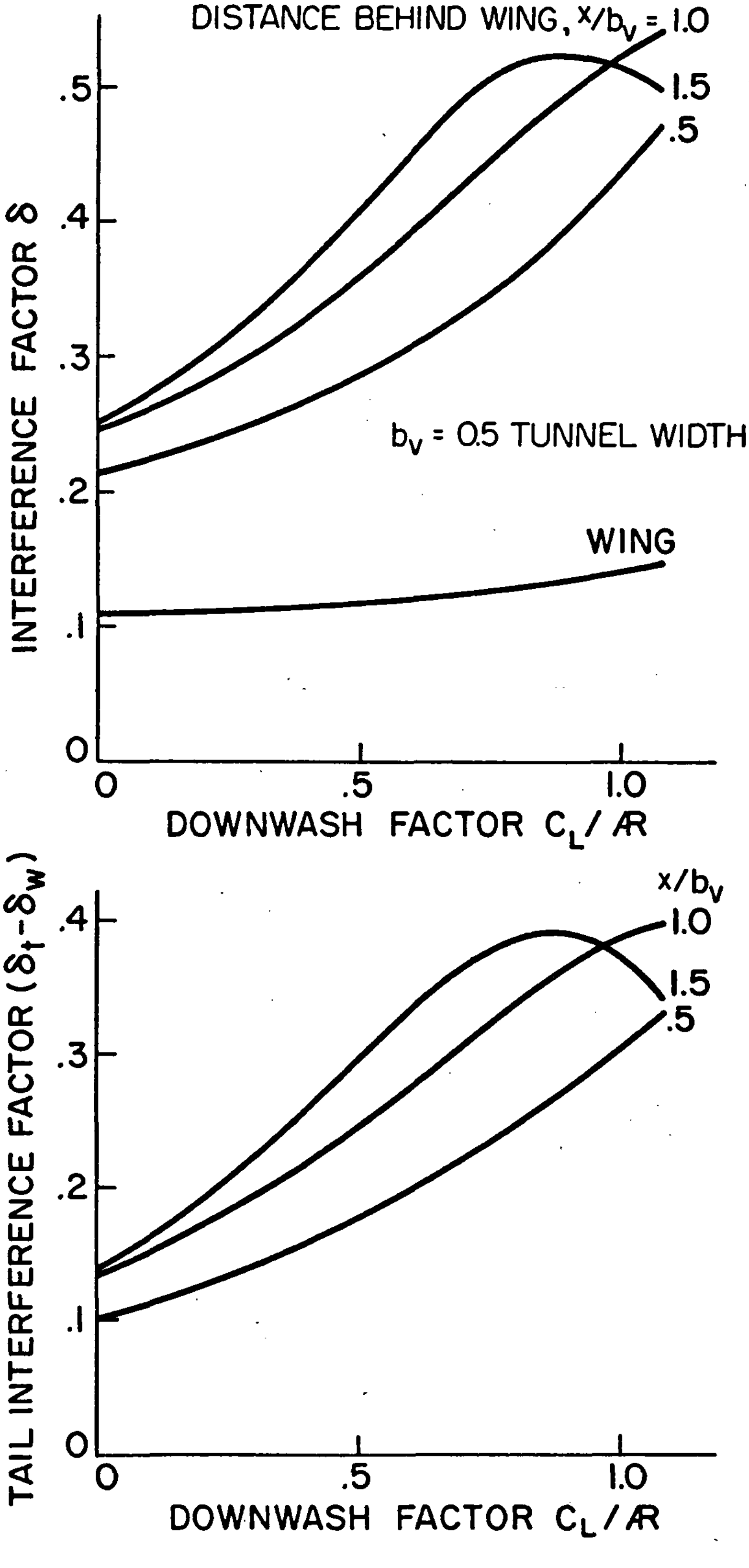

Fig. 22 Interference factors at wing and tail at .4 b_v below tunnel centerline.

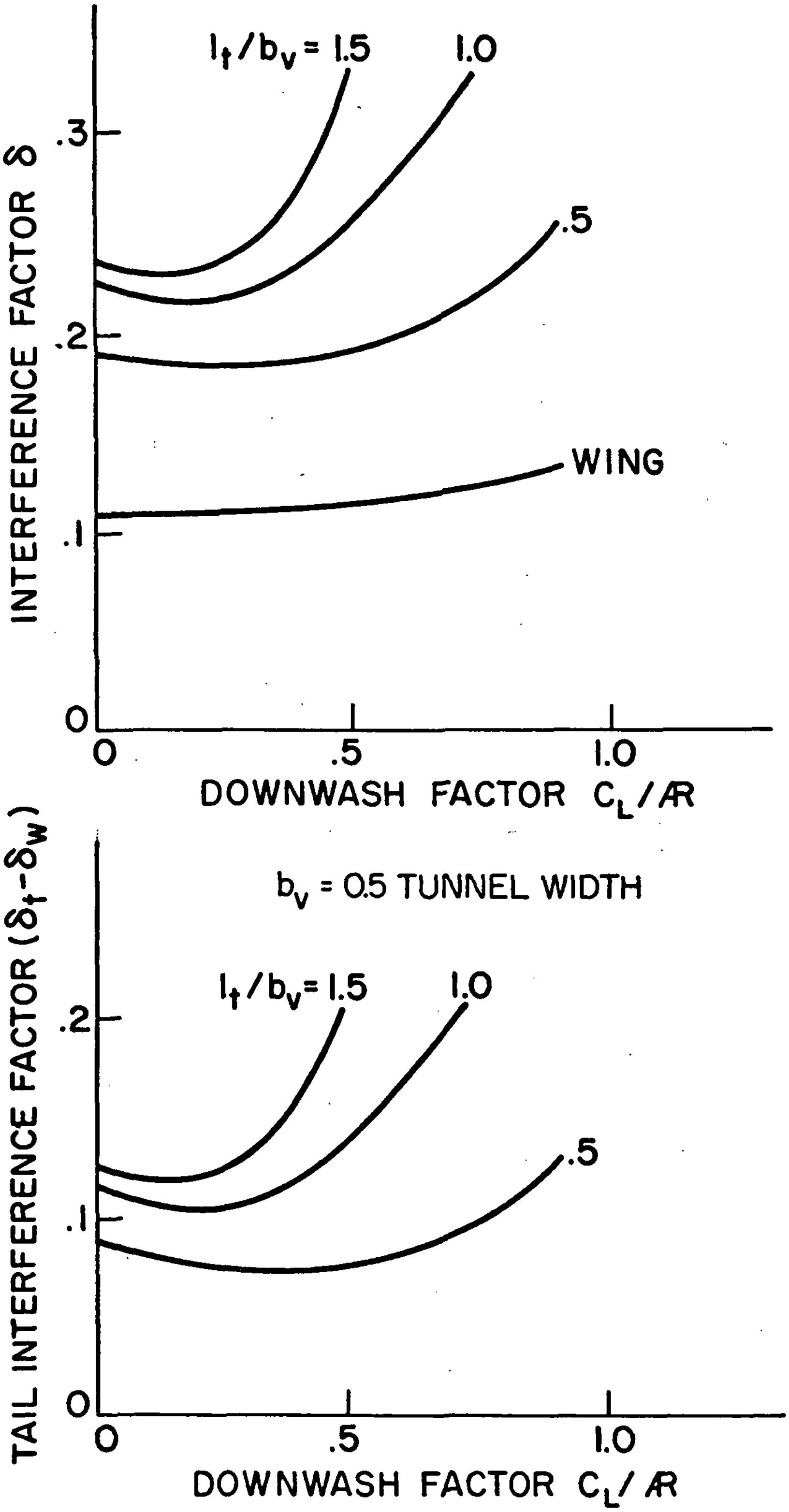

Fig. 23 Interference factors at wing and tail. Effect of tail displacement included. Tail height .2 b_v above wing plane.

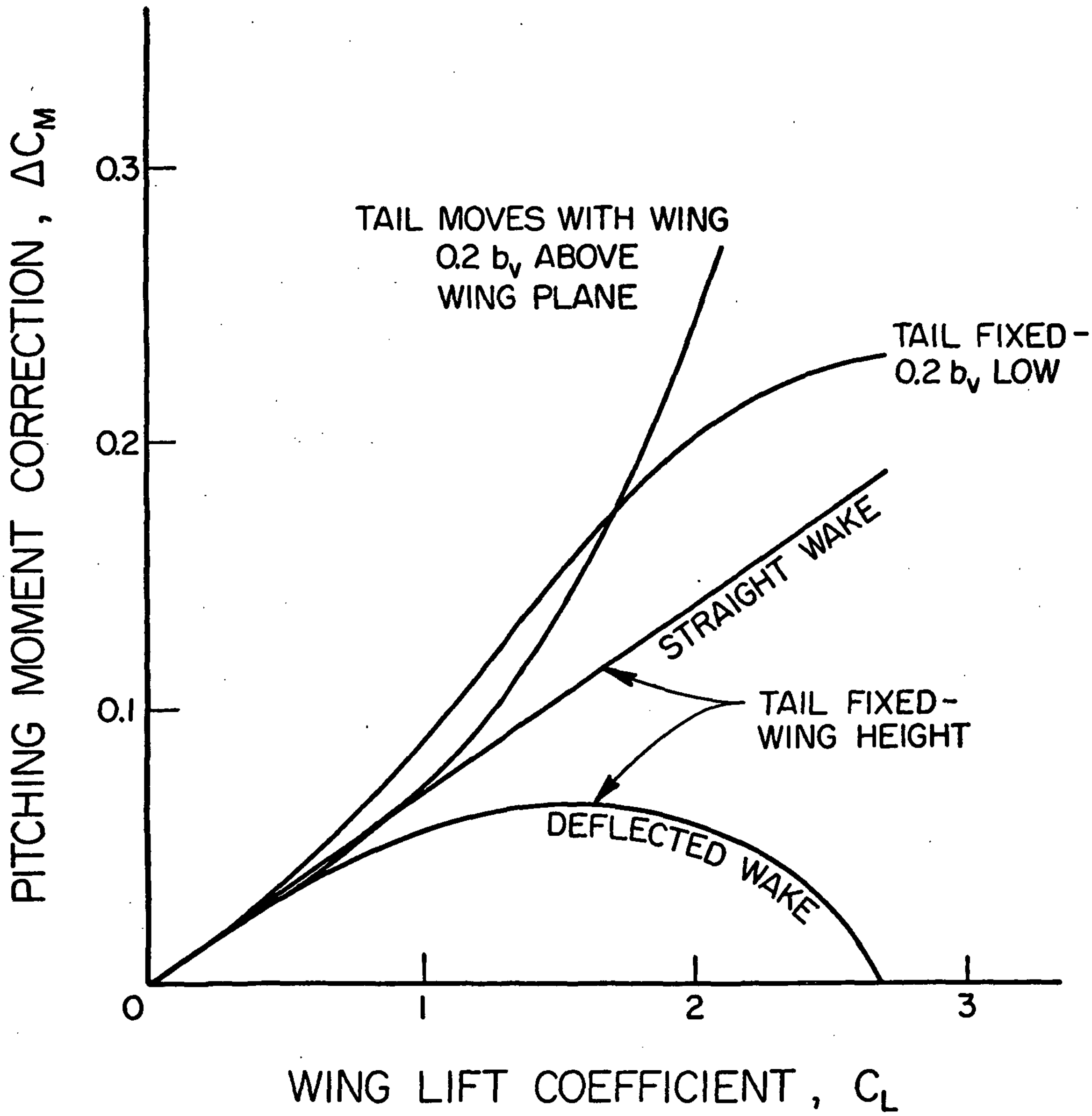

Fig. 24. Pitching moment corrections for several tail locations.

APPENDIX A

COMPARISON OF THE INDUCED VELOCITY OF A DISTRIBUTED VORTEX SHEET WITH THAT DUE TO A SINGULAR VORTEX

Betz* has shown that the first moment (center of gravity location) of a group of vortex filaments in a trailing vortex sheet is constant as they move about in the process of rolling up into a cylindrical arrangement. It is well known that the spanwise location of the center of gravity of the vortex sheet trailing from an elliptical wing is at $\pi/4$ times the semispan, measured from the plane of symmetry of the wing. It is also well known that the induced velocity at some large distance from the vortex sheet may be computed accurately by replacing the vortex sheet with a single vortex of the same total strength located at the center of gravity of the sheet it replaces. What is not widely known is the variation close to the sheet when this substitution is made. The following analysis is presented to show the ratio of the induced velocity in the near field computed using the trailing sheet, to that computed using a concentrated vortex located at the center of gravity of the sheet.

Consider the Trefftz plane, but just behind an elliptically loaded wing, as shown below.

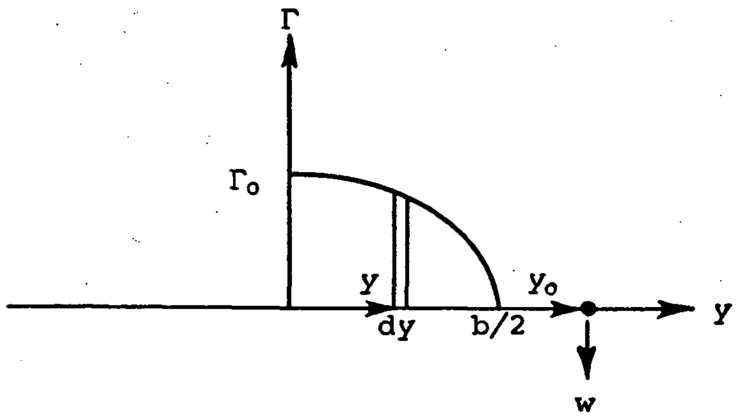

*Betz, A., "Behavior of Vortex Systems," NACA T.M. 713, June 1933.

The circulation on the wing is given by

$$\Gamma = \Gamma_o \sqrt{1 - \left(\frac{y}{b/2}\right)^2}$$

and the strength of the vortex trailing from the point y is

$$d\Gamma = \left(\frac{d\Gamma}{dy}\right) dy$$

This element of the vortex sheet induces a downwash velocity at a point y_o

$$dw_{y_o y} = \frac{d\Gamma}{4\pi (y_o - y)}$$

These equations are combined, and non-dimensionalized by letting $y = \frac{y}{b/2}$ and $y_o = \frac{y_o}{b/2}$. The integral is evaluated only over $0 < y < 1$ because we are only interested in the effect of one half of the wing on the other half.

$$w_{y_o y} = \frac{-\Gamma_o}{4\pi \frac{b}{2}} \int_o^1 \frac{y\, dy}{(y_o - y)\sqrt{1 - y^2}}$$

The integral can be put into a standard form by making the transformation

$$x = y_o - y$$

Then,

$$y = y_o - x$$

$$y^2 = y_o^2 - 2\, y_o\, x + x^2$$

$$dy = - dx$$

and the limits of integration become

$$\text{when} \quad y = 0 \quad , \; x = y_0$$

$$\text{when} \quad y = 1 \quad , \; x = y_0 - 1$$

Then

$$w_{y_0 y} = \frac{\Gamma_0}{4\pi \frac{b}{2}} \int_{y_0}^{y_0 - 1} \frac{(y_0 - x)\, dx}{x\sqrt{(1 - y_0{}^2) + 2y_0 x - x^2}}$$

This is integrated for values of $-1 < y_0 < 0$, using integrals number 161 and 182 from Pierce, <u>A Short Table of Integrals</u>, Ginn and Company, 1929. The result is

$$w_{y_0 y} = \frac{\Gamma_0}{4\pi \frac{b}{2}} \left[\frac{\pi}{2} - \frac{y_0}{\sqrt{1 - y_0{}^2}} \ln\left(\frac{- y_0}{\sqrt{1 + \quad 1 - y_0{}^2}} \right) \right]$$

Now compare this solution with that of the simpler case, where the total circulation, $-\Gamma_0$, is assumed to be concentrated at $y_0 = \pi/4 \cdot b/2$, and find its effect on the other side of the wing. We have, then

$$w_{y_0 y} = \frac{-\Gamma_0}{4\pi \frac{b}{2} \left(\frac{y_0}{b/2} - \frac{\pi}{4} \right)}$$

The ratio of the downwash due to the sheet to that due to the single vortex is

$$R = \frac{w_{y_0 y}\,(\text{sheet})}{w_{y_0 y}\,(\text{single})} = \left(\frac{\pi}{4} - \frac{y}{b/2} \right) \left[\frac{\pi}{2} - \frac{y_0}{\sqrt{1 - y_0{}^2}} \ln\left(\frac{- y_0}{\sqrt{1 + \quad 1 - y_0{}^2}} \right) \right]$$

We are particularly interested in the value when $y_0 = \pi/4$, and that value is

$$R = 1.02566$$

The graph following shows the variation of this ratio over a range of distances from the wing.

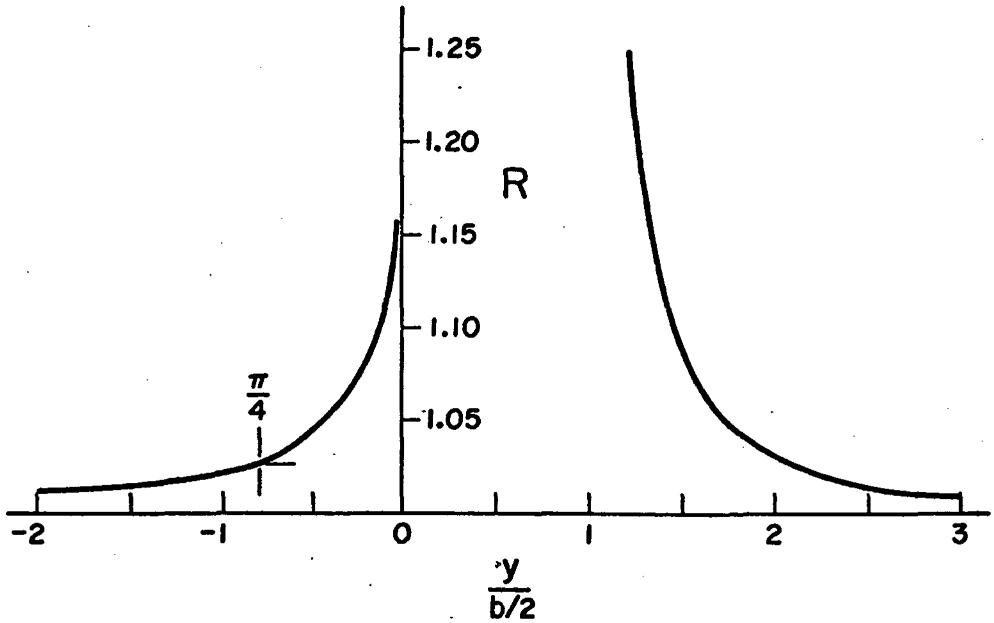

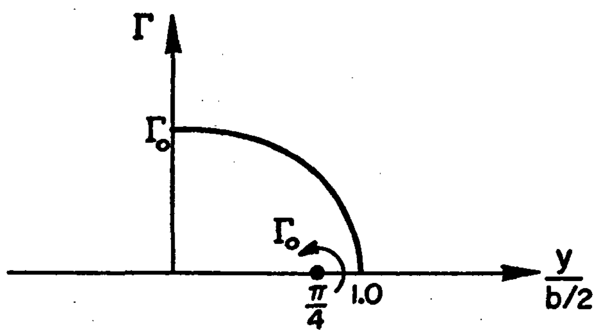

DOWNWASH ALONG THE EXTENDED LIFTING LINE

R is the ratio of downwash due to a vortex sheet trailing from one half of an elliptically loaded wing to the downwash due to a single trailing vortex of the same strength located at the center of gravity of the trailing sheet.

```
C                              APPENDIX B
C                  PROGRAM TO COMPUTE THE WAKE TRAJECTORY
C              OF A VORTEX PAIR TRAILING FROM A FINITE WING
C
      PROGRAM FRAIR (INPUT,OUTPUT,PUNCH,TAPE5=INPUT,TAPE6=OUTPUT,
     1TAPE7=PUNCH)
C
C THIS PROGRAM IS WRITTEN IN FORTRAN IV FOR THE CDC-6400 COMPUTER. THE
C APPROXIMATE STORAGE REQUIREMENT FOR THIS PROGRAM IS 14600 (OCTAL).
C EXECUTION TIME IS APPROXIMATELY 25 SECONDS PER CASE WITH 180 SURVEY
C POINTS, 30 TRAILING SEGMENTS, AND 8 ITERATIONS. NOTE THAT THIS PROGRAM
C YIELDS A PUNCHED CARD DECK OUTPUT.
C
C INPUT DATA SEQUENCE
C
C SPAN, GAMAM, SPEED, ASPECT, NW (4F10.5,I10)
C     SPAN IS WING VORTEX SPAN, FEET
C     GAMAM IS WING CIRCULATION, SQUARE FEET/SECOND
C     SPEED IS REMOTE WIND SPEED, FEET/SECOND
C     ASPECT IS ASPECT RATIO OF THE GEOMETRIC WING BEING REPRESENTED BY
C     THE VORTEX SPAN. VORTEX SPAN IS PI/4 TIMES GEOMETRIC SPAN.
C     NW IS THE NUMBER OF TRAILING SEGMENTS IN THE WAKE, LESS THAN 50
C
C DELTAX (F10.5)
      LENGTH OF TRAILING SEGMENTS, FEET. USUALLY TAKEN SPAN/10
C
C XW(1), YW(1)  (2F10.5)
C     X AND Y COORDINATES OF CENTER OF BOUND VORTEX, USUALLY 0.0, 0.0
C     X AXIS IS POSITIVE DOWNSTREAM, Y IS POSITIVE UPWARD, Z TO RIGHT
C     LOOKING DOWNSTREAM
C
C TLMN, TLMX, DELTX (3F10.5)
      MINIMUM AND MAXIMUM TAIL LENGTHS, FRACTION OF SPAN, DEFINING
C     LONGITUDINAL REGION TO BE SURVEYED, AND INCREMENT BETWEEN
C     SURVEY POINTS, FRACTION OF SPAN.
C
C THMN, THMX, DELTY (3F10.5)
C     MINIMUM AND MAXIMUM TAIL HEIGHTS, FRACTION OF SPAN, DEFINING
C     VERTICAL REGION TO BE SURVEYED, AND INCREMENT BETWEEN SURVEY
C     POINTS, FRACTION OF SPAN.
C
C THSP, DELTZ (2F10.5)
C     SEMISPAN OF TAIL, FRACTION OF SPAN, DEFINING LATERAL REGION TO
C     BE SURVEYED, AND INCREMENT BETWEEN SURVEY POINTS, FRACTION OF
C     SPAN.
C
C KK (I1)
C     INTEGER VARIABLE SET EQUAL TO ONE IF SURVEY REGION ABOVE IS
C     REFERENCED TO WING, AND TO ANY OTHER VALUE IF REFERENCED TO
C     SPACE COORDINATES.
C
C ADDITIONAL CASES
C     REPEAT THE PRECEDING SET OF SEVEN DATA CARDS FOR AS MANY CASES
C     AS DESIRED
C
C PUNCHED OUTPUT RESULTING FROM EACH CASE WILL BE AS FOLLOWS
```

```
C
C CARD 1-3. VORTEX SPAN, REMOTE VELOCITY, WING CIRCULATION, ASPECT
C RATIO, LIFT, DRAG, TOTAL X-VELOCITY AT WING CENTER SPAN, TOTAL
C Y-VELOCITY AT WING CENTER, WING GEOMETRIC ANGLE OF ATTACK (4E20.10)
C
C CARD 4 AND FOLLOWING CARDS, COORDINATES OF SURVEY POINTS XCI, YCJ,
C AND ZCJ (SPACE FIXED) AND TOTAL X, Y, AND Z VELOCITY COMPONENTS
C AT EACH SURVEY POINT. (4E20.10)
C
C LAST CARD. THE NUMBER 10000 IS PUNCHED TO INDICATE THE END OF
C EACH CASE. THIS SPECIAL PUNCHING IS USED BY THE WING-IN-TUNNEL
C PROGRAM TO LOCATE THE END OF EACH DATA DBCK. (40X, E20.10)
C
C
1      FORMAT (4F10.5,I10)
2      FORMAT (F10.5)
3      FORMAT (18H ITERATION NUMBER  ,I2)
4      FORMAT (10F10.5)
5      FORMAT (3F10.5)
6      FORMAT (10F12.6)
7      FORMAT (2F10.5)
8      FORMAT (13H CL/ASPECT =  ,F8.5,15X,13HCDI/ASPECT =   ,F8.5)
9      FORMAT (I3,5F10.5)
10     FORMAT (2I10)
11     FORMAT (I2)
12     FORMAT (7F15.5)
4100   FORMAT (74H-NOTE - ALL DISTANCES MEASURED FROM ASSUMED LIFTING LIN
      1E POSITION AT XW(1)   )
4150   FORMAT (18H WAKE COORDINATES  ,/, 9X,2HXW,13X,2HYW,13X,2HZW,13X,
      13HDSM)
4160   FORMAT (4F15.5)
4170   FORMAT (1H0,8HGAMAM = ,F10.4)
4175   FORMAT (1X,I2,3F10.4,2X,3F10.4,2X,3F10.4)
4180   FORMAT (19H ANGLE OF ATTACK = ,F6.3,12H RADIANS OR ,F7.3,8H DEGREE
      1S   )
4190   FORMAT (22H ANGLE OF ZERO LIFT = ,F6.3,12H RADIANS OR ,F7.3,8H DEG
      1REES   )
4200   FORMAT (23H TAIL SPAN (ABSOLUTE) =,F9.4,2X,21HTAIL SPAN/WING SPAN
      1=,F9.4)
4250   FORMAT (1H1,5X,7HSPAN = ,F6.3,21X,18HREMOTE VELOCITY = ,F9.3,
      17X,14HCIRCULATION = ,F9.3,/,6X,15HASPECT RATIO = ,F6.3,13X,7HLIFT
      1= ,F9.4,18X,7HDRAG = ,F9.5,/,6X,13HVX AT WING = ,F10.4,11X,
      113HVY AT WING = ,F10.4,11X,18HGEOMETRIC ALPHA = ,F6.2,8H DEGREES,
      1/,/,/,8X,16HWING COORDINATES,18X,17HEARTH COORDINATES,17X,
      119HVELOCITY COMPONENTS   )
4260   FORMAT (1H ,3F10.4,5X,3F10.4,5X,3F10.4)
4270   FORMAT (12H TAIL SPAN = ,F8.4,4X,23HTAIL SPAN/WING SPAN =  ,F8.4)
4280   FORMAT (4E20.10)
4281   FORMAT (40X,E20.10)
4285   FORMAT (4F10.4)
4290   FORMAT (1H0,12H2-D ALPHA = ,F8.5,12H RADIANS OR ,F7.3,8H DEGREES)
4295   FORMAT (1H ,16HINDUCED ALPHA = ,F8.5,12H RADIANS OR ,F7.3,5H DEG.)
4300   FORMAT (1H ,18HGEOMETRIC ALPHA = ,F8.5,9H RAD. OR ,F7.3,5H DEG.)
4310   FORMAT (1H1)
4320   FORMAT (1H0,44X,3HX =,F9.4)
4330   FORMAT (1H0,44X,3HY =,F9.4)
```

```
4340  FORMAT (1H ,41X,18HREFERENCED TO WING)
4350  FORMAT (1H ,40X,20HREFERENCED TO TUNNEL)
      REAL LIFT
      DIMENSION VX(7),VY(7),VZ(7)
      DIMENSION VMX(7),VMY(7),VMZ(7)
      DIMENSION VCX(7),VCY(7),VCZ(7)
      DIMENSION XW(50), YW(50), ZW(50), RW(2,2), DSM(50),VBAR(2)
      DIMENSION ALPHA(7) , BETA(7)
      RHO = .002378
30    CONTINUE
      READ (5,1) SPAN,GAMAM,SPEED,ASPECT,NW
      IF (EOF,5) 60,31
31    READ (5,2) DELTAX
      READ (5,7) XW(1),YW(1)
      IF (EOF,5) 60,80
C
C COMPUTE INITIAL COORDINATES, WING DIMENSIONS, TRAILING SEGMENTS
80    CONTINUE
      NW1 = NW + 1
      ZW(1) = SPAN/2.
      CHORD = SPAN/(ASPECT*.785398163**2)
      ALFAA=ASIN(GAMAM*2./(6.2831853*CHORD*SPEED))
      XCI = 0.75*CHORD*SQRT(1.-(.78539816**2))
      XW(2) = XW(1) + XCI*COS(ALFAA)
      YW(2) = YW(1) - XCI*SIN(ALFAA)
      ZW(2) = ZW(1)
      XCI = DELTAX + XW(2)
      YCJ = YW(2)
      ZCJ = ZW(1)
      DO 90 N=3,NW
      ZW(N) = ZCJ
      YW(N) = YCJ
      XW(N) = XCI
      XCI = XCI + DELTAX
90    CONTINUE
      XW(NW1) = XW(NW) + 1000.0
      YW(NW1) = YCJ
      ZW(NW1) = ZCJ
      DO 81 I=1,NW
      J = I+1
81    DSM(I) = SQRT((XW(I)-XW(J))**2+(YW(I)-YW(J))**2+(ZW(I)-ZW(J))**2)
C
C CARRY OUT ITERATIVE SOLUTION
      NUMIT = GAMAM/19. + 3.
      WRITE (6,4310)
      DO 100 NUMBER = 1,NUMIT
      CALL WKIT        (XW,YW,ZW,DSM,GAMAM,SPEED,SPAN,NW,NW1,
     1                  ALPHAO,ALPHAI,ALFAA,CHORD)
      IF ((NUMIT-NUMBER).GT.3) GO TO 95
      WRITE (6,3) NUMBER
      WRITE (6,4150)
      WRITE (6,4160) (XW(L),YW(L),ZW(L),DSM(L),L=1,NW1)
      CALL LCOMP       (XW,YW,ZW,DSM,GAMAM,SPEED,SPAN,NW,NW1,LIFT,RHO,
     1VXWC,VYWC,DRAG)
      WRITE (6,4170) GAMAM
      ALPHAO = -ALPHAO
```

```
      ALFAA = -ALFAA
      DEG=ALPHA0*57.29578
      WRITE (6,4290) ALPHA0,DEG
      DEG=ALPHAI*57.29578
      WRITE (6,4295) ALPHAI,DEG
      DEG = ALFAA*57.29578
      WRITE (6,4300) ALFAA,DEG
95    XCI = XW(1)
      DO 1000 L = 4,NW1
      IF (XW(L).LT.XCI) GO TO 999
1000  CONTINUE
100   CONTINUE
C
C SET UP COORDINATES FOR VELOCITY SURVEY
      READ (5,5) TLMN,TLMX,DELTX
      READ (5,5) THMN,THMX,DELTY
      READ (5,7) THSP,DELTZ
      NTL=INT((TLMX-TLMN)/DELTX+0.5)+1
      NTH=INT((THMX-THMN)/DELTY+0.5)+1
      NTS=INT(THSP/DELTZ+0.5)+1
      COSA=COS(ALFAA)
      SINA=SIN(-ALFAA)
      WRITE (7,4280) SPAN,SPEED,GAMAM,ASPECT,LIFT,DRAG,VXWC,VYWC,ALFAA
      READ (5,40) KK
40    FORMAT (I1)
      DO 400 I=1,NTH
      YC=(THMN+FLOAT(I-1)*DELTY)*SPAN
      WRITE (6,4250) SPAN,SPEED,GAMAM,ASPECT,LIFT,DRAG,VXWC,VYWC,DEG
      WRITE (6,4330) YC
      IF (KK.EQ.1) WRITE (6,4340)
      IF (KK.NE.1) WRITE (6,4350)
      DO 400 J=1,NTL
      XC=(TLMN+FLOAT(J-1)*DELTX)*SPAN
      WRITE (6,4320) XC
      IF (KK.EQ.1) WRITE (6,4340)
      IF (KK.NE.1) WRITE (6,4350)
      DO 400 K=1,NTS
      IF (KK.NE.1) GO TO 51
      XCI=XC*COSA+XW(1)-YC*SINA
      YCJ=XC*SINA+YC*COSA+YW(1)
      ZCJ=FLOAT(K-1)*DELTZ*SPAN
      GO TO 52
51    CONTINUE
      XCI=XC+XW(1)
      YCJ=YC+YW(1)
      ZCJ=FLOAT(K-1)*DELTZ*SPAN
52    CONTINUE
C
C COMPUTE VELOCITY COMPONENTS AT SURVEY POINTS
      CALL VCOMP      (XCI,YCJ,ZCJ,                DSM,GAMAM,SPAN,SPEED,
     1VXMOD,VYMOD,VZMOD,VXTOT,VYTOT,VZTOT,XW,YW,ZW,NW,.FALSE.)
C
C REFERENCE SPACE FIXED COORDINATES TO BOUND VORTEX
      XCI=XCI-XW(1)
      YCJ=YCJ-YW(1)
      WRITE (7,4280) XCI,YCJ,ZCJ,VXTOT,VYTOT,VZTOT
```

```
      WRITE (6,4260) XC,YC,ZCJ,XCI,YCJ,ZCJ,VXTOT,VYTOT,VZTOT
400   CONTINUE
      ZCJ=10000.
      WRITE (7,4281) ZCJ
C
C READ INPUT DATA FOR NEXT CASE
      GO TO 30
939   CONTINUE
60    STOP
      END
```

```
      SUBROUTINE WKIT (XW,YW,ZW,DSM,GAMAM,SPEED,SPAN,NW,NW1
     1                        ,ALPHA0,ALPHAI,ALFAA,CHORD)
C
C SUBROUTINE TO ITERATE TRAILING WAKE POSITION
C
      DIMENSION XW(50),YW(50),ZW(50),DSM(50),RW(2,2),VBAR(2)
      LOGICAL SKP,WTEST
      SKP = .FALSE.
C
C MAKE TWO PASSES, FIRST FOR X-Y MOVEMENT, SECOND FOR X-Z MOVEMENT
      DO 20 N = 1,2
31    NNN = NW
40    DO 47 M = 1,NNN
      WTEST = .FALSE.
      IF (M.EQ.1) WTEST = .TRUE.
      IF ((M.EQ.1).AND.SKP) GO TO 47
C
C CHOOSE COORDINATES FOR VELOCITY COMPUTATION
41    XCI = XW(M)
      YCJ = YW(M)
      IF (M.EQ.1) GO TO 42
      ZCJ = ZW(M)
      GO TO 43
42    ZCJ = 0.0
43    CONTINUE
C
C COMPUTE VELOCITY COMPONENTS AT CHOSEN COORDINATES
      CALL VWKIT      (XCI,YCJ,ZCJ,             DSM,GAMAM,SPAN,SPEED,
     1VXMOD,VYMOD,VZMOD,VXTOT,VYTOT,VZTOT,XW,YW,ZW,NW,WTEST)
      VXM = VXTOT
      VYM = VYTOT
      VZM = VZTOT
      VEL = SQRT(VXTOT**2 + VYTOT**2 + VZTOT**2)
      J = M+1
C
C COMPUTE NEW ANGLE OF ATTACK OR SEGMENT ORIENTATION, AND SHIFT
C TO BE APPLIED TO FOLLOWING SEGMENTS
      IF (M.NE.1) GO TO 45
      ALPHA0=ASIN(-GAMAM*2./(6.2831853*CHORD*VEL))
      ALPHAI = ATAN(VYM/VXM)
      ALFAA = ALPHA0 + ALPHAI
      XSHFT = DSM(1)*COS(ALFAA) + XW(1) - XW(2)
      YSHFT = DSM(1)*SIN(ALFAA) + YW(1) - YW(2)
      ZSHFT = 0.0
      GO TO 57
45    DCWX = VXM/VEL
      XSHFT = DSM(M)*DCWX + XW(M)
      XSHFT = XSHFT - XW(J)
      IF (SKP) GO TO 49
      DCWY = VYM/VEL
      YSHFT = DSM(M)*DCWY + YW(M)
      YSHFT = YSHFT - YW(J)
      GO TO 57
49    DCWZ = VZM/VEL
      ZSHFT = DSM(M)*DCWZ + ZW(M)
      ZSHFT = ZSHFT - ZW(J)
```

```
      IF (J.EQ.NW1) ZSHFT = 0.
C
C COMPUTE NEW COORDINATES OF TRAILING SEGMENTS DOWNSTREAM OF
C NEWLY ORIENTED SEGMENT
57    DO 48 L=J,NW1
      XW(L) = XW(L) + XSHFT
      IF (SKP) GO TO 59
58    YW(L) = YW(L) + YSHFT
      GO TO 50
59    ZW(L) = ZW(L) + ZSHFT
50    K = L-1
      DSM(K) = SQRT((XW(L)-XW(K))**2+(YW(L)-YW(K))**2+(ZW(L)-ZW(K))**2)
48    CONTINUE
47    CONTINUE
C
C RETURN FOR NEXT PASS
      SKP = .NOT.SKP
20    CONTINUE
      RETURN
      END
```

```
      SUBROUTINE LCOMP (XW,YW,ZW,DSM,GAMAM,SPEED,SPAN,NW,NW1,LIFT,RHO,
     1                                    VXTOT,VYTOT,DRAG)
C
C SUBROUTINE TO COMPUTE LIFT AND INDUCED DRAG ON WING
C
      DIMENSION XW(50),YW(50),ZW(50),DSM(50),RW(2,2),VBAR(2),ALPHA(7),
     1BETA(7)
      REAL LIFT
1     FORMAT (1H0,6HLIFT =,F10.4,5X,6HDRAG =,F10.4)
2     FORMAT (1H0,17HCL/ASPECT RATIO =,F10.4,5X,17HCD/ASPECT RATIO =,
     1F10.4)
3     FORMAT (1H0,23HVX AT WING CENTERLINE =,F10.5,/,1H0,23HVY AT WING C
     1ENTERLINE =,F10.5)
      KK = 1
      XCI = XW(KK)
      YCJ = YW(KK)
      ZCJ = 0.
      CALL VLCOMP    (XCI,YCJ,ZCJ,              DSM,GAMAM,SPAN,SPEED,
     1VXMOD,VYMOD,VZMOD,VXTOT,VYTOT,VZTOT,XW,YW,ZW,NW,.FALSE.)
      LIFT = RHO*VXTOT*SPAN*GAMAM
      DRAG = -RHO*VYTOT*SPAN*GAMAM
      CDIAR = (3.14159/4.)**2/(.5*RHO*(SPEED**2)*(SPAN**2))
      CLAR = LIFT*CDIAR
      CDIAR = DRAG*CDIAR
      WRITE (5,1) LIFT,DRAG
      WRITE (6,2) CLAR,CDIAR
      WRITE (6,3) VXTOT,VYTOT
C
      RETURN
      END
```

```
      SUBROUTINE VWKIT (XCI ,YREF,ZREF,            DSM,GAMAM,SPAN,SPEED
     1,VXMOD,VYMOD,VZMOD,VXTOT,VYTOT,VZTOT,XW,YW,ZW,NW,WTEST)
C
C SUBROUTINE TO COMPUTE VELOCITY COMPONENTS
C
      DIMENSION XW(50),YW(50),ZW(50),DSM(50),RW(2,2),VBAR(2)
      LOGICAL WTEST,LTEST
      LTEST = .FALSE.
      GO TO 10
      ENTRY VCOMP
      LTEST = .FALSE.
      GO TO 10
      ENTRY VLCOMP
      LTEST = .TRUE.
10    VXM=0.0
      VYM = 0.0
      VZM = 0.0
      YCJ = YREF
      ZCJ = ZREF
      P = 6.2831853
C
C INITIALIZE VARIABLES TO COMPUTE VELOCITY INDUCED BY THE SEGMENT
C PAIR UNDER CONSIDERATION
      XWK = XW(1)
      YWK = YW(1)
      ZWK = ZW(1)
      RW12 = (XWK-XCI)**2 + (YWK-YCJ)**2
      RW112 = RW12 + (ZWK-ZCJ)**2
      RW122 = RW12 + (ZWK+ZCJ)**2
      RW11 = SQRT(RW112)
      RW12 = SQRT(RW122)
43    DO 46 K = 1,NW
      J = K+1
      XWJ = XW(J)
      YWJ = YW(J)
      ZWJ = ZW(J)
      RW22 = (XWJ-XCI)**2 + (YWJ-YCJ)**2
      RW212 = RW22 + (ZWJ-ZCJ)**2
      RW222 = RW22 + (ZWJ+ZCJ)**2
      RW21 = SQRT(RW212)
      RW22 = SQRT(RW222)
      DSMK = DSM(K)
      DSMK2 = DSMK**2
      H = 4.*RW112*DSMK2 - (RW112-RW212+DSMK2)**2
      IF (H.LT.1.E-10) GO TO 44
      VBAR1 = -GAMAM*(DSMK2-(RW11-RW21)**2)*(RW11+RW21)/(P*RW11*RW21*H)
      GO TO 45
44    VBAR1 = 0.0
45    H = 4.*RW122*DSMK2-(RW122-RW222+DSMK2)**2
      IF (H.LT.1.E-10) GO TO 47
      VBAR2 = -GAMAM*(DSMK2-(RW12-RW22)**2)*(RW12+RW22)/(P*RW12*RW22*H)
      GO TO 48
47    VBAR2 = 0.0
48    CONTINUE
C
C COMPUTE VELOCITY COMPONENTS INDUCED BY EACH SEGMENT PAIR
```

```
      VXM = VBAR1*((YWK-YCJ)*(ZWJ-ZWK)-(ZWK-ZCJ)*(YWJ-YWK))
     1      -VBAR2*((YWK-YCJ)*(ZWK-ZWJ)-((-ZWK-ZCJ)*(YWJ-YWK)) + VXM
      VYM = VBAR1*((ZWK-ZCJ)*(XWJ-XWK)-(XWK-XCI)*(ZWJ-ZWK))
     1      -VBAR2*((-ZWK-ZCJ)*(XWJ-XWK)-(XWK-XCI)*(ZWK-ZWJ)) + VYM
      IF (LTEST) GO TO 55
      VZM = (VBAR1-VBAR2)*((XWK-XCI)*(YWJ-YWK)-(YWK-YCJ)*(XWJ-XWK)) +VZM
55    CONTINUE
      RW11 = RW21
      RW12 = RW22
      RW112 = RW212
      RW122 = RW222
      XWK = XWJ
      YWK = YWJ
      ZWK = ZWJ
45    CONTINUE
      IF (WTEST) GO TO 60
      XWK = XW(1)
      YWK = YW(1)
      ZWK = ZW(1)
      HM2 = (XWK-XCI)**2 + (YWK-YCJ)**2
      IF (HM2.LT..00001) GO TO 60
      RM1 = SQRT(HM2 + (ZWK-ZCJ)**2)
      RM2 = SQRT(HM2 + (ZWK+ZCJ)**2)
      P = 25.13274
C
C COMPUTE VELOCITY INDUCED BY BOUND VORTEX
      VXM = GAMAM*(RM1+RM2)*(SPAN**2 -(RM1-RM2)**2)*(YCJ-YWK)/(P*SPAN*
     1RM1*RM2*HM2) + VXM
      VYM = GAMAM*(RM1+RM2)*(SPAN**2 -(RM1-RM2)**2)*(XWK-XCI)/(P*SPAN*
     2RM1*RM2*HM2) + VYM
   60 CONTINUE
95    VXMOD = VXM
      VYMOD = VYM
      VZMOD = VZM
C
C STORE TOTAL VELOCITIES
      VXTOT = VXM + SPEED
      VYTOT = VYM
      VZTOT = VZM
      RETURN
      END
```

```
C                               APPENDIX C
C
C      PROGRAM TO COMPUTE LINEARIZED WALL INTERFERENCE FACTORS
C               FOR TUNNELS OF ARBITRARY CROSS SECTION
C
      PROGRAM STWKWT(INPUT,OUTPUT,TAPE5=INPUT,TAPE6=OUTPUT)
C
C THIS PROGRAM COMPUTES LINEARIZED WIND TUNNEL WALL INTERFERENCE FACTORS
C FOR WIND TUNNELS WITH VERTICAL AND LATERAL PLANES OF SYMMETRY IN THE
C SPECIAL CASE OF THE MODEL LOCATED ON THE PLANE OF VERTICAL SYMMETRY.
C THE MODEL IS A SIMPLE HORSESHOE VORTEX SYSTEM.
C THE CROSS SECTION OF THE TUNNEL MUST REMAIN CONSTANT OVER THE FULL
C LENGTH.
C
C THIS IS A FORTRAN IV PROGRAM WRITTEN FOR THE CDC 6400 COMPUTER.
C STORAGE REQUIREMENT FOR THIS PROGRAM IS APPROXIMATELY 46000 (OCTAL)
C LOCATIONS ON THE CDC 6400.
C EXECUTION TIME ON THE CDC 6400 IS APPROXIMATELY 95 SECONDS FOR ONE
C CASE INCLUDING THE MATRIX INVERSION.
C
C INPUT DATA SEQUENCE.
C
C TITLE (8A10)
C      ANY TITLE MAY BE USED TO ACCOMPANY OUTPUT.
C
C MM, NN (2I2)
C      MM IS THE NUMBER OF COORDINATE PAIRS DEFINING THE COMPLETE CROSS-
C      SECTIONAL SHAPE OF THE TUNNEL. MM CANNOT EXCEED 20.
C      NN IS THE NUMBER OF VORTEX RECTANGLES MAKING UP THE LENGTH OF THE
C      TUNNEL. NN CANNOT EXCEED 25.
C
C Y, Z (2F15.5)
C      Y AND Z ARE THE COORDINATES, IN FEET, OF THE POINTS DEFINING THE
C      SHAPE OF THE TUNNEL. MM CARDS ARE REQUIRED.
C      THE ORIGIN OF THE COORDINATE SYSTEM IS TAKEN ON THE TUNNEL CENTER
C      LINE WITH X POSITIVE DOWNSTREAM, Y POSITIVE UPWARD, AND Z POSITIVE
C      TO THE RIGHT LOOKING DOWNSTREAM. THE FIRST CARD IN THE SEQUENCE IS
C      THE FIRST COORDINATE TO THE RIGHT (POSITIVE Z) OF THE POSITIVE Y
C      AXIS, AND SUBSEQUENT POINTS ARE TAKEN CLOCKWISE AROUND THE TUNNEL.
C      SEGMENT LENGTHS BETWEEN ADJACENT POINTS SHOULD BE EQUAL.
C
C DELTAX (F15.5)
C      LENGTH IN FEET OF THE VORTEX RECTANGLES IN THE STREAMWISE
C      DIRECTION. SHOULD BE EQUAL TO THE LENGTH OF SEGMENTS IN THE
C      CROSS-SECTION.
C
C SPAN (F15.5)
C      VORTEX SPAN, IN FEET, OF THE WING.
C
C ADDITIONAL CASES
C      REPEAT THE LAST CARD, SPAN (F15.5), FOR AS MANY CASES AS DESIRED.
C
1     FORMAT (2I2)
2     FORMAT (2F15.5)
3     FORMAT (F15.5)
4     FORMAT (4F15.5)
```

```
5       FORMAT (1F10.5)
7       FORMAT (3F15.5)
9       FORMAT (8A10)
210     FORMAT (1H1,20X,8A10)
211     FORMAT (1H0,50X,21HM O D E L    D A T A ,/,/,25X,7HSPAN = ,
       1F6.3, 5X,4HXM =  ,F6.3, 5X, 4HYM =  ,F6.3,5X,13HCIRCULATION =   ,
       2F7.3   )
212     FORMAT (1H0,48X,23HT U N N E L    D A T A ,/,/,35X,9HPOINT NO.
       1,7X,1HY,9X,1HZ,8X,14HLENGTH OF SIDE , /,(/,38X,I2,7X,F8.4,2X,F8.4,
       29X,F7.4))
213     FORMAT (1H1,54X,13HR E S U L T S,/,/,5X,11HCOORDINATES,5X,
       110HCORRECTION,6X,16HTOTAL VELOCITIES,13X,25HTUNNEL INDUCED VELOCIT
       2IES,10X,24HMODEL INDUCED VELOCITIES,/,4X,1HX,5X,1HY,5X,1HZ,7X,
       33HDEL,6X,2HVX,9X,2HVY,9X,2HVZ,9X,3HVXC,8X,3HVYC,8X,3HVZC,8X,3HVXM,
       48X,3HVYM,8X,3HVZM )
214     FORMAT (1H0,3F6.2,F8.3,3F11.4,3F11.4,3F11.4)
215     FORMAT (/,/,48X,17HSECTION LENGTH =   ,F7.4)
216     FORMAT (/,/,45X,22HCROSS SECTIONAL AREA = ,F10.4)
        INTEGER A,B,C,D,E
        LOGICAL OPT1, OPT2
        DIMENSION X(26),Y(20),Z(20),SINPHI(20),COSPHI(20),XCPT(25),
       1YCPT(11),ZCPT(11),SIDE(20),CC(100,100),S(25),GAMAK(100),
       1GAMA(25,11),ZM(2)
        DIMENSION R(26,20),HL(25,20),HD(20),HYZ(20)
        DIMENSION GL(11), GD(11)
        DIMENSION TITLE(8)
        ID = 26
        JD = 25
        KD = 20
        LD = 11
        MD = 100
C
C READ TUNNEL AND MODEL DESCRIPTION FROM CARDS
34      READ (5,9) (TITLE(I), I=1,8)
        IF (EOF,5) 700,35
35      READ (5,1) MM,NN
        IF ((MM.GT.20).OR.(NN.GT.25)) GO TO 700
        N1 = NN + 1
        READ (5,2) (Y(I),Z(I),I=1,MM)
        READ (5,3) DELTAX
C
C
C COMPUTE THE COORDINATES OF THE TUNNEL.
        CALL COORD (X,Y,Z,XCPT,YCPT,ZCPT,S,SINPHI,COSPHI,DELTAX,
       1SIDE,OPT1,OPT2,MM,NN,LL,KK,N1,NK,ID,JD,KD,LD,AREA)
C
C GENERATE THE MATRIX OF COEFFICIENTS.
        CALL MATRIX (X,Y,Z,XCPT,YCPT,ZCPT,SINPHI,COSPHI,SIDE,S,CC,
       1MM,NN,LL,KK,N1,NK,OPT1,OPT2,R,HL,HD,HYZ,ID,JD,KD,LD,MD)
C
C
C COMPUTE INVERSE OF THE CC MATRIX, STORE RESULT IN CC ARRAY.
70      CALL INVR(CC,NK,MD)
C
C
C READ MODEL DATA FROM PUNCHED CARDS.
```

```
75    READ (5,3) SPAN
      IF (EOF,5) 700,80
80    CONTINUE
C
C GENERATE THE RIGHT HAND SIDE OF THE MATRIX EQUATION.
      CALL        RHS(SPAN,XM,YM,ZM,GAMAM,XCPT,YCPT,ZCPT,SINPHI,
     1COSPHI,GAMAK,JD,KD,LD,MD,NN,KK)
C
C
C MULTIPLY RIGHT HAND SIDE BY MATRIX INVERSE, STORE RESULT IN GAMA ARRAY
      M = 0
      DO 150 I = 1,NN
      DO 150 J = 1,KK
      M = M + 1
      XCI = 0.0
      DO 130 K = 1,NK
130   XCI = XCI + CC(M,K)*GAMAK(K)
      GAMA(I,J) = XCI
      L = LL + 1 - J
      GAMA(I,L) = -XCI
      IF ((.NOT.OPT2).AND.(J.EQ.KK)) GAMA(I,J+1) = 0.0
150   CONTINUE
C
C
C WRITE RESULTS OF COMPUTATIONS.
500   FORMAT (30H1 CALCULATED VORTEX STRENGTHS  )
      WRITE (6,500)
      DO 502 J = 1,NN
      WRITE (6,501) (GAMA(J,K), K=1,LL)
501   FORMAT (/,11F11.6)
502   CONTINUE
250   FORMAT (81H0OPT1 = .TRUE. THIS IMPLIES VORTEX SINGULARITY AT TOP A
     1ND BOTTOM CENTER OF TUNNEL  )
      IF (OPT1) WRITE (6,250)
251   FORMAT (85H0OPT1 = .FALSE. THIS IMPLIES NO VORTEX SINGULARITY AT T
     1OP AND BOTTOM CENTER OF TUNNEL  )
      IF (.NOT.OPT1) WRITE (6,251)
252   FORMAT (76H0OPT2 = .TRUE. THIS IMPLIES VORTEX SINGULARITY ON PLANE
     1 OF VERTICAL SYMMETRY  )
      IF (OPT2) WRITE (6,252)
253   FORMAT (80H0OPT2 = .FALSE. THIS IMPLIES NO VORTEX SINGULARITY ON P
     1LANE OF VERTICAL SYMMETRY  )
      IF (.NOT.OPT2) WRITE (6,253)
4000  FORMAT (27H1RESULTANT VORTEX STRENGTHS  )
4002  FORMAT (13H0RING NUMBER  ,I2,8X,15HX COORDINATE = ,F10.4,8X,17HMOD
     1EL DISTANCE =  ,F10.4,8X,22HMODEL DISTANCE/SPAN =  ,F11.4,(/,
     111F11.6))
4004  FORMAT (15H0SECTION NUMBER  ,I3,/,11F11.6)
4010  WRITE (6,4000)
4015  DO 4140 L=1,N1
4020  M=L-1
4025  DO 4075 I=1,LL
4030  IF (L-2) 4050, 4060, 4040
4040  IF (L-N1) 4060, 4070, 4140
4050  GL(I) = GAMA(L,I)
4055  GO TO 4075
```

```
4060  GL(I) = GAMA(L,I) - GAMA(M,I)
4065  GO TO 4075
4070  GL(I) = -GAMA(M,I)
4075  CONTINUE
4077  XOR = X(L)-XM
4078  XCI = XOR/SPAN
4080  WRITE (6,4002) L,X(L),XOR,XCI,(GL(I), I=1,LL)
4100  IF (L-N1) 4110, 4140, 4140
4110  DO 4125 I=2,LL
4115  J=I-1
4120  GL(J) = GAMA(L,J) - GAMA(L,I)
4125  CONTINUE
4130  MMM = LL - 1
4135  WRITE (6,4004) L,(GL(J),J=1,MMM)
4140  CONTINUE
      WRITE (6,210) TITLE
      WRITE (6,212) (I,Y(I),Z(I),SIDE(I), I=1,MM)
      WRITE (6,215) DELTAX
      WRITE (6,216) AREA
      WRITE (6,211) SPAN,XM,YM,GAMAM
C
C
C
C NOW BEGIN SURVEY OF TUNNEL FLOW FIELD.
C PERFORM SURVEY IN THE PLANE OF THE MODEL.  SURVEY FROM APPROXIMATE
C GEOMETRIC WINGTIP TO CENTERLINE OF TUNNEL WITH FIXED X COORDINATE,
C THEN SURVEY ALONG CENTERLINE OF TUNNEL DOWNSTREAM FROM BOUND VORTEX.
C SURVEY INCREMENT IN BOTH DIRECTIONS IS (VORTEX SPAN)/20
C SURVEY BEGINS AT BOUND VORTEX AND CONTINUES FOR THREE VORTEX SPANS
C DOWNSTREAM OF THE BOUND VORTEX.
C
      WRITE (6,213)
      DTP = SPAN/20.0
C SET XTP, YTP, ZTP TO INITIAL SURVEY COORDINATES.
      XTP = XM
      YTP = YM
      ZTP = SPAN*13./20.
600   CONTINUE
      CALL SURVEY (XTP,YTP,ZTP,X,Y,Z,XM,YM,ZM,SINPHI,COSPHI,S,
     1GAMA,SIDE,OPT1,SPAN,GAMAM,VXC,VYC,VZC,VXT,VYT,VZT,VXM,VYM,VZM,
     1LL,MM,NN,N1,R,HL,HD,HYZ,ID,JD,KD,LD   )
      XOR = XTP-XM
      DEL = VYC*AREA/SPAN/GAMAM/2.
C
C V*T ARE TOTAL VELOCITY COMPONENTS (SUM OF V*C AND V*M).
C V*C ARE VELOCITY COMPONENTS INDUCED BY TUNNEL WALLS.
C V*M ARE VELOCITY COMPONENTS INDUCED BY MODEL.
C XOR IS X COORDINATE OF SURVEY POINT RELATIVE TO BOUND VORTEX.
      WRITE (6,214) XOR,YTP,ZTP,DEL,VXT,VYT,VZT,VXC,VYC,VZC,VXM,VYM,VZM
      IF (ZTP.GT.0.0) GO TO 601
      XTP = XTP + DTP
      ZTP = 0.0
      IF (XTP.LE.XM+3.0*SPAN) GO TO 600
C
C READ DATA FOR NEXT MODEL FROM PUNCHED CARDS.
      GO TO 75
```

```
C
601   ZTP = ZTP - DTP
      GO TO 600
603   CONTINUE
700   STOP
      END
```

```
      SUBROUTINE COORD (X,Y,Z,XCPT,YCPT,ZCPT,S,SINPHI,COSPHI,DELTAX,
     1SIDE,OPT1,OPT2,MM,NN,LL,KK,N1,NK,ID,JD,KD,LD,AREA)
C
C THIS IS A SUBROUTINE TO COMPUTE THE TUNNEL COORDINATES.
C
      LOGICAL OPT1,OPT2
      DIMENSION X(ID),Y(KD),Z(KD),XCPT(JD),YCPT(LD),ZCPT(LD),S(JD),
     1SINPHI(KD),COSPHI(KD),SIDE(KD)
C
C COMPUTE VORTEX RING X-COORDINATES.
      XCI = 0.0
      DO 20 I=1,NN
      X(I) = XCI
20    XCI = XCI + DELTAX
      X(N1) = 1000.0 + X(NN)
C
C TEST TUNNEL SHAPE COORDINATES AND DETERMINE TOTAL NUMBER OF
C UNKNOWNS (NK).
      OPT1 = Z(MM).EQ.0.0
      I = MM/4
      J = (MM/4) + 1
      OPT2 = (Y(I).EQ.0.0).OR.(Y(J).EQ.0.0)
      IF (.NOT.OPT1) GO TO 10
      LL = MM/2
      KK = MM/4
      GO TO 14
10    IF (.NOT.OPT2) GO TO 12
      KK = MM/4 + 1
      GO TO 13
12    KK = MM/4
13    LL = MM/2 + 1
14    CONTINUE
      NL = NN * LL
      NM = NN*MM
      NK = NN*KK
      IF (NK.LE.100) GO TO 17
C
C IF NK IS GREATER THAN 100, TERMINATE EXECUTION.
      WRITE (6,15) NK
15    FORMAT (1H0,25HDIMENSIONS EXCEEDED, NK =,I3,16H REDUCE MM OR NN )
      STOP
C
C GENERATE VORTEX RECTANGLE PARAMETERS.
17    DO 21 I = 1,NN
21    S(I)=X(I+1) - X(I)
      DO 23 I=2,MM
22    SIDE(I) = SQRT((Y(I) - Y(I-1))**2 + (Z(I) - Z(I-1))**2)
      SINPHI(I) = ((Y(I)-Y(I-1))/(SIDE(I)))
23    COSPHI(I) = ((Z(I)-Z(I-1))/(SIDE(I)))
      SIDE(1) = SQRT((Y(1) - Y(MM))**2 + (Z(1) - Z(MM))**2)
      SINPHI(1) = ((Y(1)-Y(MM))/(SIDE(1)))
      COSPHI(1) = ((Z(1)-Z(MM))/(SIDE(1)))
C
C GENERATE CONTROL POINT LOCATIONS.
      DO 24 I = 2,LL
      YCPT(I) = (Y(I)+Y(I-1))/(2.)
```

```
24    ZCPT(I) = (Z(I)+Z(I-1))/(2.)
      ZCPT(1) = (Z(1)+Z(MM))/(2.)
      YCPT(1) = (Y(1)+Y(MM))/(2.)
      MMM = NN - 1
      DO 25 I = 1,MMM
25    XCPT(I) = (X(I+1) + X(I))/(2.)
      XCPT(NN) = X(NN) + DELTAX/2.0
C
C GENERATE TUNNEL CROSS SECTIONAL AREA.
      AREA = 0.0
      J = MM
      DO 30 I = 1,MM
      AREA = AREA + ABS(Y(I)-Y(J))*ABS(Z(I)+Z(J))
30    J = I
      AREA = AREA/2.
C
C RETURN TO CALLING PROGRAM.
C
      RETURN
      END
```

```
      SUBROUTINE MATRIX (X,Y,Z,XCPT,YCPT,ZCPT,SINPHI,COSPHI,SIDE,S,CC,
     1MM,NN,LL,KK,N1,NK,OPT1,OPT2,R,HL,HD,HYZ,ID,JD,KD,LD,MD)
C
C THIS IS A SUBROUTINE TO GENERATE THE MATRIX OF COEFFICIENTS FOR THE
C SPECIAL CASE OF VERTICAL SYMMETRY.
C
      LOGICAL OPT1,OPT2
      INTEGER A,B,C,D,E
      DIMENSION X(ID),Y(KD),Z(KD),SINPHI(KD),COSPHI(KD),XCPT(JD),
     1YCPT(LD),ZCPT(LD),R(ID,KD),SIDE(KD),CC(MD,MD),HL(ID,KD),HD(KD),
     1S(JD),HYZ(KD)
      P = 25.13274
C CYCLE THROUGH CONTROL POINTS.
      M = 0
      DO 50 I=1,NN
      DO 49 J = 1,KK
      M = M + 1
C
C SELECT VARIABLES FOR THIS CONTROL POINT.
      SINJ = SINPHI(J)
      COSJ = COSPHI(J)
      XCI = XCPT(I)
      YCJ = YCPT(J)
      ZCJ = ZCPT(J)
C
C
C GENERATE COORDINATES OF VORTEX RECTANGLES RELATIVE TO PRESENT CONTROL
C POINT.
      DO 26 JJ=1,MM
      HD(JJ) = SQRT((YCJ-Y(JJ))**2 + (ZCJ-Z(JJ))**2)
      HYZ(JJ)=SQRT(((ZCJ-Z(JJ))*SINPHI(JJ) - (YCJ-Y(JJ))*COSPHI(JJ))**2)
      DO 26 II=1,N1
      R(II,JJ)=SQRT((XCI-X(II))**2+(YCJ-Y(JJ))**2+(ZCJ-Z(JJ))**2)
25    HL(II,JJ)=SQRT((X(II)-XCI)**2 + HYZ(JJ)**2)
C
C CYCLE THROUGH VORTEX UNKNOWNS.
      N = 0
      DO 48 K=1,NN
      DO 47 L=1,KK
      N = N + 1
C
C
C SELECT VARIABLES FOR THIS PARTICULAR RECTANGLE OR RECTANGLES.
      B = L
      E = K+1
      MNIMIZ = 0
101   IF (OPT1) GO TO 15
      A = B-1
      C = 2*LL-B
      D = C-1
      IF (B-1) 50,29,27
27    IF (LL-B) 50,29,28
15    IF (B-1) 50,18,17
17    IF (LL-B) 50,19,11
11    A = B-1
      C = MM-A
```

```
      D = MM-B
      GO TO 28
18    A = MM
      C = MM
      D = MM-1
      GO TO 28
19    A = LL-1
      C = LL+1
      D = LL
      GO TO 28
28    RKA = R(K,A)
      RKC = R(K,C)
      REA = R(E,A)
      REC = R(E,C)
      HLKC = HL(K,C)
      HLEC = HL(E,C)
      HDA = HD(A)
      HDC = HD(C)
      YA = Y(A)
      ZA = Z(A)
      ZC = Z(C)
      HYZA = HYZ(A)
      HYZC = HYZ(C)
29    SINL = SINPHI(B)
      COSL = COSPHI(B)
      RKB = R(K,B)
      RKD = R(K,D)
      REB = R(E,B)
      RED = R(E,D)
      HLKB = HL(K,B)
      HLEB = HL(E,B)
      HDB = HD(B)
      HDD = HD(D)
      SIDEB = SIDE(B)
      DK=S(K)
      YB = Y(B)
      ZB = Z(B)
      ZD = Z(D)
      XK = X(K)
      XE = X(E)
      HYZB = HYZ(B)
      HYZD = HYZ(D)
C
C
C COMPUTE VELOCITY COMPONENTS INDUCED BY RECTANGLE OR RECTANGLES,
C TAKE ANY SPECIAL CASES INTO ACCOUNT.
      IF (COSJ.EQ.0.00000) GO TO 35
      IF (B-1) 50,16,31
31    IF (LL-B) 50,16,32
15    IF (.NOT.OPT1) GO TO 33
32    IF (COSL.EQ.0.00000) GO TO 62
      VY=(COSL/(P*SIDEB)*(-((RKA+RKB)*(SIDEB**2-(RKA-RKB)**2)/((
     2HLKB**2)*RKA*RKB) + (RKD+RKC)*(SIDEB**2 -(RKC-RKD)**2)/((HLKC**2)
     2*RKC*RKD))*(XK-XCI) + ((REA+REB)*(SIDEB**2 -(REA-REB)**2)/((
     2HLEB**2)*REA*REB) + (REC+RED)*(SIDEB**2 -(REC-RED)**2)/((HLEC**2)
     2*REC*RED))*(XE-XCI)) + 1./(P*DK)*(((RKB+REB)*(DK**2 -(
```

```
     2RKB-REB)**2)/((HDB**2)*RKB*REB))*(ZB-ZCJ)-((RKD+RED)*(DK**2-(RKD-
     2RED)**2)/((HDD**2)*RKD*RED))*(ZD-ZCJ)+((RKC+REC)*(DK**2-(RKC-REC)
     2**2)/((HDC**2)*RKC*REC))*(ZC-ZCJ)-((RKA+REA)*(DK**2-(RKA-REA)**2)
     2/((HDA**2)*RKA*REA))*(ZA-ZCJ)))
      GO TO 36
62    VY =                          (1./(P*DK)*(((RKB+REB)*(DK**2 -(
     2RKB-REB)**2)/((HDB**2)*RKB*REB))*(ZB-ZCJ)-((RKD+RED)*(DK**2-(RKD-
     2RED)**2)/((HDD**2)*RKD*RED))*(ZD-ZCJ)+((RKC+REC)*(DK**2-(RKC-REC)
     2**2)/((HDC**2)*RKC*REC))*(ZC-ZCJ)-((RKA+REA)*(DK**2-(RKA-REA)**2)
     2/((HDA**2)*RKA*REA))*(ZA-ZCJ)))
      GO TO 36
33    IF (COSL.EQ.0.00000) GO TO 63
      VY = (COSL/(P*SIDEB)*(-((RKD+RKB)*(SIDEB**2-(RKD-RKB)**2)/((
     2HLKB**2)*RKD*RKB))*(XK-XCI) + ((RED+REB)*(SIDEB**2 -(RED-REB)**
     22)/((HLEB**2)*RED*REB))*(XE-XCI)) + 1./(P*DK)*(((RKB+REB)*(DK**
     22-(RKB-REB)**2)/((HDB**2)*RKB*REB))*(ZB-ZCJ)-((RKD+RED)*(DK**2-
     2(RKD-RED)**2)/((HDD**2)*RKD*RED))*(ZD-ZCJ)))
      GO TO 36
63    VY =                                    (1./(P*DK)*(((RKB+REB)*(DK**
     22-(RKB-REB)**2)/((HDB**2)*RKB*REB))*(ZB-ZCJ)-((RKD+RED)*(DK**2-
     2(RKD-RED)**2)/((HDD**2)*RKD*RED))*(ZD-ZCJ)))
      GO TO 36
35    VY = 0.00000
36    IF (SINJ.EQ.0.00000) GO TO 42
      IF (B-1) 50,55,38
38    IF (LL-B) 50,55,39
55    IF (.NOT.OPT1) GO TO 40
39    IF (SINL.EQ.0.00000) GO TO 64
      VZ = (SINL/(P*SIDEB)*(((RKA+RKB)*(SIDEB**2 -(RKA-RKB)**2)/((
     3HLKB**2)*RKA*RKB) - (RKC+RKD)*(SIDEB**2 -(RKC-RKD)**2)/((HLKC**2)
     3*RKC*RKD))*(XK-XCI) + ((REC+RED)*(SIDEB**2 -(REC-RED)**2)/((
     3HLEC**2)*REC*RED) - (REA+REB)*(SIDEB**2 -(REA-REB)**2)/((HLEB**2)
     3*REA*REB))*(XE-XCI)) + 1./(P*DK)*(((RKA+REA)*(DK**2 -(RKA
     3-REA)**2)/((HDA**2)*RKA*REA) - (RKC+REC)*(DK**2 -(RKC-REC)**2)/((
     3HDC**2)*RKC*REC))*(YA-YCJ)  +  ((RKD+RED)*(DK**2 -(RKD-RED)**2)/
     3((HDD**2)*RKD*RED) - (RKB+REB)*(DK**2 -(RKB-REB)**2)/((HDB**2)*
     3RKB*REB))*(YB-YCJ)))
      GO TO 43
64    VZ =                      (1./(P*DK)*(((RKA+REA)*(DK**2 -(RKA
     3-REA)**2)/((HDA**2)*RKA*REA) - (RKC+REC)*(DK**2 -(RKC-REC)**2)/((
     3HDC**2)*RKC*REC))*(YA-YCJ)  +  ((RKD+RED)*(DK**2 -(RKD-RED)**2)/
     3((HDD**2)*RKD*RED) - (RKB+REB)*(DK**2 -(RKB-REB)**2)/((HDB**2)*
     3RKB*REB))*(YB-YCJ)))
      GO TO 43
40    VZ = (1./(P*DK)*(((RKD+RED)*(DK**2 -(RKD-RED)**2)/((HDD**2)*RKD*
     3RED) -(RKB + REB)*(DK**2-(RKB-REB)**2)/((HDB**2)*RKB*REB))*
     3(YB-YCJ)))
      GO TO 43
42    VZ = 0.00000
43    IF (MNIMIZ) 50,105,106
105   B = LL+1-B
      MNIMIZ = 1
C
C STORE NORMAL VELOCITY IN CC ARRAY, ACCOUNT FOR VERTICAL SYMMETRY.
      CC1 = VY*COSJ - VZ*SINJ
      GO TO 101
```

```
106   CC(M,N) = CC1 - VY*COSJ + VZ*SINJ
C
47    CONTINUE
48    CONTINUE
49    CONTINUE
50    CONTINUE
C
C THE MATRIX IS COMPLETE, RETURN TO CALLING PROGRAM.
C
      RETURN
      END
```

```
      SUBROUTINE INVR(A,N,ISIZE)
C
C THIS IS A SUBROUTINE TO INVERT THE MATRIX A.
C THE INPUT MATRIX A IS DESTROYED AND REPLACED BY ITS INVERSE.
C A IS ASSUMED TO CONTAIN N ROWS AND COLUMNS OF DATA.
C A IS ASSUMED TO BE DIMENSIONED ISIZE BY ISIZE.
C
C
      DIMENSION IPIVOT(100),A(ISIZE,ISIZE),INDEX(100,2),PIVOT(100)
      EQUIVALENCE (IROW,JROW),(ICOLUM,JCOLUM),(AMAX,T,SWAP)
C
C
   15 DO 20 J=1,N
   20 IPIVOT(J)=0
   30 DO 550 I=1,N
C
C     SEARCH FOR PIVOT ELEMENT
C
   40 AMAX=0.0
   45 DO 105 J=1,N
   50 IF (IPIVOT(J)-1) 60, 105, 60
   60 DO 100 K=1,N
   70 IF (IPIVOT(K)-1) 80, 100, 740
   80 IF(ABS(AMAX)-ABS(A(J,K)))85,100,100
   85 IROW=J
   90 ICOLUM=K
   95 AMAX=A(J,K)
  100 CONTINUE
  105 CONTINUE
  110 IPIVOT(ICOLUM)=IPIVOT(ICOLUM)+1
C
C     INTERCHANGE ROWS TO PUT PIVOT ELEMENT ON DIAGONAL
C
  130 IF (IROW-ICOLUM) 140, 250, 140
  140 CONTINUE
  150 DO 200 L=1,N
  160 SWAP=A(IROW,L)
  170 A(IROW,L)=A(ICOLUM,L)
  200 A(ICOLUM,L)=SWAP
  260 INDEX(I,1)=IROW
  270 INDEX(I,2)=ICOLUM
  310 PIVOT(I)=A(ICOLUM,ICOLUM)
C
C     DIVIDE PIVOT ROW BY PIVOT ELEMENT
C
  330 A(ICOLUM,ICOLUM)=1.0
  340 DO 350 L=1,N
  350 A(ICOLUM,L)=A(ICOLUM,L)/PIVOT(I)
C
C     REDUCE NON-PIVOT ROWS
C
  380 DO 550 L1=1,N
  390 IF(L1-ICOLUM) 400, 550, 400
  400 T=A(L1,ICOLUM)
  420 A(L1,ICOLUM)=0.0
  430 DO 450 L=1,N
```

```
  450 A(L1,L)=A(L1,L)-A(ICOLUM,L)*T
  550 CONTINUE
C
C     INTERCHANGE COLUMNS
C
  600 DO 710 I=1,N
  610 L=N+1-I
  620 IF (INDEX(L,1)-INDEX(L,2)) 630, 710, 630
  630 JROW=INDEX(L,1)
  640 JCOLUM=INDEX(L,2)
  650 DO 705 K=1,N
  660 SWAP=A(K,JROW)
  670 A(K,JROW)=A(K,JCOLUM)
  700 A(K,JCOLUM)=SWAP
  705 CONTINUE
  710 CONTINUE
  740 RETURN
      END
```

```
      SUBROUTINE RHS(SPAN,XM,YM,ZM,GAMAM,XCPT,YCPT,ZCPT,SINPHI,
     1COSPHI,GAMAK,JD,KD,LD,MD,NN,KK)
C
C THIS IS A SUBROUTINE TO COMPUTE THE RIGHT HAND SIDE OF THE
C MATRIX EQUATION FOR THE STRAIGHT WAKE IN WIND TUNNEL PROGRAM.
C
C
      DIMENSION XCPT(JD),YCPT(LD),ZCPT(LD),SINPHI(KD),COSPHI(KD),
     1ZM(2),GAMAK(MD)
C
C GENERATE MODEL COORDINATES FOR USE IN GENERATING THE GAMAK MATRIX AND
C FOR LATER USE IN THE SURVEY SUBROUTINE.
      GAMAM = 1.0
      I = NN/2 + 1
      XM = XCPT(I)
      YM = 0.0
      ZM(1) = SPAN/2.
      ZM(2) = -ZM(1)
      ZM1 = ZM(1)
      ZM2 = ZM(2)
C
C GENERATE THE RIGHT HAND SIDE OF THE MATRIX EQUATION.
      P = 25.13274
C
C CYCLE THROUGH CONTROL POINTS.
      M = 0
      DO 50 I = 1,NN
      DO 59 J = 1,KK
      M = M + 1
C
C SELECT VARIABLES FOR THIS CONTROL POINT.
      SINJ = SINPHI(J)
      COSJ = COSPHI(J)
      XCI = XCPT(I)
      YCJ = YCPT(J)
      ZCJ = ZCPT(J)
C
C COMPUTE VELOCITY INDUCED AT CONTROL POINT BY MODEL.
      RM1 = SQRT((XM-XCI)**2 + (YM - YCJ)**2 + (ZM(1) - ZCJ)**2)
      RM2 = SQRT((XM-XCI)**2 + (YM - YCJ)**2 + (ZM(2)-ZCJ)**2)
      HM1 = SQRT((YCJ-YM)**2 + (ZCJ - ZM(1))**2)
      HM2 = SQRT((YCJ - YM)**2 + (XCI-XM)**2)
      HM3 = SQRT((YCJ-YM)**2 + (ZCJ-ZM(2))**2)
      IF (COSJ.EQ.0.00000) GO TO 51
      VYM = GAMAM*((RM1+RM2)*(SPAN**2 -(RM1-RM2)**2)*(XM-XCI)/(P*SPAN*
     2RM1*RM2*(HM2**2))+2./P*((1.+(XCI-XM)/(RM1))*(ZCJ-ZM1)/(HM1**2)+
     2(1.+(XCI-XM)/(RM2))*(ZM2-ZCJ)/(HM3**2)))
      GO TO 52
51    VYM=0.00000
52    IF (SINJ.EQ.0.00000) GO TO 53
      VZM = GAMAM*((YCJ-YM)*2./P)*((1. +(XCI-XM)/RM2)/(HM3**2) - (1. +(
     3XCI-XM)/(RM1))/(HM1**2))
      GO TO 54
53    VZM = 0.00000
C
C STORE NORMAL VELOCITY COMPONENT IN GAMAK ARRAY.
```

```
54    GAMAK(M)  = VZM*SINJ - VYM*COSJ
59    CONTINUE
60    CONTINUE
C
C RIGHT HAND SIDE IS COMPLETE, RETURN TO CALLING PROGRAM.
      RETURN
      END
```

```
      SUBROUTINE SURVEY (XTP,YTP,ZTP,X,Y,Z,XM,YM,ZM,SINPHI,COSPHI,S,
     1GAMA,SIDE,OPT1,SPAN,GAMAM,VXC,VYC,VZC,VXT,VYT,VZT,VXM,VYM,VZM,
     1LL,MM,NN,N1,R,HL,HD,HYZ,ID,JD,KD,LD    )
C
C THIS IS A SUBROUTINE TO COMPUTE VELOCITY COMPONENTS AT COORDINATES
C XTP, YTP,ZTP.
C
      LOGICAL OPT1
      INTEGER A,B,C,D,E
      DIMENSION X(ID),Y(KD),Z(KD),SINPHI(KD),COSPHI(KD),
     1                    R(ID,KD),SIDE(KD),HL(ID,KD),HD(KD),S(JD),
     1GAMA(JD,LD),ZM(2),HM(3),HYZ(KD),RM(2)
C
C DEFINE POSITION OF MODEL AND VORTEX RECTANGLES RELATIVE TO SURVEY
C POINT.
      ZM1 = ZM(1)
      ZM2 = ZM(2)
601   RM(1) = SQRT((XM-XTP)**2 + (YM - YTP)**2 + (ZM(1) - ZTP)**2)
      RM(2) = SQRT((XM-XTP)**2 + (YM - YTP)**2 + (ZM(2)-ZTP)**2)
      HM1 = SQRT((YTP-YM)**2 + (ZTP - ZM(1))**2)
      HM2 = SQRT((YTP - YM)**2 + (XTP-XM)**2)
      HM3 = SQRT((YTP-YM)**2 + (ZTP-ZM(2))**2)
      DO 127 J = 1,MM
      HD(J) = SQRT((YTP-Y(J))**2 + (ZTP - Z(J))**2)
      HYZ(J) = SQRT(((ZTP-Z(J))*SINPHI(J)-(YTP-Y(J))*COSPHI(J))**2)
      DO 127 I = 1,N1
      R(I,J) = SQRT((XTP-X(I))**2 + (YTP-Y(J))**2 + (ZTP-Z(J))**2)
127   HL(I,J)=SQRT((X(I)-XTP)**2 + HYZ(J)**2)
      VXC = 0.0
      VYC = 0.0
      VZC = 0.0
C
C CYCLE THROUGH VORTEX STRENGTHS.
      DO 150 K = 1,NN
      DO 150 L = 1,LL
C
C SELECT PARAMETERS FOR THIS PARTICULAR VORTEX STRENGTH.
      B = L
      E = K+1
      IF (OPT1) GO TO 110
      A = L-1
      C = LL*2-L
      D = C-1
      IF (L-1) 150,129,125
125   IF (LL-L) 150,129,128
110   IF (L-1) 150,113,111
111   IF (LL-L) 150,114,112
112   A = L-1
      C = MM-A
      D = MM-B
      GO TO 128
113   A = MM
      C = MM
      D = MM-1
      GO TO 128
114   A = LL-1
```

```
      C = LL+1
      D = LL
      GO TO 128
128   RKA = R(K,A)
      RKC = R(K,C)
      REA = R(E,A)
      REC = R(E,C)
      HLKC = HL(K,C)
      HLEC = HL(E,C)
      HDA = HD(A)
      HDC = HD(C)
      YA = Y(A)
      ZA = Z(A)
      ZC = Z(C)
      HYZA = HYZ(A)
      HYZC = HYZ(C)
129   SINL = SINPHI(L)
      COSL = COSPHI(L)
      RKB = R(K,B)
      RKD = R(K,D)
      REB = R(E,B)
      RED = R(E,D)
      HLKB = HL(K,B)
      HLEB = HL(E,B)
      HDB = HD(B)
      HDD = HD(D)
      SIDEB = SIDE(B)
      DK = S(K)
      YB = Y(B)
      ZB = Z(B)
      ZD = Z(D)
      XK = X(K)
      XE = X(E)
      HYZB = HYZ(B)
      HYZD = HYZ(D)
      P = 25.13274
C
C COMPUTE VELOCITY INDUCED BY VORTEX RECTANGLE OR RECTANGLES, TAKE ANY
C SPECIAL CASES INTO ACCOUNT.
      IF (L-1) 150,115,131
131   IF (LL-L) 150,115,132
115   IF (OPT1) GO TO 132
130   VXPS = 0.0
      VYPS = 0.0
      VZPS = 0.0
      IF (YTP.EQ.0.0) GO TO 200
      VXPS = 1./(P*SIDEB)*(HYZB*((RKD+RKB)*(SIDEB**2-(RKD-RKB)**2)/((
     1HLKB**2)*RKD*RKB) - (RED+REB)*(SIDEB**2-(RED-REB)**2)/((HLEB**2)
     1*RED*REB)))*GAMA(K,L)
200   IF (COSL.EQ.0.0) GO TO 66
      VYPS = (COSL/(P*SIDEB)*(-((RKD+RKB)*(SIDEB**2-(RKD-RKB)**2)/((
     2HLKB**2)*RKD*RKB))*(XK-XTP) + ((RED+REB)*(SIDEB**2 -(RED-REB)**
     22)/((HLEB**2)*RED*REB))*(XE-XTP)) + 1./(P*DK)*(((RKB+REB)*(DK**
     22-(RKB-REB)**2)/((HDB**2)*RKB*REB))*(ZB-ZTP)-((RKD+RED)*(DK**2-
     2(RKD-RED)**2)/((HDD**2)*RKD*RED))*(ZD-ZTP)))*GAMA(K,L)
      GO TO 67
```

```
65     VYPS =                            (1./(P*DK)*(((RKB+REB)*(DK**
      22-(RKB-REB)**2)/((HDB**2)*RKB*REB))*(ZB-ZTP)-((RKD+RED)*(DK**2-
      2(RKD-RED)**2)/((HDD**2)*RKD*RED))*(ZD-ZTP)))*GAMA(K,L)
67     IF (YTP.EQ.0.0) GO TO 201
       IF (ZTP.EQ.0.0) GO TO 201
       VZPS = (1./(P*DK)*(((RKD+RED)*(DK**2 -(RKD-RED)**2)/((HDD**2)*RKD*
      3RED) -(RKB + REB)*(DK**2-(RKB-REB)**2)/((HDB**2)*RKB*REB))*
      3(YB-YTP)))*GAMA(K,L)
201    VXC = VXC + VXPS
       VYC = VYC + VYPS
       VZC = VZC + VZPS
       GO TO 150
132    VX = 0.0
       VY = 0.0
       VZ = 0.0
       IF (YTP.EQ.0.0) GO TO 202
       VX =(1./(P*SIDEB)*((HYZB*((RKA+RKB)*(SIDEB**2 -(RKA-RKB)**2)/((
      1HLKB**2)*RKA*RKB) - (REA+REB)*(SIDEB**2 -(REA-REB)**2)/((HLEB**2)
      1*REA*REB))) + (HYZC*((RKD+RKC)*(SIDEB**2 -(RKD-RKC)**2)/((
      1HLKC**2)*RKC*RKD) - (RED+REC)*(SIDEB**2 -(RED-REC)**2)/((HLEC**2)
      1*REC*RED)))))*GAMA(K,L)
202    IF (COSL.EQ.0.0) GO TO 68
       VY=(COSL/(P*SIDEB)*(-((RKA+RKB)*(SIDEB**2-(RKA-RKB)**2)/((
      2HLKB**2)*RKA*RKB) + (RKD+RKC)*(SIDEB**2 -(RKC-RKD)**2)/((HLKC**2)
      2*RKC*RKD))*(XK-XTP) + ((REA+REB)*(SIDEB**2 -(REA-REB)**2)/((
      2HLEB**2)*REA*REB) + (REC+RED)*(SIDEB**2 -(REC-RED)**2)/((HLEC**2)
      2*REC*RED))*(XE-XTP)) + 1./(P*DK)*(((RKB+REB)*(DK**2 -(
      2RKB-REB)**2)/((HDB**2)*RKB*REB))*(ZB-ZTP)-((RKD+RED)*(DK**2-(RKD-
      2RED)**2)/((HDD**2)*RKD*RED))*(ZD-ZTP)+((RKC+REC)*(DK**2-(RKC-REC)
      2**2)/((HDC**2)*RKC*REC))*(ZC-ZTP)-((RKA+REA)*(DK**2-(RKA-REA)**2)
      2/((HDA**2)*RKA*REA))*(ZA-ZTP)))*GAMA(K,L)
       GO TO 69
68     VY =                    (1./(P*DK)*(((RKB+REB)*(DK**2 -(
      2RKB-REB)**2)/((HDB**2)*RKB*REB))*(ZB-ZTP)-((RKD+RED)*(DK**2-(RKD-
      2RED)**2)/((HDD**2)*RKD*RED))*(ZD-ZTP)+((RKC+REC)*(DK**2-(RKC-REC)
      2**2)/((HDC**2)*RKC*REC))*(ZC-ZTP)-((RKA+REA)*(DK**2-(RKA-REA)**2)
      2/((HDA**2)*RKA*REA))*(ZA-ZTP)))*GAMA(K,L)
69     IF (YTP.EQ.0.0) GO TO 71
       IF (ZTP.EQ.0.0) GO TO 71
       IF (SINL.EQ.0.00000) GO TO 70
       VZ = (SINL/(P*SIDEB)*(((RKA+RKB)*(SIDEB**2 -(RKA-RKB)**2)/((
      3HLKB**2)*RKA*RKB) - (RKC+RKD)*(SIDEB**2 -(RKC-RKD)**2)/((HLKC**2)
      3*RKC*RKD))*(XK-XTP) + ((REC+RED)*(SIDEB**2 -(REC-RED)**2)/((
      3HLEC**2)*REC*RED) - (REA+REB)*(SIDEB**2 -(REA-REB)**2)/((HLEB**2)
      3*REA*REB))*(XE-XTP)) + 1./(P*DK)*(((RKA+REA)*(DK**2 -(RKA
      3-REA)**2)/((HDA**2)*RKA*REA) - (RKC+REC)*(DK**2 -(RKC-REC)**2)/((
      3HDC**2)*RKC*REC))*(YA-YTP) + ((RKD+RED)*(DK**2 -(RKD-RED)**2)/
      3((HDD**2)*RKD*RED) - (RKB+REB)*(DK**2 -(RKB-REB)**2)/((HDB**2)*
      3RKB*REB))*(YB-YTP)))*GAMA(K,L)
       GO TO 71
70     VZ =                   (1./(P*DK)*(((RKA+REA)*(DK**2 -(RKA
      3-REA)**2)/((HDA**2)*RKA*REA) - (RKC+REC)*(DK**2 -(RKC-REC)**2)/((
      3HDC**2)*RKC*REC))*(YA-YTP) + ((RKD+RED)*(DK**2 -(RKD-RED)**2)/
      3((HDD**2)*RKD*RED) - (RKB+REB)*(DK**2 -(RKB-REB)**2)/((HDB**2)*
      3RKB*REB))*(YB-YTP)))*GAMA(K,L)
71     VXC = VXC + VX
```

```
      VYC = VYC + VY
      VZC = VZC + VZ
150   CONTINUE
C
C COMPUTE VELOCITY INDUCED BY MODEL.
      RM1 = RM(1)
      RM2 = RM(2)
      VXM = 0.0
      VYM = 0.0
      VZM = 0.0
      IF (HM1.LT.1.E-10) GO TO 155
      VYM = GAMAM*2./P*(1.+(XTP-XM)/RM1)/(HM1**2)
      VZM = -VYM*(YTP-YM)
      VYM = VYM*(ZTP-ZM1)
155   IF (HM3.LT.1.E-10) GO TO 160
      VXM = GAMAM*2./P*(1.+(XTP-XM)/RM2)/(HM3**2)
      VZM = VXM*(YTP-YM) + VZM
      VYM = VXM*(ZM2-ZTP) + VYM
      VXM = 0.0
160   IF (HM2.LT.1.E-10) GO TO 165
      VXM = GAMAM*(RM1+RM2)*(SPAN**2-(RM1-RM2)**2)/(P*SPAN*RM1*RM2*
     1(HM2**2))
      VYM = VYM + VXM*(XM-XTP)
      VXM = VXM*(YTP-YM)
C
C COMPUTE TOTAL VELOCITY COMPONENTS.
165   VXT = VXC + VXM
      VYT = VYC + VYM
      VZT = VZC + VZM
      RETURN
      END
```

```
C                                 APPENDIX D
C
C          PROGRAM TO COMPUTE NON-LINEAR WIND TUNNEL WALL INTERFERENCE
C                  FACTORS FOR HIGHLY LOADED LIFTING SYSTEMS
C
      PROGRAM WINGT (INPUT,OUTPUT,TAPE5=INPUT,TAPE6=OUTPUT)
C
C THIS PROGRAM IS WRITTEN IN FORTRAN IV FOR THE CDC 6400 COMPUTER.
C APPROXIMATE STORAGE REQUIREMENT IS 52000 (OCTAL).
C EXECUTION TIME IS APPROXIMATELY 230 SECONDS PER CASE WITH 29 TRAILING
C SEGMENTS, 7 ITERATIONS, AND 100 SURVEY POINTS.
C
C THE WIND TUNNEL CROSS-SECTION MUST HAVE A PLANE OF LATERAL SYMMETRY
C AND MUST REMAIN CONSTANT OVER THE LENGTH OF THE TUNNEL
C
C INPUT DATA SEQUENCE
C
C I (I1)
C     AN INTEGER PARAMETER WHICH DETERMINES THE Z COORDINATE OF TOP
C     AND BOTTOM CENTER CONTROL POINTS.  IF I.NE.1 THESE CONTROL POINTS
C     WILL BE LOCATED ON THE CENTERPLANE OF THE TUNNEL (I.E. Z=0.0).
C     IF I.EQ.1 THESE CONTROL POINTS WILL BE LOCATED AT Z(1)/2
C
C MM, NN (2I2)
C     MM IS THE NUMBER OF COORDINATE PAIRS DEFINING THE COMPLETE CROSS-
C     SECTIONAL SHAPE OF THE TUNNEL. MM CANNOT EXCEED 20.
C     NN IS THE NUMBER OF VORTEX RECTANGLES MAKING UP THE LENGTH OF
C     THE TUNNEL. NN CANNOT EXCEED 14.
C
C Y(I), Z(I) (2F10.5)
C     Y AND Z ARE THE COORDINATES, IN FEET, OF THE POINTS DEFINING THE
C     CROSS-SECTION SHAPE OF THE TUNNEL.  MM CARDS ARE REQUIRED.
C     THE ORIGIN OF THE COORDINATE SYSTEM IS TAKEN ON THE TUNNEL CENTER
C     LINE WITH X POSITIVE DOWNSTREAM, Y POSITIVE UPWARD, AND Z POSITIVE
C     TO THE RIGHT LOOKING DOWNSTREAM. THE FIRST CARD IN THE SEQUENCE IS
C     THE FIRST COORDINATE TO THE RIGHT (POSITIVE Z) OF THE POSITIVE Y
C     AXIS, AND SUBSEQUENT POINTS ARE TAKEN CLOCKWISE AROUND THE TUNNEL.
C     SEGMENT LENGTHS BETWEEN ADJACENT POINTS SHOULD BE EQUAL, EXCEPT
C     THAT, IF CONVENIENT SPACING REQUIRES POINTS ON TOP AND BOTTOM
C     CENTER LINE, THOSE POINTS ARE OMITTED AND THE FIRST DATA CARD
C     ABOVE, I, IS SET TO 1.0.
C
C DELTAX (F10.5)
C     LENGTH IN FEET OF THE VORTEX RECTANGLES IN THE STREAMWISE
C     DIRECTION. SHOULD BE EQUAL TO THE LENGTH OF SEGMENTS IN THE
C     CROSS-SECTION.
C
C BVDATA (F10.5)
C     THE VORTEX SPAN OF THE WING IN FREE AIR WHICH PRODUCED THE PUNCHED
C     CARD DATA TO BE USED IN THIS PROGRAM.
C
C BVOTW (F10.5)
C     THE RATIO OF VORTEX SPAN TO MAXIMUM TUNNEL WIDTH TO BE USED IN
C     THIS COMPUTATION.
C
C YW(1) (F10.5)
```

```
C     THE VERTICAL LOCATION OF THE MODEL BOUND VORTEX IN THE TUNNEL.
C
C DELTAX (F10.5)
C     THE VORTEX SEGMENT LENGTH TO BE USED IN CONSTRUCTING THE
C     TRAILING VORTEX PAIR IN THE TUNNEL.  NEED NOT BE THE SAME
C     AS THAT USED IN THE FREE AIR PROGRAM, USUALLY SPAN/10
C
C ZMAX, YMIN  (2F10.5)
C     MAXIMUM Z COORDINATE AND MINIMUM Y COORDINATE TO BE ALLOWED
C     IN SURVEY OF WALL INTERFERENCE VALUES. THESE PARAMETERS WILL
C     BE USED TO DETERMINE IF A SURVEY POINT LIES TOO NEAR THE TUNNEL
C     FLOOR OR SIDE WALLS FOR ACCURATE INTERFERENCE COMPUTATION.
C
C SPAN, SPEED, GAMAM, ASPECT, FAL, VXWC, VYWC, ALFA. (4E20.10)
C     THESE THREE CARDS DEFINE THE MODEL TO BE USED IN THIS COMPUTATION,
C     AND ARE PART OF THE DECK PUNCHED BY THE WING-IN-FREE-AIR PROGRAM.
C     SPAN IS WING VORTEX SPAN, FEET.
C     SPEED IS REMOTE WIND SPEED IN THE TUNNEL, FEET/SECOND
C     GAMAM IS MODEL WING CIRCULATION, FEET SQUARED/SECOND. IF GAMAM IS
C     LESS THAN OR EQUAL TO ZERO, THE ZERO LIFT CASE IS PERFORMED.
C     ASPECT IS THE ASPECT RATIO OF THE WING.
C     FAL AND FAD ARE THE LIFT AND DRAG OF THE WING IN FREE AIR, POUNDS.
C     VXWC AND VYWC ARE VELOCITY COMPONENTS AT THE CENTER OF THE BOUND
C     VORTEX IN FREE AIR.
C     ALFA IS THE WING ANGLE OF ATTACK IN FREE AIR.
C
C XFA, YFA, ZFA, VXTOT, VYTOT, VZTOT. (4E20.10)
C     THESE ARE THE COORDINATES AND VELOCITIES SURVEYED BY THE
C     WING-IN-FREE-AIR PROGRAM AND PUNCHED IN A CARD DECK. THE
C     COORDINATES ARE REFERENCED TO THE WING.
C     NOTE THAT ZFA AND YFA ARE ALSO PROGRAM BRANCHING PARAMETERS.
C     IF (ZFA.EQ.10000.) THE PROGRAM TRANSFERS TO NEW MODEL DATA.
C     THEN IF (YFA.EQ.10000.) THE PRESENT MODEL WAKE COORDINATES
C     ARE USED FOR THE FIRST ITERATION OF THE NEW WING. THIS REDUCES
C     THE NUMBER OF ITERATIONS.
C
1     FORMAT (2I2)
2     FORMAT (2F10.5)
3     FORMAT (F10.5)
4     FORMAT (4F10.5)
5     FORMAT (1F10.5)
6     FORMAT (I2)
7     FORMAT (2F10.5)
8     FORMAT (I1)
9     FORMAT (I3,7F10.5)
11    FORMAT (4E20.10)
12    FORMAT (3F10.5)
13    FORMAT (5F10.5)
30    FORMAT (1H1,13X,19HTUNNEL  COORDINATES,/,/,14X,1HY,13X,1HZ,
     1(/,10X,F10.5,4X,F10.5))
31    FORMAT (/,/,15X,10HX STATIONS,(/,4X,5F6.2))
32    FORMAT (1H0,22HCROSS SECTIONAL AREA =,F10.4)
5000  FORMAT (1H0,14HTAIL LENGTH = ,F7.2,5X,14HTAIL HEIGHT = ,F6.2,5X,
     119HSPANWISE STATION = ,F6.2)
5010  FORMAT (1H ,13H(F.A.)  VX = ,F9.3,6X,5HVY = ,F9.3,6X,5HVZ = ,
     1F9.3,6X,8HALPHA = ,F7.4,6X,7HBETA = ,F7.4)
```

```
5020  FORMAT (1H ,13H(TUN.)  VX = ,F9.3,6X,5HVY = ,F9.3,6X,5HVZ = ,
     1F9.3,6X,8HALPHA = ,F7.4,6X,7HBETA = ,F7.4)
5030  FORMAT (1H ,13H(COR.)  VX = ,F9.3,6X,5HVY = ,F9.3,6X,5HVZ = ,
     1F9.3,6X,8HALPHA = ,F7.4,6X,7HBETA = ,F7.4)
5040  FORMAT (1H ,34HCORRECTION FACTORS   DEL(ALPHA) = ,F8.3,10X,12HDEL(
     1BETA) = ,F8.3,10X,5HDQ = ,F8.4)
5100  FORMAT (1H1,12HWING SPAN = ,F6.2,10X,8HGAMAM = ,F7.2,10X,15HASPECT
     1 RATIO = ,F6.2,10X,18HREMOTE VELOCITY = ,F8.2)
5110  FORMAT (1H ,23H(F.A. CENTER)   LIFT = ,F8.3,10X,7HDRAG = ,F7.4,
     110X,5HVX = ,F8.3,10X,5HVY = F8.3)
5120  FORMAT (1H ,23H(TUN. CENTER)   LIFT = ,F8.3,10X,7HDRAG = ,F7.4,
     110X,5HVX = ,F8.3,10X,5HVY = ,F8.3)
5130  FORMAT (1H ,23H(COR. CENTER)   LIFT = ,F8.3,10X,7HDRAG = ,F7.4,
     110X,5HVX = ,F8.3,10X,5HVY = ,F8.3)
5140  FORMAT (1H ,34HCORRECTION FACTORS   DEL(ALPHA) = ,F8.3,10X,
     15HDQ = ,F8.4)
      DIMENSION X(15),Y(20),Z(20),SINPHI(20),COSPHI(20),XCPT(14),
     1YCPT(10),ZCPT(10),R(15,20),SIDE(20),HL(15,20),HD(20),S(14),ZM(2),
     1HM(3),HYZ(20),RM(2),GL(10)
      DIMENSION CC(100,100),GAMA(14,10),GAMAK(100,1)
      DIMENSION XW(40),YW(40),ZW(40),RW(2,2),DSM(39),VBAR(2)
      LOGICAL STWK,OPT1
      REAL LIFT
      RHO = .002378
      YFA=0.0
14    CONTINUE
C
C READ DATA DESCRIBING TUNNEL FROM PUNCHED CARDS.
      READ (5,8) I
      OPT1 = I.EQ.1
34    READ (5,1) MM,NN
      READ (5,7) (Y(I),Z(I), I=1,MM)
      READ (5,3) DELTAX
C
C TEST DIMENSIONS
      IF ((MM.GT.20).OR.(NN.GT.14)) GO TO 906
C
C TEST SCALING OF TUNNEL, IF NECESSARY CHANGE SCALE SO THAT THE WING
C SPAN OF MODEL IN TUNNEL CORRESPONDS TO THAT OF MODEL IN FREE AIR.
      XCI = Z(1)
C READ SCALING DATA FROM PUNCHED CARDS.
      READ (5,3) BVDATA
      READ (5,3) BVOTW
      DO 35 I = 2,MM
      IF (Z(I).GT.XCI) XCI = Z(I)
35    CONTINUE
      YCJ = BVDATA/BVOTW/2.
      XCI = YCJ/XCI
C IF THE SCALING FACTOR IS UNITY DO NOT CHANGE TUNNEL SIZE.
      IF (XCI.EQ.1.) GO TO 37
      DO 36 I=1,MM
      Y(I) = Y(I)*XCI
      Z(I) = Z(I)*XCI
36    CONTINUE
      DELTAX = DELTAX*XCI
37    CONTINUE
```

```
C
C COMPUTE THE CROSS SECTIONAL AREA OF THE TUNNEL.
      AREA = 0.0
      DO 38 I = 2,MM
      AREA = AREA + ABS(Y(I)-Y(I-1))*ABS(Z(I)+Z(I-1))
38    CONTINUE
      AREA = AREA/2.
C
C
C NOW COMPUTE THE TUNNEL PARAMETERS TO BE USED IN THE COMPUTATION.
      LL = MM/2 + 1
      NL = NN * LL
      IF (NL.GT.100) GO TO 906
      NM = NN*MM
      N1 = NN + 1
      XCI = 0.0
      DO 20 I=1,NN
      X(I) = XCI
20    XCI = XCI + DELTAX
      X(N1) = 1000.0 + X(NN)
      DO 21 I = 1,NN
21    S(I)=X(I+1) - X(I)
      DO 23 I=2,MM
22    SIDE(I) = SQRT((Y(I) - Y(I-1))**2 + (Z(I) - Z(I-1))**2)
      SINPHI(I) = ((Y(I)-Y(I-1))/(SIDE(I)))
23    COSPHI(I) = ((Z(I)-Z(I-1))/(SIDE(I)))
      SIDE(1) = SQRT((Y(1) - Y(MM))**2 + (Z(1) - Z(MM))**2)
      SINPHI(1) = ((Y(1)-Y(MM))/(SIDE(1)))
      COSPHI(1) = ((Z(1)-Z(MM))/(SIDE(1)))
      DO 24 I = 2,LL
      YCPT(I) = (Y(I)+Y(I-1))/(2.)
24    ZCPT(I) = (Z(I)+Z(I-1))/(2.)
      ZCPT(1) = (Z(1)+Z(MM))/(2.)
      YCPT(1) = (Y(1)+Y(MM))/(2.)
      IF (.NOT.OPT1) GO TO 91
      ZCPT(1) = Z(1)/2.
      ZCPT(LL)=Z(LL-1)/2.
91    MMM=NN-1
      DO 25 I = 1,MMM
25    XCPT(I) = (X(I+1) + X(I))/(2.)
      XCPT(NN) = X(NN) + DELTAX/2.0
C ALL TUNNEL PARAMETERS HAVE BEEN COMPUTED.
C
C
C GENERATE THE MATRIX OF COEFFICIENTS.
      CALL MATRIX      (MM,NN,LL,N1,X,Y,Z,SINPHI,COSPHI,SIDE,S,XCPT,
     1YCPT,ZCPT,CC)
C
C INVERT THE MATRIX OF COEFFICIENTS.
      CALL INVR(CC,NL,100,100)
C
C WRITE A DESCRIPTION OF TUNNEL.
      WRITE (6,30) (Y(I),Z(I), I=1,MM)
      WRITE (6,31) (X(I), I=1,N1)
      WRITE (6,32) AREA
C
```

```
C READ MODEL INFORMATION FROM PUNCHED CARDS.
      READ (5,3) YW(1)
      READ (5,3) DELTAX
      READ (5,7) ZMAX,YMIN
15    CONTINUE
      READ (5,11) SPAN,SPEED,GAMAM,ASPECT,FAL,FAD,VXWC,VYWC,ALFA
      IF (EOF,5) 907,16
16    CONTINUE
      IF (YFA.EQ.10000.) GO TO 40
C
C NOW GENERATE MODEL PARAMETERS.
      IF (GAMAM.GT.0.0) NW=30
      I = NN/2
      XW(1) = X(I)
      XW(2) = XW(1)
      YW(2) = YW(1)
      ZW(1) = 0.0
      ZW(2) = SPAN/2.
      ZW(3) = ZW(2)
      STWK=(GAMAM.LE.0.0)
      IF (STWK) GO TO 18
      NW1 = NW + 1
      CHORD = SPAN/(ASPECT*.785398163**2)
      ALFAA = ASIN(GAMAM/(3.1415927*CHORD*SPEED))
      XCI = 0.75*CHORD*SQRT(1.-(.78539816**2))
      XW(3) = XW(2) + XCI*COS(ALFAA)
      YW(3) = YW(2) - XCI*SIN(ALFAA)
      XCI = DELTAX + XW(3)
      YCJ = YW(3)
      ZCJ = ZW(3)
      DO 90 N = 4,NW
      ZW(N) = ZCJ
      YW(N) = YCJ
      XW(N) = XCI
      XCI = XCI + DELTAX
90    CONTINUE
      XW(NW1) = XW(NW) + 1000.0
      YW(NW1) = YCJ
      ZW(NW1) = ZCJ
      GO TO 19
C
C IF THE STRAIGHT WAKE (ZERO LIFT COEFFICIENT) SOLUTION IS REQUIRED
C SET UP A HORSESHOE VORTEX MODEL.  SET SPEED TO 1000., GAMAM TO 1.0.
18    XW(3) = XW(2) + 1000.
      YW(3) = YW(2)
      SPEED = 1000.
      GAMAM = 1.0
C
C COMPUTE THE LIFT AND INDUCED DRAG OF THE WING IN FREE AIR.
      FAL = RHO*SPEED*SPAN*GAMAM
      FAD = RHO*(GAMAM**2)/3.14159
      NW = 2
      NW1 = NW + 1
19    DO 81 I = 1,NW
      J = I+1
81    DSM(I) = SQRT((XW(I)-XW(J))**2+(YW(I)-YW(J))**2+(ZW(I)-ZW(J))**2)
```

```
      Q = .5*RHO*SPEED**2
C
C BEGIN ITERATIVE PROCEDURE.  NUMIT IS THE NUMBER OF ITERATIONS TO BE
C USED.  IF THIS CASE REPRESENTS A SMALL CHANGE FROM A PREVIOUS
C EQUILIBRIUM STATE, REDUCE NUMIT.
      NUMIT = GAMAM/19. + 2.
40    CONTINUE
      IF (YFA.EQ.10000.) NUMIT = GAMAM/30. + 2.
900   DO 901 NUMBER = 1,NUMIT
C
C COMPUTE THE RIGHT HAND SIDE OF THE MATRIX EQUATION.
       CALL RHS      (XCPT,YCPT,ZCPT,XW,YW,ZW,DSM,GAMAM,SPAN,SPEED,
     1GAMAK,NN,LL,NW,SINPHI,COSPHI)
C
C COMPUTE THE VORTEX STRENGTHS.
1001  DO 101 I=1,NL
      J = (I-1)/LL + 1
      K = (1-J)*LL + I
      XCI = 0.0
      DO 100 L=1,NL
100   XCI = XCI+CC(I,L)*GAMAK(L,1)
      GAMA(J,K) = XCI
101   CONTINUE
C
C IF THIS IS WITHIN THREE ITERATIONS OF THE LAST WRITE COMPUTED VORTEX
C STRENGTHS.
      IF ((NUMIT-NUMBER).GE.3) GO TO 110
3999  FORMAT (19H1ITERATION NUMBER ,I2)
      WRITE (6,3999) NUMBER
500   FORMAT (30H0 CALCULATED VORTEX STRENGTHS )
      WRITE (6,500)
      DO 502 J = 1,NN
      WRITE (6,501) (GAMA(J,K), K=1,LL)
501   FORMAT (/,11F11.5)
502   CONTINUE
4000  FORMAT (27H1RESULTANT VORTEX STRENGTHS    )
4002  FORMAT (13H0RING NUMBER  ,I2,/,11F11.5)
4004  FORMAT (15H0SECTION NUMBER  ,I3 ,/, 11F11.5)
4010  WRITE (6,4000)
4015  DO 4140 L=1,N1
4020  M=L-1
4025  DO 4075 I=1,LL
4030  IF (L-2) 4050, 4060, 4040
4040  IF (L-N1) 4060, 4070, 4140
4050  GL(I) = GAMA(L,I)
4055  GO TO 4075
4060  GL(I) = GAMA(L,I) - GAMA(M,I)
4065  GO TO 4075
4070  GL(I) = -GAMA(M,I)
4075  CONTINUE
4080  WRITE (6,4002) L,(GL(I), I=1,LL)
4100  IF (L-N1) 4110, 4140, 4140
4110  DO 4125 I=2,LL
4115  J=I-1
4120  GL(J) = GAMA(L,J) - GAMA(L,I)
4125  CONTINUE
```

```
4130   MMM = LL - 1
4135   WRITE (6,4004) L,(GL(J),J=1,MMM)
4140   CONTINUE
C
C
C PERFORM WAKE ITERATION PROCESS.
110    CONTINUE
       CALL WKIT        (XW,YW,ZW,X,Y,Z,SINPHI,COSPHI,SIDE,S,GAMA,DSM,
     1GAMAM,SPEED,SPAN,NW,NN,MM,N1,LL,NW1,RHO,Q,FAL,FAD,CHORD,LIFT,DRAG,
     1STWK,VXTC,VYTC,ALPHAO,ALPHAI,ALFAA,VXMC,VYMC)
C
C IF THIS IS THE LINEAR CASE (ZERO LIFT COEFFICIENT) GO DIRECTLY TO
C WALL CORRECTION SURVEY, DO NOT PERFORM ANY ITERATIONS.
       IF (STWK) GO TO 810
901    CONTINUE
       GO TO 811
C
C COMPUTE VXWC AND VYWC FOR SPECIAL CASE OF ZERO LIFT COEFFICIENT.
810    VXWC = VXMC + SPEED
       VYWC=VYMC
C
C WRITE A DESCRIPTION OF MODEL AND TUNNEL OPERATING CONDITIONS.
811    WRITE (6,4240) GAMAM
4240   FORMAT (1H0,19HMODEL CIRCULATION =,F10.5)
       WRITE (6,4195) SPAN
4195   FORMAT (14H0VORTEX SPAN = ,F10.5)
       WRITE (6,4200) Q
4200   FORMAT (11H0TUNNEL Q =  ,F10.5)
       WRITE (6,4185) SPEED
4185   FORMAT (26H0TUNNEL NOMINAL VELOCITY =  ,F10.5)
       WRITE (6,5100) SPAN,GAMAM,ASPECT,SPEED
C
C WRITE FREE AIR RESULTS.
       WRITE (6,5110) FAL,FAD,VXWC,VYWC
C
C WRITE TUNNEL RESULTS.
       WRITE (6,5120) LIFT,DRAG,VXTC,VYTC
       FAL=FAL-LIFT
       FAD=FAD-DRAG
       DA=VXWC-VXTC
       DB=VYWC-VYTC
C
C WRITE CHANGES DUE TO TUNNEL.
       WRITE (6,5130) FAL,FAD,DA,DB
       DA=(ATAN(-VYWC/VXWC)-ATAN(-VYTC/VXTC))*AREA*Q/LIFT
       DQ=(VXWC**2+VYWC**2-VXTC**2-VYTC**2)/(SPEED**2)
C
C WRITE ANGLE OF ATTACK CORRECTION FACTOR AND DYNAMIC PRESSURE RATIO.
       WRITE (6,5140) DA,DQ
801    CONTINUE
       READ (5,11) XFA,YFA,ZFA,VXTOT,VYTOT,VZTOT
       IF (EOF,5) 907,802
802    CONTINUE
       IF (ZFA.EQ.10000.) GO TO 15
       IF (ZFA.GT.ZMAX) GO TO 801
       DA=ATAN(YFA/XFA)
```

```
      DB=ALFA+DA
      TL=SQRT(YFA**2+XFA**2)
      TH=TL*SIN(DB)
      TL=TL*COS(DB)
      XCI=XW(1)+TL*COS(ALFAA)+TH*SIN(ALFAA)
      YCJ=YW(1)-TL*SIN(ALFAA)+TH*COS(ALFAA)
      ZCJ=ZFA
      IF (YCJ.LT.YMIN) GO TO 801
      CALL XYZVEL        (XCI,YCJ,ZCJ,XW,YW,ZW,X,Y,Z,SINPHI,COSPHI,SIDE,S
     1,GAMA,DSM,GAMAM,SPEED,SPAN,NW,NN,MM,N1,LL,VXT,VYT,VZT,VXR,VYR,
     1VZR,VXM,VYM,VZM)
      IF (.NOT.STWK) GO TO 850
      VXTOT=VXM+SPEED
      VYTOT=VYM
      VZTOT=VZM
850   WRITE (6,5000) TL,TH,ZCJ
      ALPHA=ATAN(-VYTOT/VXTOT)
      BETA=ATAN(VZTOT/VXTOT)
      WRITE (6,5010) VXTOT,VYTOT,VZTOT,ALPHA,BETA
      DA=ATAN(-VYT/VXT)
      DB=ATAN(VZT/VXT)
      WRITE (6,5020) VXT,VYT,VZT,DA,DB
      DQ=VXTOT**2+VYTOT**2+VZTOT**2
      VXTOT=VXTOT-VXT
      VYTOT=VYTOT-VYT
      VZTOT=VZTOT-VZT
      DA=ALPHA-DA
      DB=BETA-DB
      WRITE (6,5030) VXTOT,VYTOT,VZTOT,DA,DB
      DA=DA*AREA*Q/LIFT
      DB=DB*AREA*Q/LIFT
      DQ=(DQ-(VXT**2+VYT**2+VZT**2))/(SPEED**2)
      WRITE (6,5040) DA,DB,DQ
      GO TO 801
906   CONTINUE
      WRITE (6,902)
902   FORMAT (52H0DIMENSIONED STORAGE EXCEEDED - EXECUTION TERMINATED   )
907   CONTINUE
      STOP
      END
```

```
      SUBROUTINE MATRIX (MM,NN,LL,N1,X,Y,Z,SINPHI,COSPHI,SIDE,S,XCPT,
     1YCPT,ZCPT,CC)
C
C THIS IS A SUBROUTINE TO COMPUTE THE MATRIX OF COEFFICIENTS.
C
      DIMENSION X(15),Y(20),Z(20),SINPHI(20),COSPHI(20),XCPT(14),
     1YCPT(10),ZCPT(10),R(15,20),SIDE(20),HL(15,20),HD(20),S(14),ZM(2),
     1HM(3),HYZ(20),RM(2),GL(10)
      DIMENSION CC(100,100)
      INTEGER A,B,C,D,E
      M = 0
C
C CYCLE THROUGH CONTROL POINTS (I.E. ROWS OF COEFFICIENT MATRIX).
      DO 50 I = 1,NN
      DO 49 J = 1,LL
      M = M + 1
C
C
C RECALL PARAMETERS FOR THIS CONTROL POINT, GENERATE PARAMETERS FOR
C VORTEX NET WITH RESPECT TO THIS CONTROL POINT.
      P = 25.13274
      SINJ = SINPHI(J)
      COSJ = COSPHI(J)
      XCI = XCPT(I)
      YCJ = YCPT(J)
      ZCJ = ZCPT(J)
37    DO 26 JJ=1,MM
      HD(JJ) = SQRT((YCJ-Y(JJ))**2 + (ZCJ-Z(JJ))**2)
      HYZ(JJ)=SQRT(((ZCJ-Z(JJ))*SINPHI(JJ) - (YCJ-Y(JJ))*COSPHI(JJ))**2)
      DO 26 II=1,N1
      R(II,JJ)=SQRT((XCI-X(II))**2+(YCJ-Y(JJ))**2+(ZCJ-Z(JJ))**2)
26    HL(II,JJ)=SQRT((X(II)-XCI)**2 + HYZ(JJ)**2)
      N = 0
C
C CYCLE THROUGH VORTEX RECTANGLES (I.E. COMPUTE ELEMENTS IN THIS ROW
C OF THE COEFFICIENT MATRIX).
      DO 48 K=1,NN
      DO 47 L=1,LL
      N = N + 1
C
C RECALL VARIABLES FOR THIS PARTICULAR VORTEX RECTANGLE PAIR.
      A = (L-1)
      B = L
      C = 2*LL-L
      D = C-1
      E = K+1
C
C IF THIS IS A SINGLE VORTEX ON THE TOP OR BOTTOM OF THE TUNNEL, NOT
C ALL PARAMETERS ARE NEEDED.
      IF (L-1) 50,29,27
27    IF (LL-L) 50, 29, 28
28    RKA = R(K,A)
      RKC = R(K,C)
      REA = R(E,A)
      REC = R(E,C)
      HLKC = HL(K,C)
```

```
      HLEC = HL(E,C)
      HDA = HD(A)
      HDC = HD(C)
      YA = Y(A)
      ZA = Z(A)
      ZC = Z(C)
      HYZA = HYZ(A)
      HYZC = HYZ(C)
29    SINL = SINPHI(L)
      COSL = COSPHI(L)
      RKB = R(K,B)
      RKD = R(K,D)
      REB = R(E,B)
      RED = R(E,D)
      HLKB = HL(K,B)
      HLEB = HL(E,B)
      HDB = HD(B)
      HDD = HD(D)
      SIDEB = SIDE(B)
      DK=S(K)
      YB = Y(B)
      ZB = Z(B)
      ZD = Z(D)
      XK = X(K)
      XE = X(E)
      HYZB = HYZ(B)
      HYZD = HYZ(D)
      IF (COSJ.EQ.0.00000) GO TO 35
C
C
C COMPUTE THE Y, Z VELOCITY COMPONENTS INDUCED BY VORTEX RECTANGLE
C OR RECTANGLE PAIR.
C USE EQUATIONS APPLYING TO VARIOUS SPECIAL CASES.
      IF(L-1) 50,33,31
31    IF (LL-L) 50,33,32
32    IF (COSL.EQ.0.00000) GO TO 62
      VY=(COSL/(P*SIDEB)*(-((RKA+RKB)*(SIDEB**2-(RKA-RKB)**2)/((
     2HLKB**2)*RKA*RKB) + (RKD+RKC)*(SIDEB**2 -(RKC-RKD)**2)/((HLKC**2)
     2*RKC*RKD))*(XK-XCI) + ((REA+REB)*(SIDEB**2 -(REA-REB)**2)/((
     2HLEB**2)*REA*REB) + (REC+RED)*(SIDEB**2 -(REC-RED)**2)/((HLEC**2)
     2*REC*RED))*(XE-XCI))  +  1./(P*DK)*(((RKB+REB)*(DK**2 -(
     2RKB-REB)**2)/((HDB**2)*RKB*REB))*(ZB-ZCJ)-((RKD+RED)*(DK**2-(RKD-
     2RED)**2)/((HDD**2)*RKD*RED))*(ZD-ZCJ)+((RKC+REC)*(DK**2-(RKC-REC)
     2**2)/((HDC**2)*RKC*REC))*(ZC-ZCJ)-((RKA+REA)*(DK**2-(RKA-REA)**2)
     2/((HDA**2)*RKA*REA))*(ZA-ZCJ)))
      GO TO 36
62    VY =                    (1./(P*DK)*(((RKB+REB)*(DK**2 -(
     2RKB-REB)**2)/((HDB**2)*RKB*REB))*(ZB-ZCJ)-((RKD+RED)*(DK**2-(RKD-
     2RED)**2)/((HDD**2)*RKD*RED))*(ZD-ZCJ)+((RKC+REC)*(DK**2-(RKC-REC)
     2**2)/((HDC**2)*RKC*REC))*(ZC-ZCJ)-((RKA+REA)*(DK**2-(RKA-REA)**2)
     2/((HDA**2)*RKA*REA))*(ZA-ZCJ)))
      GO TO 36
33    IF (COSL.EQ.0.00000) GO TO 63
      VY = (COSL/(P*SIDEB)*(-((RKD+RKB)*(SIDEB**2-(RKD-RKB)**2)/((
     2HLKB**2)*RKD*RKB))*(XK-XCI) + ((RED+REB)*(SIDEB**2 -(RED-REB)**
     22)/((HLEB**2)*RED*REB))*(XE-XCI)) + 1./(P*DK)*(((RKB+REB)*(DK**
```

```
     22-(RKB-REB)**2)/((HDB**2)*RKB*REB))*(ZB-ZCJ)-((RKD+RED)*(DK**2-
     2(RKD-RED)**2)/((HDD**2)*RKD*RED))*(ZD-ZCJ)))
      GO TO 36
63    VY =                                  (1./(P*DK)*((((RKB+REB)*(DK**
     22-(RKB-REB)**2)/((HDB**2)*RKB*REB))*(ZB-ZCJ)-((RKD+RED)*(DK**2-
     2(RKD-RED)**2)/((HDD**2)*RKD*RED))*(ZD-ZCJ)))
      GO TO 36
35    VY = 0.00000
36    IF (SINJ.EQ.0.00000) GO TO 42
      IF(L-1) 50,40,38
38    IF(LL-L) 50,40,39
39    IF (SINL.EQ.0.00000) GO TO 64
      VZ = (SINL/(P*SIDEB)*(((RKA+RKB)*(SIDEB**2 -(RKA-RKB)**2)/((
     3HLKB**2)*RKA*RKB) - (RKC+RKD)*(SIDEB**2 -(RKC-RKD)**2)/((HLKC**2)
     3*RKC*RKD))*(XK-XCI) + ((REC+RED)*(SIDEB**2 -(REC-RED)**2)/((
     3HLEC**2)*REC*RED) - (REA+REB)*(SIDEB**2 -(REA-REB)**2)/((HLEB**2)
     3*REA*REB))*(XE-XCI)) + 1./(P*DK)*(((RKA+REA)*(DK**2 -(RKA
     3-REA)**2)/((HDA**2)*RKA*REA) - (RKC+REC)*(DK**2 -(RKC-REC)**2)/((
     3HDC**2)*RKC*REC))*(YA-YCJ)  +  ((RKD+RED)*(DK**2 -(RKD-RED)**2)/
     3((HDD**2)*RKD*RED) - (RKB+REB)*(DK**2 -(RKB-REB)**2)/((HDB**2)*
     3RKB*REB))*(YB-YCJ)))
      GO TO 43
64    VZ =                      (1./(P*DK)*(((RKA+REA)*(DK**2 -(RKA
     3-REA)**2)/((HDA**2)*RKA*REA) - (RKC+REC)*(DK**2 -(RKC-REC)**2)/((
     3HDC**2)*RKC*REC))*(YA-YCJ)  +  ((RKD+RED)*(DK**2 -(RKD-RED)**2)/
     3((HDD**2)*RKD*RED) - (RKB+REB)*(DK**2 -(RKB-REB)**2)/((HDB**2)*
     3RKB*REB))*(YB-YCJ)))
      GO TO 43
40    VZ = (1./(P*DK)*(((RKD+RED)*(DK**2 -(RKD-RED)**2)/((HDD**2)*RKD*
     3RED) -(RKB + REB)*(DK**2-(RKB-REB)**2)/((HDB**2)*RKB*REB))*
     3(YB-YCJ)))
      GO TO 43
42    VZ = 0.00000
C
C
C THE VELOCITY COMPONENTS HAVE BEEN COMPUTED, STORE THE NORMAL VELOCITY
C AT THIS CONTROL POINT IN CC ARRAY ELEMENT M,N.
43    CC(M,N) =  VY*COSJ - VZ*SINJ
C
47    CONTINUE
48    CONTINUE
49    CONTINUE
50    CONTINUE
C
C THE MATRIX HAS BEEN GENERATED, RETURN TO CALLING PROGRAM.
C
      RETURN
      END
```

```
      SUBROUTINE INVR(A,N,ISIZE,JSIZE)
C
C     SUBROUTINE TO COMPUTE THE INVERSE OF A MATRIX OF SIZE LESS THAN
C     OR EQUAL TO 100
C
C THE MATRIX A IS REPLACED BY ITS INVERSE.
C THE MATRIX IS ASSUMED TO CONTAIN N ROWS AND COLUMNS.
C ISIZE AND JSIZE ARE THE DIMENSIONS OF A.
C NOTE THAT THIS SUBROUTINE DOES NOT TEST THE SINGULARITY OF A.
C
      DIMENSION IPIVOT(100),A(ISIZE,JSIZE),INDEX(100,2),PIVOT(100)
      EQUIVALENCE (IROW,JROW),(ICOLUM,JCOLUM),(AMAX,T,SWAP)
C
C
   15 DO 20 J=1,N
   20 IPIVOT(J)=0
   30 DO 550 I=1,N
C
C     SEARCH FOR PIVOT ELEMENT
C
   40 AMAX=0.0
   45 DO 105 J=1,N
   50 IF (IPIVOT(J)-1) 60, 105, 60
   60 DO 100 K=1,N
   70 IF (IPIVOT(K)-1) 80, 100, 740
   80 IF(ABS(AMAX)-ABS(A(J,K)))85,100,100
   85 IROW=J
   90 ICOLUM=K
   95 AMAX=A(J,K)
  100 CONTINUE
  105 CONTINUE
  110 IPIVOT(ICOLUM)=IPIVOT(ICOLUM)+1
C
C     INTERCHANGE ROWS TO PUT PIVOT ELEMENT ON DIAGONAL
C
  130 IF (IROW-ICOLUM) 140, 260, 140
  140 CONTINUE
  150 DO 200 L=1,N
  160 SWAP=A(IROW,L)
  170 A(IROW,L)=A(ICOLUM,L)
  200 A(ICOLUM,L)=SWAP
  260 INDEX(I,1)=IROW
  270 INDEX(I,2)=ICOLUM
  310 PIVOT(I)=A(ICOLUM,ICOLUM)
C
C     DIVIDE PIVOT ROW BY PIVOT ELEMENT
C
  330 A(ICOLUM,ICOLUM)=1.0
  340 DO 350 L=1,N
  350 A(ICOLUM,L)=A(ICOLUM,L)/PIVOT(I)
C
C     REDUCE NON-PIVOT ROWS
C
  380 DO 550 L1=1,N
  390 IF(L1-ICOLUM) 400, 550, 400
  400 T=A(L1,ICOLUM)
```

```
  420 A(L1,ICOLUM)=0.0
  430 DO 450 L=1,N
  450 A(L1,L)=A(L1,L)-A(ICOLUM,L)*T
  550 CONTINUE
C
C     INTERCHANGE COLUMNS
C
  600 DO 710 I=1,N
  610 L=N+1-I
  620 IF (INDEX(L,1)-INDEX(L,2)) 630, 710, 630
  630 JROW=INDEX(L,1)
  640 JCOLUM=INDEX(L,2)
  650 DO 705 K=1,N
  660 SWAP=A(K,JROW)
  670 A(K,JROW)=A(K,JCOLUM)
  700 A(K,JCOLUM)=SWAP
  705 CONTINUE
  710 CONTINUE
  740 RETURN
      END
```

```
      SUBROUTINE RHS (XCPT,YCPT,ZCPT,XW,YW,ZW,DSM,GAMAM,SPAN,SPEED,
     1GAMAK,NN,LL,NW,SINPHI,COSPHI)
C
C THIS IS A SUBROUTINE TO COMPUTE THE RIGHT HAND SIDE OF THE MATRIX
C EQUATION DEFINING THE VORTEX STRENGTHS.
C
      DIMENSION XW(40),YW(40),ZW(40),RW(2,2),DSM(39),VBAR(2)
      DIMENSION GAMAK(100,1)
      DIMENSION SINPHI(20),COSPHI(20),XCPT(14),YCPT(10),ZCPT(10)
      P = 6.2831853
      M = 0
C
C CYCLE THROUGH CONTROL POINTS.
900   DO 50 I=1,NN
      DO 49 J=1,LL
      M = M + 1
C
      VYM = 0.0
      VZM = 0.0
      SINJ = SINPHI(J)
      COSJ = COSPHI(J)
      XCI = XCPT(I)
      YCJ = YCPT(J)
      ZCJ = ZCPT(J)
C
C COMPUTE VELOCITY INDUCED BY MODEL.
      DO 46 K=1,NW
      JJ = K
      DO 45 L=1,2
      RW(L,1) = SQRT((XW(JJ)-XCI)**2+(YW(JJ)-YCJ)**2+(ZW(JJ)-ZCJ)**2)
      RW(L,2) = SQRT((XW(JJ)-XCI)**2+(YW(JJ)-YCJ)**2+(ZW(JJ)+ZCJ)**2)
      JJ = K+1
45    CONTINUE
      DO 44 L=1,2
44    VBAR(L) =-GAMAM*(DSM(K)**2-(RW(1,L)-RW(2,L))**2)*(RW(1,L)+RW(2,L))
     1/(P*RW(1,L)*RW(2,L)*(4.0*(RW(1,L)**2)*(DSM(K)**2)-(RW(1,L)**2-RW(2
     2,L)**2+DSM(K)**2)**2))
      L = K+1
      IF (COSJ.EQ.0.0) GO TO 41
      VYM = VBAR(1)*((ZW(K)-ZCJ)*(XW(L)-XW(K))-(XW(K)-XCI)*(ZW(L)-ZW(K)))
     1)-VBAR(2)*((-ZW(K)-ZCJ)*(XW(L)-XW(K))-(XW(K)-XCI)*(ZW(K)-ZW(L)))
     2+ VYM
41    IF (SINJ.EQ.0.0) GO TO 46
      VZM = (VBAR(1)-VBAR(2))*((XW(K)-XCI)*(YW(L)-YW(K))-(YW(K)-YCJ)*
     1(XW(L)-XW(K))) + VZM
45    CONTINUE
C
C STORE NORMAL VELOCITY IN GAMAK ARRAY ELEMENT M.
54    GAMAK(M,1) =  VZM*SINJ - VYM*COSJ
49    CONTINUE
50    CONTINUE
C
C THE RIGHT HAND SIDE HAS BEEN GENERATED, RETURN TO CALLING PROGRAM.
C
      RETURN
      END
```

```
      SUBROUTINE WKIT (XW,YW,ZW,X,Y,Z,SINPHI,COSPHI,SIDE,S,GAMA,DSM,
     1GAMAM,SPEED,SPAN,NW,NN,MM,N1,LL,VW1,RHO,Q,FAL,FAD,CHORD,LIFT,DRAG,
     1STWK,VXTC,VYTC,ALPHAO,ALPHAI,ALFAA,VXMC,VYMC)
C
C THIS IS A SUBROUTINE TO ITERATE THE TRAILING VORTEX PAIR POSITION
C AND TO COMPUTE LIFT AND INDUCED DRAG VALUES BASED UPON THE VELOCITY
C AT THE CENTER OF THE BOUND VORTEX.
C
      DIMENSION X(15),Y(20),Z(20),SINPHI(20),COSPHI(20),SIDE(20),S(14)
      DIMENSION GAMA(14,10)
      DIMENSION XW(40),YW(40),ZW(40),RW(2,2),DSM(39),VBAR(2)
      INTEGER A,B,C,D,E
      LOGICAL STWK
      REAL LIFT
      ALPHAI = 0.0
      ALFAA = 0.0
      ALPHAO = 0.0
C
C IF THIS IS TO BE THE LINEARIZED CASE, DO NOT ITERATE THE TRAILING
C PAIR.  GO DIRECTLY TO COMPUTE THE LIFT AND DRAG.
      IF (STWK) GO TO 704
      MMMM = NW-1
C
C CYCLE THROUGH VERTICAL AND LATERAL SHIFT OPERATIONS.
      DO 701 LSHFT = 1,2
C
C CYCLE THROUGH WAKE SEGMENTS.
      DO 700 M = 2,MMMM
      IF ((M.EQ.2).AND.(LSHFT.EQ.2)) GO TO 700
C
C SELECT COORDINATES FOR VELOCITY COMPUTATION.  NOTE ZCJ = 0.0 FOR CASE
C OF FIRST TRAILING VORTEX SEGMENT.
      XCI = XW(M)
      YCJ = YW(M)
      IF (M.EQ.2) GO TO 20
      ZCJ = ZW(M)
      GO TO 30
20    ZCJ = 0.0
30    CONTINUE
C
C COMPUTE VELOCITY AT THIS POINT.
      CALL XYZVEL       (XCI,YCJ,ZCJ,XW,YW,ZW,X,Y,Z,SINPHI,COSPHI,SIDE,S
     1,GAMA,DSM,GAMAM,SPEED,SPAN,NW,NN,MM,N1,LL,VXT,VYT,VZT,VXR,VYR,
     1VZR,VXM,VYM,VZM)
      VEL = SQRT(VXT**2 + VYT**2 + VZT**2)
      J = M+1
      IF (M.NE.2) GO TO 743
C
C IF THIS IS THE FIRST SEGMENT, COMPUTE NEW ANGLE OF ATTACK.
      ALPHAO = ASIN(-GAMAM*2./(6.2831853*CHORD*VEL))
      ALPHAI = ATAN(VYT/VXT)
      ALFAA = ALPHAO + ALPHAI
C
C COMPUTE COORDINATE SHIFT.
      XSHFT = DSM(1)*COS(ALFAA) + XW(1) - XW(2)
      YSHFT = DSM(1)*SIN(ALFAA) + YW(1) - YW(2)
```

```
      ZSHFT = 0.0
      GO TO 57
743   CONTINUE
      DCWX = VXT/VEL
      DCWY = VYT/VEL
      DCWZ = VZT/VEL
      XSHFT = DSM(M)*DCWX + XW(M)
      XSHFT = XSHFT - XW(J)
      IF (LSHFT.EQ.2) GO TO 149
      YSHFT = DSM(M)*DCWY + YW(M)
      YSHFT = YSHFT - YW(J)
      GO TO 57
149   ZSHFT = DSM(M)*DCWZ + ZW(M)
      ZSHFT = ZSHFT - ZW(J)
C
C SHIFT ALL COORDINATES DOWNSTREAM OF VELOCITY COMPUTATION POINT.
57    DO 748 L=J,NW1
      K=L-1
      XW(L) = XW(L) + XSHFT
      IF (LSHFT.EQ.2) GO TO 59
58    YW(L) = YW(L) + YSHFT
      GO TO 148
59    ZW(L) = ZW(L) + ZSHFT
C
C COMPUTE NEW SEGMENT LENGTH.
148   DSM(K) = SQRT((XW(L)-XW(K))**2+(YW(L)-YW(K))**2+(ZW(L)-ZW(K))**2)
748   CONTINUE
700   CONTINUE
701   CONTINUE
4150  FORMAT (18H0WAKE COORDINATES  ,/, 9X,2HXW,13X,2HYW,13X,2HZW)
C
C WRITE RESULT OF ITERATION PROCESS.
      WRITE (6,4150)
4160  FORMAT (3F15.5)
      XCI = XW(1)
      DO 703 I = 1,NW
      YCJ = XW(I) - XCI
      WRITE (6,4160) YCJ,YW(I),ZW(I)
703   CONTINUE
704   CONTINUE
C
C COMPUTE LIFT AND INDUCED DRAG OF WING, COMPARE WITH FREE AIR RESULT.
      XCI = XW(1)
      YCJ = YW(1)
      ZCJ = 0.
      CALL XYVEL      (XCI,YCJ,ZCJ,XW,YW,ZW,X,Y,Z,SINPHI,COSPHI,SIDE,S
     1,GAMA,DSM,GAMAM,SPEED,SPAN,NW,NN,MM,N1,LL,VXT,VYT,VZT,VXR,VYR,
     1VZR,VXM,VYM,VZM)
      VXTC=VXT
      VYTC=VYT
      VXMC=VXM
      VYMC=VYM
702   LIFT = RHO*SPAN*GAMAM
      DRAG = -LIFT*VYT
      LIFT = VXT*LIFT
      CLAR = ((3.14159/4.)**2)/(Q*(SPAN**2))
```

```
      CDIAR = DRAG*CLAR
      CLAR = LIFT*CLAR
      DELTAL = LIFT - FAL
      DELTAD =  DRAG-FAD
      IF (STWK) ALFAA=0.0
      ALFAA=-ALFAA
      ALPHA0=-ALPHA0
C
C WRITE RESULTS OF COMPUTATIONS.
      WRITE (6,4176) ALFAA, ALPHA0, ALPHAI
4176  FORMAT (2X,7HALFAA =,F7.4,3X,8HALPHA0 =,F7.4,3X,8HALPHAI =,F7.4)
      WRITE (6,4175) LIFT,DELTAL
4175  FORMAT (12H0WING LIFT =,F10.5,4X,22HCHANGE DUE TO TUNNEL = ,F10.5)
      WRITE (6,4177) DRAG,DELTAD
4177  FORMAT (12H0WING DRAG =,F10.5,4X,22HCHANGE DUE TO TUNNEL =,F10.5)
      WRITE (6,4200) VXT,VYT
4200  FORMAT (1H0,39HTOTAL VELOCITIES AT WING CENTER   VX = ,F10.4,5X,
     15HVY = ,F10.4)
      WRITE (6,4210) CLAR,CDIAR
4210  FORMAT (1H0,29HMEASURED IN TUNNEL   CL/AR = ,F10.5,5X,9HCDI/AR = ,
     1F10.5)
C
C RETURN TO CALLING PROGRAM.
C
      RETURN
      END
```

```
      SUBROUTINE XYZVEL (XCI,YCJ,ZCJ,XW,YW,ZW,X,Y,Z,SINPHI,COSPHI,SIDE,S
     1,GAMA,DSM,GAMAM,SPEED,SPAN,NW,NN,MM,N1,LL,VXT,VYT,VZT,VXR,VYR,
     1VZR,VXM,VYM,VZM)
C
C THIS IS A SUBROUTINE TO COMPUTE VELOCITY COMPONENTS INDUCED BY
C TUNNEL AND LIFTING SYSTEM.
C
      DIMENSION X(15),Y(20),Z(20),SINPHI(20),COSPHI(20),SIDE(20),S(14),
     1R(15,20),HL(15,20),HD(20),HYZ(20),XW(40),YW(40),ZW(40),RW(2,2),
     1DSM(39),VBAR(2),GAMA(14,10)
      INTEGER A,B,C,D,E
      LOGICAL XONLY,XNY,YNZ
C
C SET LOGICAL VARIABLES TO COMPUTE ONLY VELOCITY COMPONENTS REQUIRED.
      IF (ZCJ.EQ.0.) GO TO 10
      XONLY = .FALSE.
      XNY = .FALSE.
      YNZ = .FALSE.
      GO TO 643
      ENTRY XVEL
      XONLY = .TRUE.
      XNY = .FALSE.
      YNZ = .FALSE.
      GO TO 643
      ENTRY XYVEL
10    CONTINUE
      XNY = .TRUE.
      XONLY = .FALSE.
      YNZ = .FALSE.
      GO TO 643
      ENTRY YZVEL
      YNZ = .TRUE.
      XONLY = .FALSE.
      XNY = .FALSE.
643   XTP = XCI
      YTP = YCJ
      ZTP = ZCJ
C
C COMPUTE LOCATION OF VORTEX NET WITH RESPECT TO POINT OF VELOCITY
C COMPUTATION.
      DO 127 J = 1,MM
      HD(J) = SQRT((YTP-Y(J))**2 + (ZTP - Z(J))**2)
      HYZ(J) = SQRT(((ZTP-Z(J))*SINPHI(J)-(YTP-Y(J))*COSPHI(J))**2)
      DO 127 I = 1,N1
      R(I,J) = SQRT((XTP-X(I))**2 + (YTP-Y(J))**2 + (ZTP-Z(J))**2)
127   HL(I,J)=SQRT((X(I)-XTP)**2 + HYZ(J)**2)
      VXR = 0.00000
      VYR = 0.00000
      VZR = 0.00000
C
C CYCLE THROUGH VORTEX RECTANGLES.
      DO 150 K = 1,NN
      DO 150 L = 1,LL
C
C SELECT VARIABLES FOR THIS PARTICULAR VORTEX RECTANGLE OR RECTANGLES.
      A = L - 1
```

```
      B = L
      C = LL*2 - L
      D = C - 1
      E = K + 1
      IF (L - 1) 150, 129, 125
125   IF (LL-L) 150,129,128
128   RKA = R(K,A)
      RKC = R(K,C)
      REA = R(E,A)
      REC = R(E,C)
      HLKC = HL(K,C)
      HLEC = HL(E,C)
      HDA = HD(A)
      HDC = HD(C)
      YA = Y(A)
      ZA = Z(A)
      ZC = Z(C)
      HYZA = HYZ(A)
      HYZC = HYZ(C)
129   SINL = SINPHI(L)
      COSL = COSPHI(L)
      RKB = R(K,B)
      RKD = R(K,D)
      REB = R(E,B)
      RED = R(E,D)
      HLKB = HL(K,B)
      HLEB = HL(E,B)
      HDB = HD(B)
      HDD = HD(D)
      SIDEB = SIDE(B)
      DK = S(K)
      YB = Y(B)
      ZB = Z(B)
      ZD = Z(D)
      XK = X(K)
      XE = X(E)
      HYZB = HYZ(B)
      HYZD = HYZ(D)
      P = 25.13274
C
C DETERMINE WHETHER OR NOT VORTEX RECTANGLE LIES ON PLANE OF SYMMETRY.
      IF (L-1) 150, 130, 131
131   IF (LL-C) 132,130,150
130   CONTINUE
C
C VORTEX RECTANGLE LIES ON PLANE OF SYMMETRY, USE FOLLOWING EQUATION TO
C COMPUTE VELOCITY COMPONENTS TAKING SPECIAL CASES INTO ACCOUNT.
      VXPS = 0.0
      VYPS = 0.0
      VZPS = 0.0
      IF (YNZ) GO TO 135
      VXPS = 1./(P*SIDEB)*(HYZB*((RKD+RKB)*(SIDEB**2-(RKD-RKB)**2)/((
     1HLKB**2)*RKD*RKB) - (RED+REB)*(SIDEB**2-(RED-REB)**2)/((HLEB**2)
     1*RED*REB)))*GAMA(K,L)
      IF (XONLY) GO TO 72
135   IF (COSL.EQ.0.0) GO TO 56
```

```
      VYPS = (COSL/(P*SIDEB)*(-((RKD+RKB)*(SIDEB**2-(RKD-RKB)**2)/((
     2HLKB**2)*RKD*RKB))*(XK-XTP) + ((RED+REB)*(SIDEB**2 -(RED-REB)**
     22)/((HLEB**2)*RED*REB))*(XE-XTP)) + 1./(P*DK)*(((RKB+REB)*(DK**
     22-(RKB-REB)**2)/((HDB**2)*RKB*REB))*(ZB-ZTP)-((RKD+RED)*(DK**2-
     2(RKD-RED)**2)/((HDD**2)*RKD*RED))*(ZD-ZTP)))*GAMA(K,L)
      IF (XNY) GO TO 72
      GO TO 67
65    VYPS =                          (1./(P*DK)*(((RKB+REB)*(DK**
     22-(RKB-REB)**2)/((HDB**2)*RKB*REB))*(ZB-ZTP)-((RKD+RED)*(DK**2-
     2(RKD-RED)**2)/((HDD**2)*RKD*RED))*(ZD-ZTP)))*GAMA(K,L)
      IF (XNY) GO TO 72
67    VZPS = (1./(P*DK)*(((RKD+RED)*(DK**2 -(RKD-RED)**2)/((HDD**2)*RKD*
     3RED) -(RKB + REB)*(DK**2-(RKB-REB)**2)/((HDB**2)*RKB*REB))*
     3(YB-YTP)))*GAMA(K,L)
      VZR = VZR + VZPS
72    VXR = VXR + VXPS
      VYR = VYR + VYPS
      GO TO 150
C
C VORTEX RECTANGLES DO NOT LIE ON PLANE OF SYMMETRY, USE FOLLOWING
C EQUATIONS TO COMPUTE VELOCITY COMPONENTS TAKING VARIOUS SPECIAL CASES
C INTO ACCOUNT.
132   CONTINUE
      VX = 0.0
      VY = 0.0
      VZ = 0.0
      IF (YNZ) GO TO 140
      VX =(1./(P*SIDEB)*((HYZB*((RKA+RKB)*(SIDEB**2 -(RKA-RKB)**2)/((
     1HLKB**2)*RKA*RKB) - (REA+REB)*(SIDEB**2 -(REA-REB)**2)/((HLEB**2)
     1*REA*REB))) + (HYZC*((RKD+RKC)*(SIDEB**2 -(RKD-RKC)**2)/((
     1HLKC**2)*RKC*RKD) - (RED+REC)*(SIDEB**2 -(RED-REC)**2)/((HLEC**2)
     1*REC*RED)))))*GAMA(K,L)
      IF (XONLY) GO TO 73
140   IF (COSL.EQ.0.0) GO TO 68
      VY=(COSL/(P*SIDEB)*(-((RKA+RKB)*(SIDEB**2-(RKA-RKB)**2)/((
     2HLKB**2)*RKA*RKB) + (RKD+RKC)*(SIDEB**2 -(RKC-RKD)**2)/((HLKC**2)
     2*RKC*RKD))*(XK-XTP) + ((REA+REB)*(SIDEB**2 -(REA-REB)**2)/((
     2HLEB**2)*REA*REB) + (REC+RED)*(SIDEB**2 -(REC-RED)**2)/((HLEC**2)
     2*REC*RED))*(XE-XTP))   +   1./(P*DK)*(((RKB+REB)*(DK**2 -(
     2RKB-REB)**2)/((HDB**2)*RKB*REB))*(ZB-ZTP)-((RKD+RED)*(DK**2-(RKD-
     2RED)**2)/((HDD**2)*RKD*RED))*(ZD-ZTP)+((RKC+REC)*(DK**2-(RKC-REC)
     2**2)/((HDC**2)*RKC*REC))*(ZC-ZTP)-((RKA+REA)*(DK**2-(RKA-REA)**2)
     2/((HDA**2)*RKA*REA))*(ZA-ZTP)))*GAMA(K,L)
      IF (XNY) GO TO 73
      GO TO 69
68    VY =                     (1./(P*DK)*(((RKB+REB)*(DK**2 -(
     2RKB-REB)**2)/((HDB**2)*RKB*REB))*(ZB-ZTP)-((RKD+RED)*(DK**2-(RKD-
     2RED)**2)/((HDD**2)*RKD*RED))*(ZD-ZTP)+((RKC+REC)*(DK**2-(RKC-REC)
     2**2)/((HDC**2)*RKC*REC))*(ZC-ZTP)-((RKA+REA)*(DK**2-(RKA-REA)**2)
     2/((HDA**2)*RKA*REA))*(ZA-ZTP)))*GAMA(K,L)
      IF (XNY) GO TO 73
69    IF (SINL.EQ.0.00000) GO TO 70
      VZ = (SINL/(P*SIDEB)*(((RKA+RKB)*(SIDEB**2 -(RKA-RKB)**2)/((
     3HLKB**2)*RKA*RKB) - (RKC+RKD)*(SIDEB**2 -(RKC-RKD)**2)/((HLKC**2)
     3*RKC*RKD))*(XK-XTP) + ((REC+RED)*(SIDEB**2 -(REC-RED)**2)/((
     3HLEC**2)*REC*RED) - (REA+REB)*(SIDEB**2 -(REA-REB)**2)/((HLEB**2)
```

```
     3*REA*REB))*(XE-XTP)) + 1./(P*DK)*(((RKA+REA)*(DK**2 -(RKA
     3-REA)**2)/((HDA**2)*RKA*REA) - (RKC+REC)*(DK**2 -(RKC-REC)**2)/((
     3HDC**2)*RKC*REC))*(YA-YTP)  +  ((RKD+RED)*(DK**2 -(RKD-RED)**2)/
     3((HDD**2)*RKD*RED) - (RKB+REB)*(DK**2 -(RKB-REB)**2)/((HDB**2)*
     3RKB*REB))*(YB-YTP)))*GAMA(K,L)
      GO TO 71
70    VZ =                    (1./(P*DK)*(((RKA+REA)*(DK**2 -(RKA
     3-REA)**2)/((HDA**2)*RKA*REA) - (RKC+REC)*(DK**2 -(RKC-REC)**2)/((
     3HDC**2)*RKC*REC))*(YA-YTP)  +  ((RKD+RED)*(DK**2 -(RKD-RED)**2)/
     3((HDD**2)*RKD*RED) - (RKB+REB)*(DK**2 -(RKB-REB)**2)/((HDB**2)*
     3RKB*REB))*(YB-YTP)))*GAMA(K,L)
71    VZR = VZR + VZ
73    VXR = VXR + VX
      VYR = VYR + VY
C
C NOW COMPUTE VELOCITY INDUCED BY MODEL.
150   CONTINUE
      P = 6.2831853
      VXM = 0.0
      VYM = 0.0
      VZM = 0.0
      DO 746 K=1,NW
      J = K
      DO 745 L=1,2
      RW(L,1) = SQRT((XW(J)-XCI)**2+(YW(J)-YCJ)**2+(ZW(J)-ZCJ)**2)
      RW(L,2) = SQRT((XW(J)-XCI)**2+(YW(J)-YCJ)**2+(ZW(J)+ZCJ)**2)
      J = K + 1
745   CONTINUE
      DO 744 L=1,2
       H = 4.*(RW(1,L)**2)*(DSM(K)**2)-(RW(1,L)**2-RW(2,L)**2+DSM(K)**2)
     1**2
      IF (H.LT.((1.E-6)*4.*DSM(K)**2))  GO TO 730
      VBAR(L) =-GAMAM*(DSM(K)**2-(RW(1,L)-RW(2,L))**2)*(RW(1,L)+RW(2,L))
     1/(P*RW(1,L)*RW(2,L)*H)
      GO TO 744
730   VBAR(L) = 0.0
744   CONTINUE
      L = K+1
      IF (YNZ) GO TO 750
      VXM = VBAR(1)*((YW(K)-YCJ)*(ZW(L)-ZW(K))-(ZW(K)-ZCJ)*(YW(L)-YW(K))
     1) - VBAR(2)*((YW(K)-YCJ)*(ZW(K)-ZW(L))-(-ZW(K)-ZCJ)*(YW(L)-YW(K)))
     2 + VXM
      IF (XONLY) GO TO 746
750   CONTINUE
      VYM = VBAR(1)*((ZW(K)-ZCJ)*(XW(L)-XW(K))-(XW(K)-XCI)*(ZW(L)-ZW(K))
     1)-VBAR(2)*((-ZW(K)-ZCJ)*(XW(L)-XW(K))-(XW(K)-XCI)*(ZW(K)-ZW(L)))
     2+ VYM
      IF (XNY) GO TO 746
      VZM = (VBAR(1)-VBAR(2))*((XW(K)-XCI)*(YW(L)-YW(K))-(YW(K)-YCJ)*
     1(XW(L)-XW(K))) + VZM
746   CONTINUE
C
      VXT = VXM+VXR+SPEED
      VYT = VYM+VYR
      VZT = VZM+VZR
C
```

```
C VELOCITY COMPONENTS HAVE BEEN COMPUTED, RETURN TO CALLING PROGRAM.
C
      RETURN
      END
```

"The aeronautical and space activities of the United States shall be conducted so as to contribute . . . to the expansion of human knowledge of phenomena in the atmosphere and space. The Administration shall provide for the widest practicable and appropriate dissemination of information concerning its activities and the results thereof."

—NATIONAL AERONAUTICS AND SPACE ACT OF 1958

NASA SCIENTIFIC AND TECHNICAL PUBLICATIONS

TECHNICAL REPORTS: Scientific and technical information considered important, complete, and a lasting contribution to existing knowledge.

TECHNICAL NOTES: Information less broad in scope but nevertheless of importance as a contribution to existing knowledge.

TECHNICAL MEMORANDUMS: Information receiving limited distribution because of preliminary data, security classification, or other reasons. Also includes conference proceedings with either limited or unlimited distribution.

CONTRACTOR REPORTS: Scientific and technical information generated under a NASA contract or grant and considered an important contribution to existing knowledge.

TECHNICAL TRANSLATIONS: Information published in a foreign language considered to merit NASA distribution in English.

SPECIAL PUBLICATIONS: Information derived from or of value to NASA activities. Publications include final reports of major projects, monographs, data compilations, handbooks, sourcebooks, and special bibliographies.

TECHNOLOGY UTILIZATION PUBLICATIONS: Information on technology used by NASA that may be of particular interest in commercial and other non-aerospace applications. Publications include Tech Briefs, Technology Utilization Reports and Technology Surveys.

Details on the availability of these publications may be obtained from:

SCIENTIFIC AND TECHNICAL INFORMATION OFFICE

NATIONAL AERONAUTICS AND SPACE ADMINISTRATION

Washington, D.C. 20546